BRNO UNIVERSITY OF TECHNOLOGY
VYSOKÉ UČENÍ TECHNICKÉ V BRNĚ

FACULTY OF CHEMISTRY
FAKULTA CHEMICKÁ

INSTITUTE OF PHYSICAL AND APPLIED CHEMISTRY
ÚSTAV FYZIKÁLNÍ A SPOTŘEBNÍ CHEMIE

PREPARATION AND CHARACTERIZATION OF NANOSTRUCTURED RESORBABLE SUBSTITUTES FOR ACCELERATED SKIN HEALING

PŘÍPRAVA A CHARAKTERIZACE NANOSTRUKTUROVANÝCH VSTŘEBATELNÝCH NÁHRAD PRO AKCELEROVANÉ HOJENÍ KŮŽE

MASTER'S THESIS
DIPLOMOVÁ PRÁCE

AUTHOR
AUTOR PRÁCE

Bc. Katarína Kacvinská

SUPERVISOR
VEDOUCÍ PRÁCE

doc. Ing. Lucy Vojtová, Ph.D.

BRNO 2018

VYSOKÉ UČENÍ TECHNICKÉ V BRNĚ
FAKULTA CHEMICKÁ

Zadání diplomové práce

Číslo práce:	FCH-DIP1128/2017
Ústav:	Ústav fyzikální a spotřební chemie
Studentka:	**Bc. Katarína Kacvinská**
Studijní program:	Chemie pro medicínské aplikace
Studijní obor:	Chemie pro medicínské aplikace
Vedoucí práce:	**doc. Ing. Lucy Vojtová, Ph.D.**
Akademický rok:	2017/18

Název diplomové práce:

Příprava a charakterizace nanostrukturovaných vstřebatelných náhrad pro akcelerované hojení kůže

Zadání diplomové práce:

1. Lit. rešerše o vstřebatelných kožních náhradách a aditivech akcelerující hojení kůže
2. Příprava nanostrukturovaných multikompozitních vzorků a jejich modifikace za účelem zvýšení hojícího účinku
3. Fyzikálně–chemické a in vitro biologické testování připravených vzorků
4. Vyhodnocení, diskuze, závěr

Termín odevzdání diplomové práce: 7.5.2018

Diplomová práce se odevzdává v děkanem stanoveném počtu exemplářů na sekretariát ústavu. Toto zadání je součástí diplomové práce.

Bc. Katarína Kacvinská student(ka)	doc. Ing. Lucy Vojtová, Ph.D. vedoucí práce	prof. Ing. Miloslav Pekař, CSc. vedoucí ústavu

V Brně dne 31.1.2018

prof. Ing. Martin Weiter, Ph.D.
děkan

ABSTRACT

Together with the increasing demands on the quality of treatment in the field of burn and plastic surgery, there is the possibility of applying new technological solutions in the treatment of defects with full loss of skin thickness. This thesis deals with a preparation of a nanostructured bilayer scaffold for skin tissue engineering, which substitutes a skin dermis (lower porous layer) and a basal membrane (upper nanofibrous thin layer)). The porous layer is based on collagen, which is also characterized in presence of different polysaccharide additives: chitosan, oxidized cellulose calcium salt (CaOC), carboxymethyl cellulose sodium salt (NaCMC)), as well as a dopamine and fibroblast growth factor (FGF) addition, in order to improve biomechanical properties, regulate and promote skin healing. Thin nanofibers layer consists of electrospun gelatin in combination with polycaprolactone (PCL) and CaOC.

Two different fabrication mechanisms differing in cross-linking between the porous and nanofibrous layer are proposed. The scaffolds were evaluated in terms of biomechanical, structural and *in-vitro* properties. A uniaxial strain test has shown that the upper nanofibrous layer provides mechanical support, which is significantly enhanced with the polydopamine (PDA)-coated surface. Swelling test of porous layer showed adequate spaces to allow cells infiltration, what has been shown as decrease in presence of PDA. Degradation with collagenase and lysozyme has shown significant time prolongation and also proliferation and viability of the mouse fibroblast cells seeded on the scaffolds were significantly enhanced with PDA and FGF modification.

Novel nanostructured bilayer scaffold possess good biomechanical properties and exhibis potential in skin tissue engineering by allowing cells to adhere, proliferate and generate expracellular matrix.

KEY WORDS

Scaffold, bilayer, collagen, nanofibres, polydopamine, growth factor, biomechanical properties

ABSTRAKT

Spolu s narastajúcimi nárokmi na kvalitu liečby v oblasti popálenin a plastickej chirurgie existuje možnosť ako uplatniť nové technologické riešenie na liečbu porúch s celkovou stratou kožnej vrstvy. Diplomová práca sa zaoberá prípravou nanoštrukturovaného, dvojvrstvového skafoldu pre využitie v tkánivovom inžinierstve, ktorý nahrádza kožnú časť dermis (dolná porézna vrstva) a bazálnu membránu (horná a tenká nanovlákenná vrstva). Základom dolnej pórovitej vrstvy je kolagén, charakterizovaný v prítomnosti ďalších polysacharidových aditív: chitosan, vápenatá soľ oxidovanej celulózy (CaOC), sodná soľ karboxymetylcelulózy (NaCMC). Zároveň prídavok dopamínu a fibroblastového rastového faktoru (FGF), s cieľom zlepšiť biomechanické vlastnosti, regulovať a podporovať hojenie kože. Tenká nanovlákenná vrstva je zložená zo želatíny, polycaprolaktónu (PCL) a CaOC.

Sú navrhnuté dva rôzne mechnizmy prípravy skafoldu, ktoré sa odlišujú sa v prítomnosti sieťovaných a nesieťovaných nanovláken. Skafoldy boli charakterizované z hľadiska biomechanických, štruktúrnych vlastností a *in vitro*. Vrchná nanovlákenná vrstva poskytuje mechanickú podporu, ktorá je výrazne zvýšená prítomnosťou polydopamínu (PDA). Test botnania poréznej vrstvy skafoldu ukázal na dostatočne veľké póry, umožňujúce filtráciu buniek. Táto botnatosť bola znížená v prítomnosti PDA, ktorý má zároveň významný vplyv na časové predĺženie degrádácie v prítomnosti kolagenázy a lyzozýmu. Spolu s FGF výrazne podporil proliferizáciu a životaschopnosť myších fibroblastov.

Nanoštrukturovaný, dvojvrstvový skafold má potenciál pre budúce aplikácie pri hojení rán, kedže sa vyznačuje dobrými mechanickými vlastnosťami a umožňuje bunkám adherovať, proliferovať a formovať extra celulárny matrix.

KĽÚČOVÉ SLOVÁ

Skafold, dvojvrstva, kolagén, nanovlákna, polydopamín, rastový faktor, biomechanické vlastnosti

KACVINSKÁ, K. *A preparation and characterization of nanostructured resorable substitutes for accelerated skin healing.* Brno, 2018. 84 p. Diploma thesis, Brno university of Technology, Faculty of Chemistry, Institute of Materials Science. Supervisor doc. Ing. Lucy Vojtová, Ph.D.

DECLARATION

I declare that my diploma thesis was worked out independently and that the used references are quoted correctly and fully. The content of the above mentioned thesis is considered a property of VUT Faculty of Chemistry and can by used for commercial purposes only with the supervisor‘s and dean‘s consents.

.....

author‘s signature

PREHLÁSENIE

Prehlasujem, že som diplomovú prácu vypracovala samostatne a že všetky použité literárne zdroje som správne a úplne citovala. Táto práca je z hľadiska obsahu majetkom Fakulty chemickej VUT v Brne a môže byť použitá ku komerčným účelom len so súhlasom vedúceho diplomovej práce a dekana FCH VUT.

.....

podpis diplomanta

Acknowledgments:

I would like to thank my supervisor Doc. Ing. Lucy Vojtová, Ph.D. for helpfull advices and discussions, Ing. Pavel Janál for additional advices, Mgr. Veronika Pavliňáková, Ph.D. and Mgr. David Pavliňák, Ph.D. for helping with nanofibres formation, Ing. Petr Poláček, Ph.D for explaining the operation with rheometer and Ing. Lenka Michlovská, Ph.D for SEM images. Also I would like to thank my family for support during the whole studium. This work was supported by the CEITEC 2020 (LQ1601) with financial support from the Ministry of Education, Youth and Sports of the Czech Republic under the National Sustainability Programme II.

LIST OF CONTENT

1 Introduction

Wound healing is part of an attractive area of study that consists of deep understanding the most complex of biological mechanism of tissue repair, taking place via controlled cascade of biochemical and cellular processes. The aim of this scientific area is to design the most effective material to refund the misssing skin after burn injury, trauma, surgery, acute illness, or chronic disease. Each year millions of people worldwide are affected by skin injuries and the healing complicated process, since involves inflammation, angiogenesis, matrix deposition, and cell recruitment. Vascular disease, diabetes, or aging are usualy important factors that contribute to the treatment fail. The most convenient skin replacement should be able to mimic both dermis and epidermis layers and in a certain time, after new skin formation, be able to degrade with no harmfull effects on human body. Natural and synthetic materials have been already used for tissue engineered skin substitutes and to this date, the complete functional skin is still not available. There is a need to develop a full thickness skin replacement, that can vascularize rapidly, be easily conformed and applicable to the wound site, resist infection, keep the wound in moisture, as well as being thick flexible, resistant to the shear forces, cost effective and with long-term stability.

Theoretical part

2 Literature Review

2.1 Introduction to the structure of human skin

The human skin covers the entire external surface of the body and serves as a protective barrier that prevents internal tissues from exposure to trauma, ultraviolet (UV) radiation, temperature extremes, toxins and bacteria. It has important functions in sensory perception, immunologic surveillance, thermoregulation, and control of insensible fluid loss. The adult skin consists of three tissue layers; -an outward part is epidermis, derived from surface ectoderm; -an underlying part named dermis, derived from mesoderm and third is connective tissue, called hypodermis (**Figure 1)**.[1]

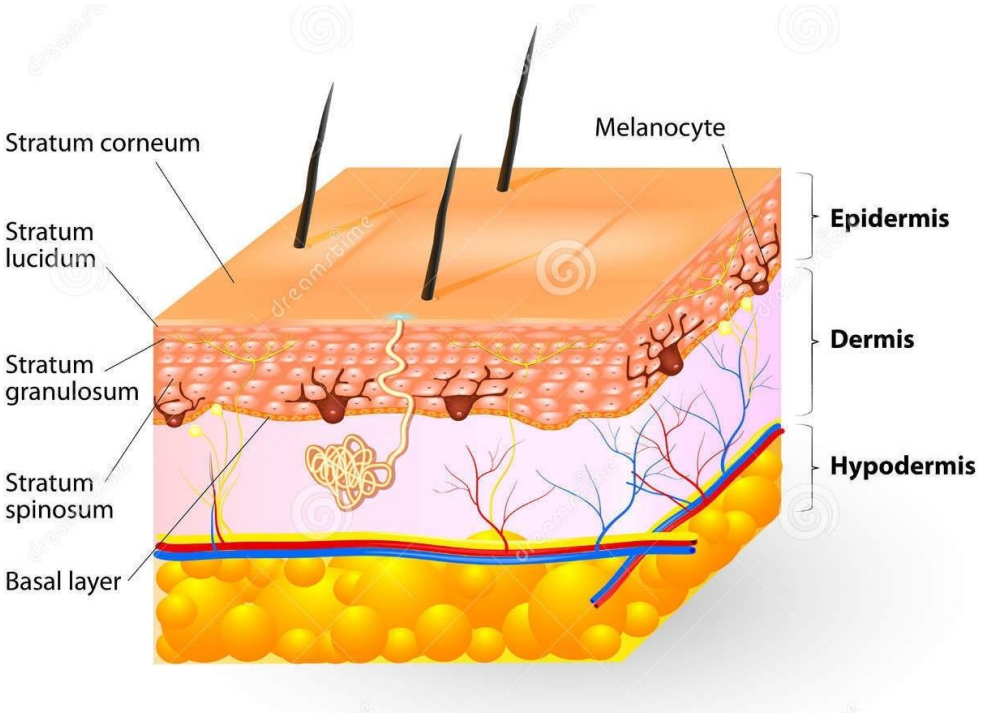

***Figure 1**-Structural depiction of layers of human skin* [1]

The epidermis layer consists mainly of keratinocytes (almost 90%), separated from the dermis by a basement membrane. It contains also melanocytes of neural crest origin, antigen-processing Langerhans cells of bone marrow origin, and pressure-sensing Merkel cells of neural crest origin.[2] The epidermis acts as a waterproof barrier and contains melanin, which is responsible to give colour to the skin.

Dermis is a collagen-rich connective tissue made of extra cellular matrix (ECM). It is relatively acellular and besides main collagen, which provides structural support to the skin, contains also elastic fibres, blood vessels, sensory structures, and fibroblasts. Fibroblasts exist in the largest number and intermediate both collagen and elastin secretion. It provides skin elasticity, mechanical flexibility and physical strength, as well as constitutes the matrix, which supports vascular bundle, nerve endings, blood vessels, sebaceous glands and sweat glands.[2][3] Collagen type I and type II form the main framework, which represents 70% of the dry skin weight. The other polymers are elastin and ground substances that support the position of collagen fibres. Glycosaminoglycan, hyaluronic acid, keratin, heparin and chondroitin belong to the ground substances, which bind collagen and elastin together and act as lubricants during stretching and relaxing of collagen fibres.[4]

The basement membrane is a layer between the epidermis and the dermis, with a role of controlling cytokines and growth factors release. It represents also semipermeable, protective barrier, to allow the cells to pass. This highly specialized structure provides dynamic interface and diffusion of bioactive molecules and has gate-keeping functions which control cell traffic.[5]

The hypodermis is a layer which represents a loose connective tissue, placed beneath the dermis. This subcutaneous layer consists of numerous amounts of flat cells and hair roots. It helps to keep body warm, i.e.,intermediates the energy transfers between body and environment.[3][4]

2.2 Wound Healing and Scar Formation

Wound healing is a natural biological process leading to reparation of damaged skin and replacement of lost tissue. It is a very well-coordinated process depending on type of wound and tissue damage. The wounds can involve first, second or third degree burn, physical trauma, inflammation, secondary infections, etc. Defect of epidermis alone is called superficial wound, defect of epidermis and dermis together along with damage of blood vessels, sweat glands, etc. is called a partial thickness wound, while damage of the subcutaneous fat layer is called full thickness wound and it leads to extensive loss of skin, hair follicles and glands.[6] All epidermal and dermal cells, ECM, plasma proteins and growth factors are participating in inflammation, proliferation, and remodelling phase, which are complete processes in wound healing.

The inflammation phase involves hemostasis, which prevents wound bleeding and in case of blood vessel injury, a platelet plug is formed and vasoconstriction is taking palce, in order to limit the amount of blood leaving the damaged vessel. Fibrin clot formation is last step in hemostasis and is produced around the platelet plug. The step is important in fibrin matrix formation and cells infiltration from the wound.[4][7] On the second or the third day of injury the monocytes are produced, followed by differentiation into macrophages with an important role of releasing cytokines, such as interleukin (IL), fibroblast growth factor (FGF) and endothelial growth factor (EGF) and initiate formation of granulation tissue.[8]

Second phase involves cells proliferation and migration and new tissue formation after 3 – 8 days of injury. This process starts with migration of the keratinocytes to the damaging place (dermis) with following formation of blood vessels. Macrophages stimulate the fibroblasts, which then differentiate into myofibroblasts and contract wound. Cellular migration is

supported by the production of hyaluronic acid (HA), which absorbs water and gives tissue the ability to resist deformation.[4][7]

The third phase of wound healing is remodelling, where endothelial cells, macrophages and myofibroblasts undergo cell death and leaving the wound rich in collagen and proteins. The tissue is after all strengthened and maintained by matrix metalloproteinases (MMPs), secreted by fibroblasts, macrophages and endothelial cells.[4] The whole process is also prompted by proteases called tissue-derived inhibitors (TIMPs). The formation of scars is attended by a lower MMP to TIMP expression ratio. In general, the scar formation is marked by increased TIMP-1 and TIMP-3 activity. Platelet-derived growth factor (PDGF) and FGF increase their expression during the formation of fibrotic tissue. However, the FGF contains multiple cytokines, which are more expressed in wound repair than in healthy tissue.[7] Scars are usual consequence of most treating steps and it needs to be considered, how to prevent or minimize its size, along with acceleration of the healing. Third-degree burns are accompanied by epidermal and dermal layers lost. This skin damage leads to thick scars formation and requires skin graftings to achieve wound closure and use of some healing additives for better cosmetic results. Some of pharmateutical products have shown improvement in the scars elimination and are introduced in the ***Table 1.*** All must be used in combination with biomaterials.[9]

Table 1. *Pharmaceutical products in wound healing and scar elimination process.*[9]

Pharmaceutical compound	**Healing effect**	**Test**
Pycnogenol	wound healing accelerator, scar reducer, inhibitory effect on matrix metalloproteinases and supports collagen matrix formation.	in vivo
Relaxin	increasing angiogenesis, scar reducer, supports well-organized collagen framework	in vivo
Astragalus membranaceus (AR)	suppressing inflammation, basal cell proliferation and angiogenesis promoter and linear alignment of the granulation tissue	in vivo
Astragaloside IV	inhibitor of the transforming growth factor beta 1 (TGF-β1) secretion, regulator of the collagen I/III ratio for scar reduction	in vivo/ in vitro
Crocodile oil	decreases expressions of TGF-β1 and Smad3 to accelerate wound healing and reducing scars	in vivo
Curcumin	suppressor of TGF-β1/SMAD pathway, reducer of pro-inflammatory cytokines, interleukins (IL-1β, IL-6, IL-8) connected with hypertrophic scarring elimination	in vivo

c-Ski	modulator of fibroblast functions, reducing scar formation by decreasing collagen production	in vivo
Jun amino-terminal kinases (JNK)	mediator of growth factor in connective tissue provides scar reduction in corneal wound	in vivo
Calpains	role in granulation tissue formation	in vivo/ in vitro
MG53	membrane repair gene inhibits myofibroblast differentiation and promotes scarless wound healing	in vivo/ in vitro

Biomaterials in combination with other natural materials and bioactive molecules have been also used in healing acceleration and scar reduction. ***Table 2.*** is showing some potenial biomaterials and their combination. All of presented materials are possesing antibacterial, antioxidant and anti-inflammatory properties with biocompatibility and biodegradability. Their structure is similar to the structure of ECM and is able to improve cell adhesion, guiding, proliferation and differentiation, as well as formation of granulation tissue.

Table 2*. Combinated biomaterials with natural polymers and bioactive molecules in wound healing and scar elimination process.*[9]

Biomaterials in combination with natural polymer	**Healing effect**	**Test**
Hyaluronic acid	free radical scavenging activity, TGF-β1 reducer and enhancing wound closure rate, improves viscoelastic properties, interactive with proteins, proteoglycans and growth factors, healing without scar formation, the best form is nanofibrous scaffold [2] [10] [11]	in vivo
Microbial cellulose	improver of healing rate, decreasing pain, reducing scar formation, removing the necrotic debris, enhancing cell growth, migration and reepithelialization, proper for second-degree burns	in vivo
Electrospun nanofibrous dressings composited of silk fibroin/gelatin and cellulose acetate	increasing expression of vascular endothelial growth factor (VEGF) and existence of collagen type I	in vivo/ in vitro
Electrospun silk fibroin nanomatrix	healing of the burned wounds and reducing scar, increasing expression of VEGF and existence of collagen type I	in vivo
Alginate (polysacharide) in form of gel and porous foam	decreasing inflammatory reaction while increase the collagen type I, the ratio of collagen I/III, rapid epithelialization, barrier function [12] [13]	in vitro
Dextran in form of hydrogel (treatment of third-degree burn)	accelerates infiltration of blood vessels, and neovessels regresion, high quality of formed epithelium with hair follicles and sebaceous glands,	in vivo

	faster stromal cell migration, high density of organizated collagen and nerve ingrowth after 40 days [14] [15] [16]	
Biomaterials with drugs and bioactive molecules	**Healing effect**	**Test**
Polyvinyl alcohol–sodium alginate gel-matrix with nitrofurazone	keeping wound moist, prevent secondary damage, mild positive effects on inflammatory and reducing wound size	in vivo
Commercial calcium alginate	keeping wound moist and regulates wound exudates	in vivo
Ginsenoside Rg3-loaded electrospun poly(lactic-co-glycolic acid) (PLGA) fibrous membranes	scar prevention, decreasing the expression of vascular endothelial growth factor (VEGF), mRNA, and collagen type I	in vivo
Norfloxacin-loaded collagen/chitosan scaffold	infection controller, inflammation reducer, new cell growth and faster wound closure promoter	in vivo
Dressing of polyester fabric containing elemental silver and zinc	collagen synthesis and reepithelialization rate promoter	in vivo

2.2.1 Role of the Enzymes in Wound Healing

In the inflammatory stage of wound healing process, enzymes called proteases are present in wound exudate. These enzymes are released by macrophages that cleanse the wound. Proteases are present in acute and chronic wound in different proportions. There are differences in the levels of proteases, proinflammatory cytokines, growth factors, and matrix components between acute and chronic wounds. In acute wounds, maintaining the right balance between tissue synthesis and degradation is crucial, because the unbalanced regulation of gene expression and activation and ihibition of enzymes can lead to degradation or deposition of ECM and healing disruption at all. In many chronic wounds these regulations are incorrect and the healing remains usualy in iflammatory phase and leads to healing problems. The persistent inflammation state is characterized by high presence of proteases and neutrophils. If expression of proteases, particularly MMPs is prolonged, ECM, growth factors and their receptors are degraded and remodeled. It is important to make a balance and control their behaviour. Collagenase, which denaturate molecules of the collagen, is in high concentration in chronic wound and its production needs to be inhibited, in order to move from the inflammatory phase to proliferation.[11][17] Proteases MMPs inhibitors are considering to improve the wound healing process in diabetic chronic wounds. It was shown,

that local therapy with doxycycline, an antibiotic from to the tetracycline family, or competitive inhibitor of MMPs can reduce inflammation.[18] A very promising regulation solution of MMPs in the chronic wound are wound dressings, which can control the wound microenvironment by incorporating the healing accelerator such as nano-oligosacharide factors, possesing anti-proteases properties. Such a matrix can be formed from collagen and oxidized regenerated cellulose (ORC). Collagen can act as protese substrate and binds inactivate MMPs, while the role of ORC consists in counteracting the positive charges associated with the metal ions of MMPs. This matrix combination is also benefical because of no affection of growth factor activity.[11]

2.2.2 Conventional Treatments for Wound Healing

There are many types of skin grafting and skin regeneration substances, which represent full epidermis or dermis or both layers. As it is illustrated in **Figure 2**, depending on the depth of the wound, the skin substitutes are devided into superficial, epidermal (involves cultured epidermal cells), dermal (including dermal components) and dermo-epidermal-bilayer structure, which is currently the most accepted structure of wound coverage. The use of an autograft and an allograft belong to this most common approache, but it has some limitations. The autograft represents a full epidermis, thin layer and a portion of the dermis with good adhesion to the wound bed, enables relief from the pain and reduce rejection rates. It is derived from the patient's own tissue, such as inner thighs, buttocks and can be reharvested a few times after healing. The thickness of underlying dermis determines the healing process, more thick dermis means faster healing and better aesthetic and cosmetic results. The lack availibility of donor sites is the main limitation, also long surgical time is required in order to obtain the autograft from donor and can cause nerve injury or damage.[19] The allograft is usefull for deeper dermal wounds and prevents them from dehydration, contamination, immune rejection and transmission of diseases. Allografts are extensively used in burn wound healing and are usualy taken from cadavers or living donors. It is always disadvantage about the human donor tissue, taking concern about bacterial and viral disease transmission or body rejection.[20] It has been reported that Allografts have a lower success rate among younger patients.[19]

Wound dresing **(Figure 2a)**, as a superficial treatment has the capacity to protect the wound and help prevent infection, whereas the others skin replacements as characterized as scaffold and guide cells for skin to regenerate.[21]

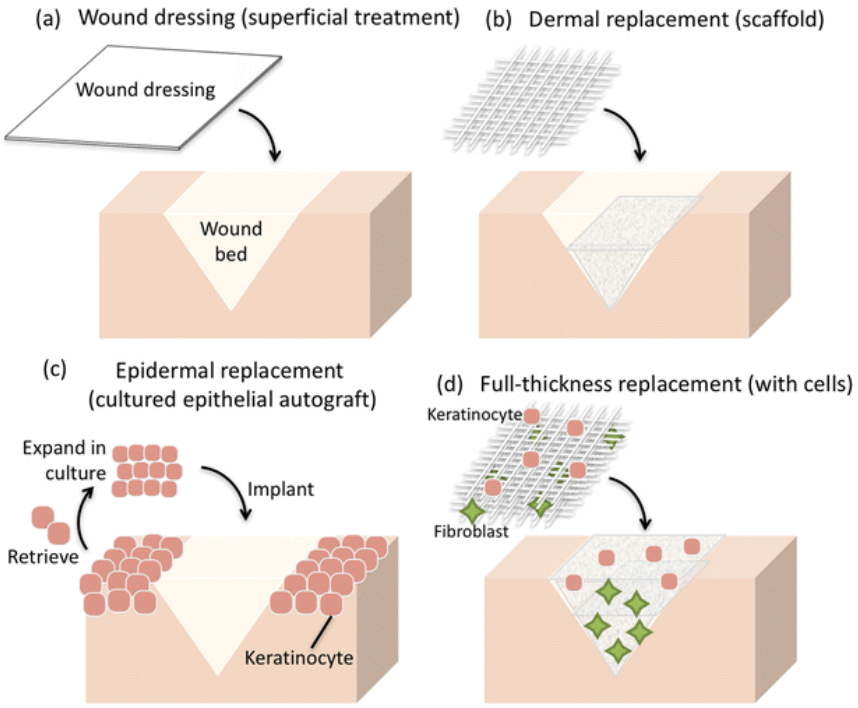

***Figure 2**-Types of engineered skin treatments* [21]

The epidermal skin substitute **(Figure. 2c)** is cellular, in which the patient's own keratinoctyes are retrieved, expanded in culture, and reapplied to the wound site. Cells can be cultured as allogenic or autologous cell suspension. Cellular allogenic skin substitutes are produced using living neonatal foreskin fibroblasts and provide only temporary coverage of the injured skin. In case of the use of cultured autologous keratinocytes, the more warious wounds can be healed with more permanent skin coverage. The use of them is on their own or along with dermal matrix, which represents full-thickness with or without cells seeded, **(Figure 2d)**. Dermal replacements are decellularized human dermis, designed mainly as barriers against fluid loss and against contamination **(Figure 2b)**.[21] There are some examples of typical, comercialy available skin substitues such as Biobrane®, Integra®, Alloderm™, and TransCyte™ all belong to the synthetic skin substatnces. Dermagraft™, Apligraf™, OrCel™ (with allogeneic cells) and Epicel™ (with autologous cells), belong to the biological skin substances.[22]

2.3 Scaffold Properties for Skin Tissue Engineering

An ideal skin scaffold should have the capability to act as a protective barrier between the wound and the environment. The most desire properties are non-toxicity, non-antigenicity, biocompatibility, biodegradability, cost-effectiveness and long shelf life. It should also prevent infection at the wound site, reduce the loss of physiological fluid from the wound and minimize local pain. This structure must be able to create suitable environment for cell guiding, their proliferation, growing, and regeneration, while proving formation of new skin. The epidermis–dermis interaction is possible to create by designing the scaffold, with elasticity, strength, sufficient oxygenation and other nutrients to support growth of epidermis and keratinocytes. Porous scaffolds are used with the aim to mimic the ECM at the wound site through various growth factors. They are usualy made by processes such as freeze-drying, fiber bonding, foaming, salt leaching and 3D printing.[4] As the most attractive matrices is nanofibrous network, perfectly mimic the native ECM fibres. It is form by electrospinning process, which provides a wide range of compositions and morphologies. The scaffold has low stiffness providing a sufficient flexibility for cells. The challenge of naturall scaffolds is scale up production and the cells secreted enzymes, which can degradate biomaterials. Therefore, synthetic biomaterials are being explored, which can be easily reproducible and customizable and have desired porosity, mechanical properties, and do not underlie the degradation.[23]

2.4 Natural Polymers for Skin Tissue Engineering

The most suitable polymers for scaffold formation in tissue engineering are native components of ECM. The very proper collagen can form intrachain and interchain bridges with its molecules, by cross-linking with components of ECM such as chitosan, polycaprolactone (PCL), or poly(lactic-co-glycolic acid) PLGA. These polymer combinations have specific role in guiding cells for its future behaviour and promotes wound healing. Remaining problems, based on combination with collagen and natural polymers, are wound contraction and scars formation.[24]

2.4.1 Collagen

Collagen belongs to the naturally occurring proteins consists of three α-domains (polypeptide chain), twisted around one another in a rope and form triple-helix, held together by hydrogen bonds. Each of these domains contains a characteristic L-handed amino acid sequence of polyproline type II helix. Every third position in the polypeptide chain involves glycine residue and repeating multiple triplet sequences contains of Gly-Y-Z, where Y and Z can be any amino acid, usualy proline and hydroxyproline, see **Figure 3**. The hydroxylation of proline residues in the Y position increases thermal stability of triple helices. Within each amino acid triplet, the hydrogen bonds are formed with four of the six main chain heteroatoms, and their formation require two of the three peptide bonds. Peptide bond is formed when amino group of a glycine residue binds with the carbonyl of an adjacent residue. Collagen is responsible for performing important biological and structural functions and usualy works in cooperation with other important proteins.[25][26]

Until now there are 30 different types of collagen that are found in various types in human body. The most abudant is collagen I contained bones, tendons and organs. Another types are collagen II in cartilage, collagen III in reticular fibres, collagen IV in the cell basement membrane and collagen V presents in hair and nails.[27]

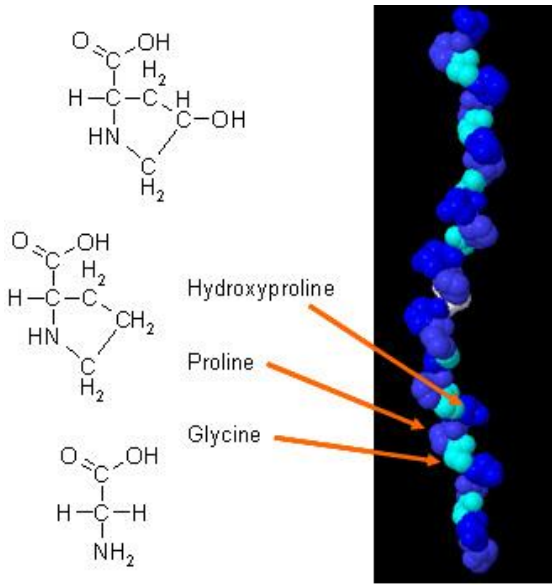

***Figure 3**-Molecular structure of collagen with glycine, proline and hydroxyproline amino acids residues* [28]

2.4.2 Collagen-Based Scaffold

The collagen-based scaffold is clinically used for skin regeneration after burns. It forms a highly organized, three dimensional structure and maintains the biological and structural integrity of ECM. It is biodegradable, non-toxic and biocompatible with specific arginine-glycine-aspartate (RGD) groups, which induces cellular adhesion by binding to integrin receptors. This interaction makes collagen being natural substrate for cell growth, proliferation, differentiation and function regulation. There are many already available gels, sheets, lattices or scaffolds based on collagen, which are used as a temporary skin burns covering and reducing scar formation. There is already engineered acellular and cellular dermis and bilayered skin, involving collagen–based materials.[24]

In vivo are collagen molecules strengthened together by covalent intramolecular and intermolecular interactions and form fibres. The problem of collagen is its fast biodegradation rate and the low mechanical strength. For this reason is collagen cross-linked.[29] There are chemical and physical cross-linking methods, where collagen can form fibres with high tensile strength and stability. The chemical cross-linking of collagen can be provided with formaldehyde, glutaraldehyde, carbodiimides, polyepoxy compounds, acyl azides, or hexamethylene diisocyanate. On the one site, it is enhancing stability, on the other site some of the reagents and compounds can be cytotoxic after degradation. To avoid cytotoxicity, collagen can be stabilized with amino groups of polycationic molecules like chitosan. By that stabilization cross-linking efficiency can be increased and cytotoxicity is minimizing. By changing matrix porosity or density, immunology and mechanical properties of collagen based scaffolds can be modified. In terms of burn healing, dehydrated collagen scaffold is one of the types of temporary skin burns covers, which is produced by freeze drying. Contrary to collagen gels, they are possessing stronger mechanical properties and many this kind of artificial skin were efficiently used in skin recovery.[30]

2.4.3 Chitosan

Chitosan is natural linear polysaccharide, which consists of β-(1 → 4)-linked 2-acetamido-2-deoxy-d-glucopyranose and 2-amino-2-deoxy-d-glucopyranose units. This structure is obtained by alkaline deacetylation of chitin and it is very similar to cellulose. Chitosan is polycationic at pH < 6 and it interacts with negatively charged molecules, such as proteins, anionic polysaccharides (e.g., alginate and carrageenan), fatty acids, bile acids, phospholipids and can also chelate metal ions (iron, copper, cadmium and magnesium).[26]

Biodegradability, non-toxicity, anti-bacterial properties and haemostatic effect make it favorable as wound and burn healing material. The biodegradability depends on human enzyme lysozyme. It was suggested that chitosan accelerates the formation of fibroblasts and increases early phase reactions related to healing.[31][32] The antibacterial property is believing to be due to the attack of negatively charged groups on the bacterial cell wall by the possitively charged chitosan polymer, what leads to the lysis of bacterial cell walls. Chitosan also inhibits the growth of bacterial cells becasue of binding to the bacterial DNA and interferencing with its transcription.[33] Chitosan can exist in various forms as films, hydrogels, fibres, powders and micro-/nanoparticles.[12]

The important fact of chitosan is the ability to form granulation tissue with angiogenesis. It has been shown that chitosan, due to the electrostatic function can incomporate growth factors into fibroblast. The fibroblast has promoted realease of interleukin, which subsequently supporting fibroblasts migration and proliferation. This all processes are improving rate of the wound healing. Collagen/chitosan scaffold is promising material structure in skin tissue engineering, however there is still no clear answer about collagen and chitosan effect on both physical and biological properties of created scaffold.[26] The porous collagen/chitosan scaffold can be fabricated by freeze drying and dehydrothermal cross-linking techniques and various forms can be created (films gels or scaffolds) to heal full-thickness burn wounds.[32]

There are plenty of chitosan-based composite biomaterials with potential applications in wound healing and tissue regeneration, such as films made up of chitosan–cellulose–silver nanoparticle mixtures, chitosan–gelatin scaffold mixtures, chitosan gelatin–antibiotic mixtures,[34] chitosan–alginate polyelectrolyte membranes,[35] tencel–chitosan–pectin composite, chitosan–fibrin nanocomposites, like nanofibrous chitosan–silk fibroin composite, beads of chitosan–fibrin or chitosan–fibrin–sodium alginate.[36]

2.4.4 Gelatin

Gelatin is a biocompatible, biodegradable and fully absorbable biopolymer, derived from the hydrolysis of collagen. It has less antigenicity and immunogenecity than collagen and it has better solubility in aqueous systems, because of far less tertiary structure than collagen. Due to its RGD sequence it enhances cell adhesion, migration, differentiation, proliferation and in the form of electrospun nanofibres has shown potential in wound healing.[37] Scaffold, which already includes cationic chitosan can be blended with free carboxyl groups of gelatin and form a network by hydrogen bonding.[38]

The formation of gelatin-alginate scaffolds or gelatin films has shown potential in burn skin tissue and it has been already applied as cartilage and nerve tissue. Gelatin can be also modified and changed its mechanical and biochemical properties.[2][39] It is also promising drug delivery carrier, becasue of its isoelectric point, which can be tailored by either alkaline or acidic environment and can load charged biomolecules. Carriers for antibacterial agents, anti-inflammatory drugs and many different antineoplastic compounds has been studied.[40]

2.4.5 Oxydized Cellulose

Oxidized cellulose (OC) is another biodegradable polymer, with potential applications in field and wound healing. It possess non-immunogenicity, antibacterial, anti-tumor activity and anti-adhesive effects.[41] Structure of cellulose presents anhydroglucose units linked together by β-D-1,4 glycosidic bonds **(Figure 4)**. Three hydroxyl groups of every anhydroglucose units can undergo oxidation and make the cellulose be bioabsorbable and biocomaptible. The bioabsorbtion is enabled via chemical depolarization and enzymatic hydrolysis mediated by glycosidases, what leads to nontoxic final products of glucuronic acid and glucose. The structure of OC is broken at pH higher than 7, while at pH 7 is relatively stable.

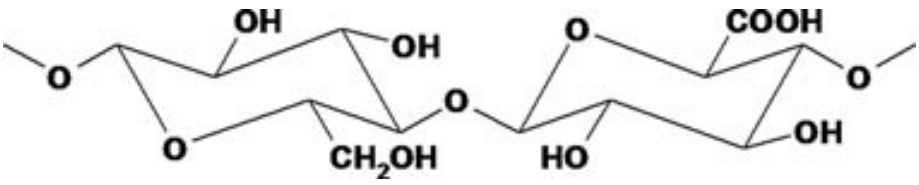

***Figure 4**-Structure of oxidized cellulose*

OC has hemostatic activity, initiating or accelerating blood coagulation. It is also promising as a carrier for controlled drug delivery and its acid character is reduced with arginin or chitosan functionalization.[42] When the healing of chronic wounds is persisting in inflammatory phase, scaffold made of OC and collagen reduces proinflammatory interleukins, reactive oxygen species and binds to the metal ions with increasing concentration of growth factors and proteinase inhibitors.[43] Marked names of OC are known as Oxycel^{TM}, Surgicel^{TM}, Gelitacel^{TM} and Interceed^{TM}.

The combination of gelatin with oxycellulose has been already studied in form of nanofibrous scaffold maded from acetic acid solution by electrospinning method.

Possibility to make nanofibres based on this combination has shown to be suitable material in medical applications, especially for lung disease. The best results were obtained with the use of twice higer amount of gelatin to OC. The OC was used in the form of sodium salt and calcium salt. It was shown that Ca^{2+} attaching exhibits more possitive properties.[44]

2.5 Carboxymethylcellulose CMC

CMC is a natural, biodegradable and biocompatible polysacharide used as a viscosity modifier or thickener to stabilize emulsions in various products (especially dietetic foods and ice cream). Its excelent water retaining capacity makes it attractive candidate for application as wound dresing, for drug delivery and skin engineering.[45] The polar carboxyl or hydroxyl groups make cellulose to be water-soluble and chemically reactive[46] and serve as active sites for preparing CMC gells. It can create more stable three-dimensional network by chemical cross-linking.[47] Its sodium salt, known as sodium carboxymethyl cellulose (NaCMC) is often used form, synthesized by the alkali-catalyzed reaction of cellulose with chloroacetic acid. CH_2COOH groups are substituted on the glucose units of the cellulose chain through an ether linkage. Sodium carboxymethyl cellulose is pale yellow, odorless, nontoxic, water-soluble powder, stable in the pH range 2–10 and insoluble in organic liquids.[48]

CMC has been used in drug delivery system, where the release of apomorphine was successfully incomporated into CMC powder. Resulted mucoadhesive polymers was able to increase its resistent in the nasal cavity and provide sustainable nasal drug delivery.[49] NaCMC has been used in developing a gastroretentive drug delivery system for administering Losartan.[50] Combination of CMC and chitosan has been shown as promising, thermally sensitive, gelling system, formed without any chemical modification or cross-linking and being highly biocompatible with biological compounds. This gel has ability to encapsulate living cells and swtich from liquid to gel in situ after injection in vivo. CMC/Chitosan combination was used for culturing chondrocytes, where the cells proliferated and remained metabolically active in 3D culture for 2 weeks with minimal cytotoxicity.[51] This combination with hydroxyapatite has been made and showed adequate mechanical support, high porosity, biocompatibility and could enhanced the mechanical strength for bone regeneration.[52] An biocompatible, selectively degradable CMC-methacrylate/polyethylene glycol dimethacrylate (PEG-DM) gel was created and modified with the adhesive peptide RGD sequence. The gel was able to support fibroblast adhesion and viability and it was

concluded as suitable applicant in bioengineering, since the cellulase and the fragment of degraded cellulose have advantages as selectively degradable components in an engineered cell scaffold or controlled release device.[53]

2.6 Polycaprolactone PCL

Polycaprolactone (PCL) is a synthetical, biocompatible, linear aliphatic polyester, which is hydrophobic, semicrystalline, relatively slow degrading and with good mechanical properties. It was already applicated as an in vivo tissue implant for various medical application and has shown a great potential in wound healing, bone tissue enginnering, cardiovascular tissue engineering and nerve regeneration. It is obtained by the polymerization to open-loop of e-caprolactone. However, PCL-based materials have not been completely introduced to the clinic applications. One potential use, is the incomporation of the nanostructured material into the PCL and modulate mechanical and degradation properties. PCL can not be degradated by enzymes within human or animal body, only by microorganisms (bacteria and fungi) and degradation rate is depending on the molecular weight, degree of crystallinity and degradation conditions.[54][55]

2.7 Hyperstable Fibroblast Growth Factor 2

Fibroblast growth factor (FGF) that signal through FGF receptor can regulate a wide spectrum of biological functions, including cellular proliferation, migration, viability and differentiation. Specificaly, human FGF2 has shown potential effects on the repair and regeneration of tissues in the ulcer, wound [56] and epithelium healing. [57]

However, the growth factor faces limitation due it to its low thermal stability *in vivo* and *in vitro.* Related with this problem, a generalizable computer-assisted protein engineering strategy was used to create a modified FGF2 with nine mutations. Protein engineering is a powerful method of changing a protein sequence to achieve a desired result, such as a change in the substrate specificity or increased stability. This approach for protein stabilization was made and the new the most thermostable nine-point mutant FGF2-G3 was able to exhibit a much greater stability, which was improved from 10 hours to more than 20 days. The FGF2-G3 showed a 19°C increase in melting temperature and greater than 48-fold improved half-life at 37°C. In terms of biological activity, it supported the undifferentiated growth of human embryonic stem cells and stimulated hair growth in mouse model.[58]

2.8 Dopamine

An attractive molecule, which can create natural adhesion between materials' surfaces or even gluing small molecules. Marine mussel protein has an ability of attaching to many surfaces in aqueous environments and it has similar nucleic acid sequences as dopamine. Due to this similarity, dopamine can be used as some medical glue and improve adhesion of metallic, inorganic, and organic materials. Dopamine is synthesized in the body from within cells and can be created by any one of three amino acids, which are provided from natural sources such as food.[59] The most attractive property of dopamin is its auto-polymerization. It was reported that the oxidative polymerization is taking place in Tris buffer of pH 8.5, where dopamine results in polydopamine (PDA) films.[60][61] **Figure 5** is showing possible mechanism of PDA formation. Conditions of longer exposure time, higher concentration and higer temperature, all those factors contribute to the thicker PDA film fomation.[62]

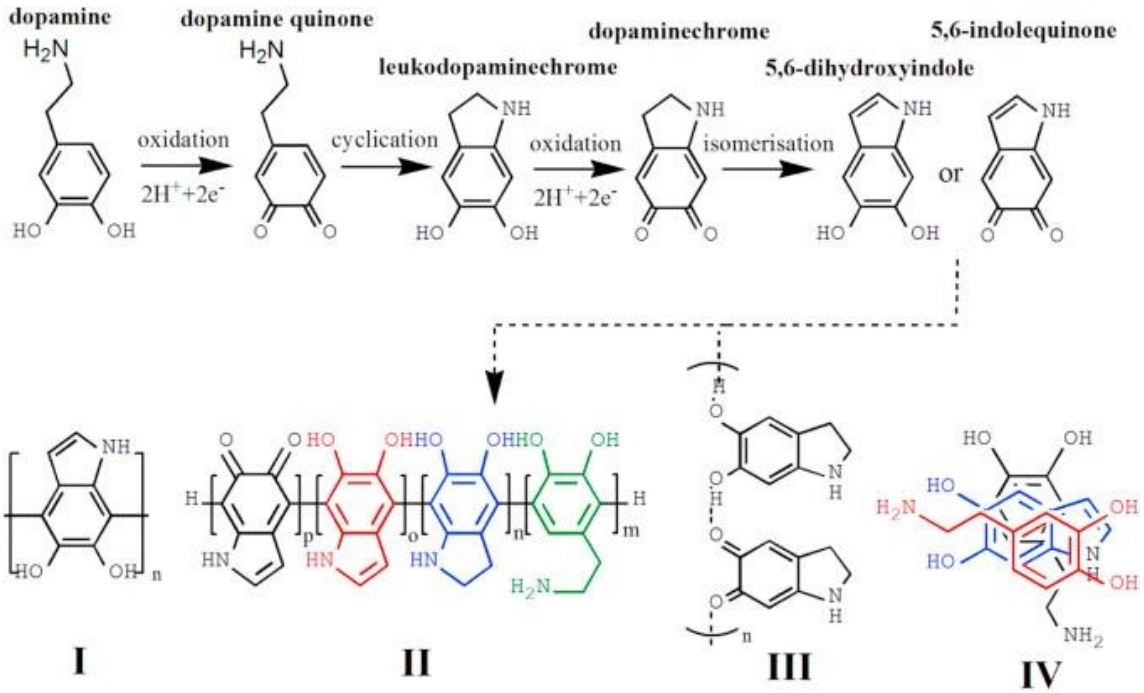

***Figure 5**-Possible PDA film formations included: 1. the oxidation of dopamine to dopamine-quinone, 2. intramolecular cyclization, 3. oxidation to dopaminechrome, 4. formation of 5,6-dihydroxyindole (DHI), 5. the oxidation to 5,6-indolequinone (IDQ), 6. the mixture of the dopamine, quinone and indole units may co-exist in solution after the first steps since the oxidation and cyclization may not be complete. Subsequently, the mixture of these units undergoes various pathways to form the PDA structures (I-IV) representing a PDA covalent polymer or a supramolecular aggregate.*[63]

Depending on the type of surface, PDA can bind via covalent or non-covalent bonds. Covalently is binded with amine groups or thiol groups via Michael addition or Schiff base reactions. Surfaces without these groups are binded via non-covalent H-bond, π-π interaction. Polydopamine can be also linked with metal oxides (such as Fe_2O_3, Fe_4O_3, ZrO_2) through chelating bonding interaction.[59] It was shown that PDA coated PCL nanofibres significantly improved endothelial cells' attachment on the nanofibres and polydopamine coated PLLA nanofibres induced osteogenic differentiation of hMSCs (human mesenchymal stem cells).[64] PDA can also conjugate biomolecules onto the polymer scaffolds. Lee et al. successfully conjugated trypsin onto the polydopamine-modified cellulose paper, while trypsin stayed with its activity.[65] Biomolecule can be easily conjugated through a reaction with the polydopamine surface in aqueous solution, while the process is keeping both the activity of bioactive molecule and structure of material.[61] Basic fibroblast growth factor (bFGF) was grafted onto the surface of PLGA electrospun fibres by immersing the fibres in solutions of dopamine and bFGF. PDA film was created and fibrous PDA coated scaffold was able to accelerate wound healing.[66]

2.9 Methods of Scaffold Preparation

The bioactive scaffolds should possess an excelent 3D architecture with porous structure, which can be done by various preparation techniques optimizing size and density of pores, structural strength, specific 3D shape, surface. Traditional tissue engineering methods are "top-down" and "bottom-up" approaches as it is depicted on **Figure 6**. The top-down approach involves seeding cells onto a biocompatible and biodegradable scaffold, in which the cells are expected to form their own full functional tissue.[67] Only thin or less blood vessels tissues (skin, bladder, cartilage) can be fabricated, since slow vascularization, low cell density, non-uniform cell distribution and worsening diffusion are remaining as limitations of those approach. Larger functional tissues and organs with higher metabolic requirements (liver, kidney) are modulated by bottom-up approach, where microscale tissue building blocks are fabricated via self-assembled cell aggregation, cell-laden modules, cell-encapsulating microscale hydrogels (microgels), cell sheets generation or direct cells printing and all can be assembled into larger tissue constructs.[68][69] Those complex structures are providing more guidance on the cellular level to direct tissue morphogenesis.[70] The bottom-up is increasingly becoming a promising tool to study and recreate vascular physiology in tissue engineering applications.[71]

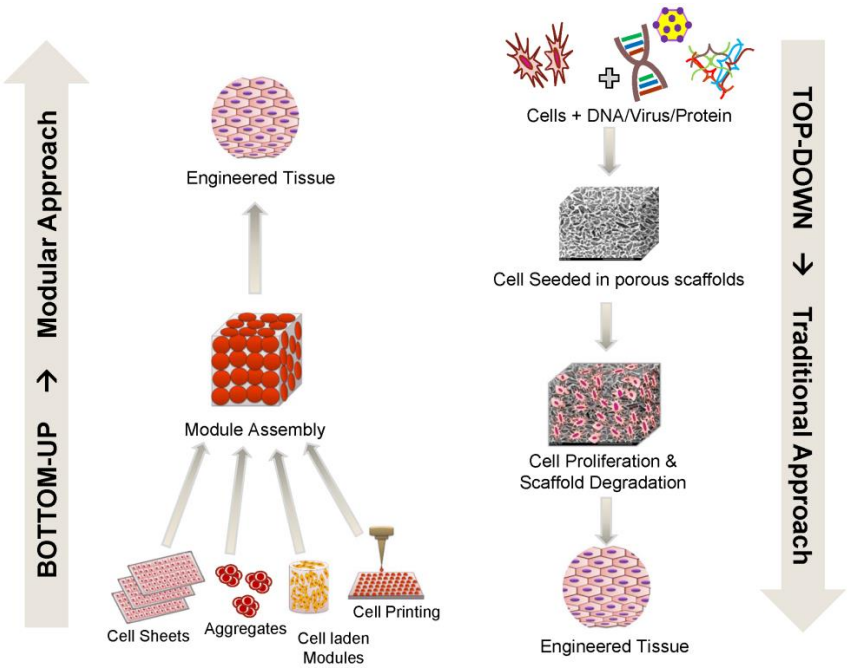

***Figure 6**-Bottom-up vs. top-down approaches in tissue engineering* [67]

From the top-down fabrication methods phase-separation, self-assembly, freeze-drying, and electrospinning will be discussed. Phase separation is induced by different thermal conditions, which means that solution of homogeneous polymer is under certain temperature thermodynamically unstable, resulting in separation of polymer solution into two phases. Phase of low polymer concentration (lean phase) and phase of high polymer concentration (rich phase).[72][73] Subsequently, the rich phase forms a matrix by process of solidifying, while the lean phase turns into pores as a result of solvent removal.[74] Phase separation can be also induced by using a nonsolvent, which results in heterogeneous pore structure.[68] Liquid-liquid phase separation was used to fabricate PLLA scaffold with a continuous three-dimensional nanofibrous network. Diameters of nanofibres ranging from 50 nm to 500 nm and a porosity was 98%.[75] Solid–liquid phase separation was used to fabricate an uniform nano-fibrous chitosan acetate with diameter of 50–500nm. Phase separation temperature and chitosan concentration can regulate the porosity and fiber size, what can be potential for tissue engineering.[76]

Technique of self-assembling is an autonomous process, characterized by autonomous components organization into patterns or structures. The occured interactions are noncovalent or weak covalent bonds (electrostatic, van der Waals, hydrophobic, ionic and hydrogen).[74] For example phospholipids, which are important amphiphilic components of the cell

membrane can self-assemble into higher order structures such as vesicles, tubules, and micelles in aqueous solution. Proteins are able to assemble into nanofibres and create three-dimensional network, which can mimic in vivo microenvironment of cells, cover long distances over their surfaces and connect neighbor cells with mechanical support.[77] Various types of nanofibres and nanoscales can be fabricated, depending on the pH and ionic concentration of the aqueous solution. Poor mechanical properties of peptides and hight cost are limitations, which make formation of stable geometrical structure challenging.[78]

From the bottom-up approach, where the cells proliferate in a cell culture, a large cell sheet modules are created and by their stacking and remodeling, the tissue with robust mechanical properties and cell-cell contacts can be created.[77] With this technique the autologous tissue-engineered blood vessels were created with physiologic mechanical properties.[79] To this date, the cell sheets have been applied to various types of organ injuries including cornea,[80] heart,[81] it has been also showed in repare of injured heart tissue by cell transplantation,[82] in injuries of esophagus,[83] and cartilage.[84]

2.8.1 Lyofilization

Lyofilization or freeze drying is a process, in which water is frozen, followed by its removal from sample. The principle is based on the physical fact, when after material freezing and pressure reducing, the temperature of the process raises to bring sublimation of frozen water. The bonds between the material and water molecules will broke and the porous structure will form. The relevant temperature of conversion to the water vapor is when the ambient partial water vapor pressure is lower than the partial pressure of the ice.[85] Before the finall foam structure is sealed, the vacuum is broked with an inert gas to dry 1-5% residual moisture. The freezing phase is considered as critical step of the lyofilization. The easiest to freeze dry are large ice crystals, which are producing by slow processes of freezing and annealing processes. In biological use the accrued large crystals can destroy cell walls, hence the freeze drying is provided fast. On the other site, fast freezing creates small crystals, which are hard to dry. Annealing can help form bigger crystals.[86] Collagen foams are generally manufactured by the lyophilization of its aqueous suspensions. The suspensions are from the minced insoluble collagen or from extracted soluble one, derived from bovine, porcine skin or equine tendon. The porosity of freeze-dried scaffold is important property and it depends on the dry matter content of the aqueous suspension to be dried as well as the freezing rate.[87]

Collagen and chitosan has been already prepared by freeze drying process and cross-linked by dehydrothermal treatment. The samples were frozen at -40°C for 24h prior to lyophilization under vacuum pressure and final biocompatible scaffolds with cell proliferation ability and mechanical strength was characterized.[88] Other highly porous 3D scaffold from PCL blended with chitosan was fabricated for the bone tissue engineering and possessed homogeneous porous structures and hydrophilic properties.[89] The freeze-drying is chracterized as an advanced technology to produce highly porous 3D scaffolds with complex pore morphology, using a wide range of materials including natural polymer, synthetic polymer, and ceramics.[90]

2.8.2 Electrospinning

The electrospinning is process of producing continuous ultrafine fibres from viscous polymer solution by applying high electrostatic forces. The process is simple and inexpensive and in case of needle electrospinning, the components involves a spinneret (usually a metal hollow needle), a high voltage source, and a collector (grounded or negatively based). Another component is a syringe pump, which drives polymer solution out of the spinneret. This pump injects the solution at the chosen flow rate and after that, the solution continues through the tube until it reaches a nozzle. Solution becomes charged on the way to the nuzzle, due to the high voltage. Equal charges at the solution surface repel each other and creating repulsive interactions. When the electrostatic force from the repulsion in the fluid overcomes the surface tension, fluid droplet deforms to a Taylor cone. When the voltage is sufficiently high a jet erupts and reaches the collector, where continuous fibres are produced. Combination of electrostatic repulsion of the charged solution and evaporation of the solvent causes continuous stretching of the jet, resulting in ultrafine fibres. The diameter of electrospun fibres are usually in the range between tens of nm and 1 mm. Final nanofibres are then collected and deposited onto the collector.

The fibres can be randomly orientated or aligned. Depends on type of collector (static or rotating) as a mat is differently orientated.[91] The whole process can be affected by type of plymer, its molecular weight, concentration, viscosity, surface tension and conductivity. Important consideration is voltage, flow rate, distance between needle tip and collector, collector’s rotating speed and ambient conditions (temperature, humidity). If the distance between the needle and collector is longer, more time is required to stretch the jet and the

created fibres will be thinner.[92] Parameters settings are the most considering determinants in terms of fiber size, properties, and characteristics.

A novel industrial needle-free multijet of electrospinning device was utilized with potential use for mass production of nanofibrous ECM (NF-ECM). The production was based on biopolymers as collagen, gelatin, PCL and PLGA. The large-scale applications for large skin regeneration area in patients with burns could be provided with this biocompatible and stem cells integrated NF-ECM.[93] Nanofibres produced by needleless technology has shown potential of gelatin and PCL electrospun nanofibres. Human dermal fibroblasts, keratinocytes and mesenchymal stem cells seeded on the nanofibres promoted cell adhesion and proliferation. Technology was related with wound healing acceleration and created nanofibres may be suitable as for cell transfer and skin regeneration.[94]

Main Goal of the Work

The main aim of this work is to develop nanostructured bilayer collagen based scaffold for full skin thickness replacement. The proposed fabrication methods should meet the criteria of both the scaffold stiffness and the scaffold stretch, where the main influence has the presence of nanofibres, which differ in cross-linked and non cross-linked with porous layer. Finally, in-vitro studies, together with structural properties should meet all requirements.

Experimental part

3 Materials and methods

3.1 Chemicals

- Bovine Collagen type I., 8 % (Výzkumný ústav pletařský a.s., Czech Republic).
- Chitosan from shrimp shells, 70 % DDA, low viscosity (Sigma-Aldrich, Germany).
- Carboxymethylcellulose sodium salt (Holzbecher, Czech Republic)
- Oxidized cellulose calcium salt (Synthesia, Czech Republic)
- *N*-(3-Dimethylaminopropyl)-*N′*-ethylcarbodiimide hydrochloride (EDC), *N*-hydroxysuccinimide (NHS), 98% (Sigma-Aldrich, Germany)
- Ethanol 96% p.a. (PENTA s.r.o., the Czech Republic)
- Sodium phosphate dibasic for molecular biology (≥98,5 %) (Sigma-Aldrich, Germany)
- Dopamin hydrochloride, Tris (hydroxymethyl) aminomethane hydrochloride (Tris HCl-buffer) (Sigma Aldrich)
- Ultrapure water (type II according to ISO 3696) prepared on Elix 5UV Water Purification System (Merck, Czech Republic)
- Sodium Chloride (NaCl), Potassium Chloride (KCl), Disodium hydrogen phosphatedodecahydrate ($Na_2HPO_4 \cdot 12H_2O$), Potassium dihydrogen phosphate (KH_2PO_4) (Lach-ner, Czech Republic)Collagenase from *Clostridium* histolyticum, (≥ 125 CDU/mg), lyophilised powder (Sigma-Aldrich, Germany)
- Lysozyme human, recombinand, expressed in rice (120 530 units/mg protein) lyophilised powder (Sigma-Aldrich, Germany)
- FGF2-STAB® (stable Fibroblast growth factor 2), (Enantis Brno, Czech Republic)
- Mouse monoclonal IgG_1-FGF-2 Antibody (G-2): sc-365106 (Santa Cruz Biotechnology)
- Anti-Mouse IgG-Peroxidase antibody produced in goat (Sigma-Aldrich, Germany)
- Bovine Serum Albumin (BSA), (Sigma-Aldrich, Germany)

3.2 Equipments

- Analytical balances – DENVER INSTRUMENT
- SI-234A, Disintegrator – IKA Ultra Turrax ® T18 basic
- Freeze-dryer – Epsilon 2-10D LSCplus, (Martin Christ, Germany)
- Scanning electron microscope – Mira3 XMU, (Tescan, Czech Republic))
- Nanospider NS LAB 500 (Elmarco, Czech Republic), placed at the Department of Physical Electronics of Masaryk University in Brno, Czech Republic
- Rheometer, Instrument Type: RSAG2 (TA Instruments)

3.3 Preparation of Samples

Samples were prepared in two series differ in steps operations with following evaluation of structural and biomechanical properties and *in-vitro* behavior.

3.3.1 Preparation of Collagen Scaffold

Bovine collagen in concentration of 0.5 % was prepared according to our previous work.[95] Briefly the collagen was cut in small pieces and seelled-up for 10 min in destilled water. With a following step of disintegration, collagen was homogenized and fullfiled into prepared plates in volume of 80 ml. Freeze-dried process was set up for two days. After completed freeze-drying process, the samples where cross-linked with EDC/NHS ethanol solution. For 500 ml of EDC/NHS cross-linking agent in concentration of 0.025 M/0.01 M was used. The agent was washed out from the samples after 2 hours of cross-linking. Washing out was carried out two times with 0.1 M Na_2HPO_4 and three times with destilled water.

3.3.2 Preparation of Collagen/Chitosan Scaffold

Adequate ammount of chitosan from shrimp shells was weighted and dissolved in 0.5 % collagen solution. Disintegration step was repeated and new clean plates were fullfiled with a new mixture of 0.5 % collagen and 0.5 % chitosan. The samples were then freeze-dried for two days and cross-linked with EDC/NHS ethanol solution.

3.3.3 Preparation of Collagen/CaOC and Collagen/CMC Scaffold

The same preparation process, as for the step before was used to make 0.5 % CaOC and 0.5 % CMC in 0.5 % collagen.

3.3.4 Preparation of PDA–Modified Collagen Scaffolds

Selected samples were before freeze drying, directly immersed in solution of dopamine hydrochloride in concentration of 2 mg/ml in 0.01M Tris HCl. The samples were keept in dopamine for 24 hours. Tris-buffer was used as the initiator of polymerization, resulting in blacked coloured polydomapine (PDA). Polymerization of dopamine hydrochloride was taking place at room temperature, under areobic conditions. After immersion, all the samples coated with PDA where washed out 3 – 4 times in destilled water, until all unbinded dopamine was gone. Subsequently, the samples where freeze-dried for two days.

3.3.5 FGF Grafting onto the PDA–modified Collagen Scaffold

Fibroblast growth factor (FGF) solution (0.1 μg/ml FGF2) was added into collagen PDA-coated scaffolds, which were prepared in 48 wells plates. The FGF was also added into scaffolds without PDA. All the samples immersed in FGF solution were keeped in fridge for one day and subsequently freeze dried. Samples in the 48 wells plates were evaluated in terms of FGF release, cell proliferation and cytotoxicity.

3.3.6 Preparation of Electrospun Gelatin/PCL/CaOC Nanofibres

All the scaffolds from the preparation steps were covered with the layer of nanofibres, prepared as followed: the polymer solution of gelatin/PCL/CaOC 70/30/10 (6.3wt.% Gelatin, 2.7wt.% PCL and 0.5 wt.% CaOC) was prepared in concentrated glacial acetic acid and stirred overnight. Process of electrospinning was carried out using laboratory machine Nanospider NS LAB 500 at the Department of Physical Electronics of Masaryk University in Brno. Setting parameters were following: flow rate of 25 $mm.min^{-1}$, applied spinning voltage of 60 kV, distance between spinning and collecting electrode was 15 cm and spinning electrode was rotating at a speed of 5 *rpm*. Ambient conditions were 23 °C, 980 kPa and 40 % of humidity. Prepared scaffolds were next tested for their biomechanical properties in order to find the most suitable one to improve wound healing.

3.4 Characterization of Samples

3.4.1 Structure and Morfology of Prepared Scaffolds

Scanning electron microscop (SEM), Tescan MIRA3 SEM was using a beam of high-energy electrons and focused them over a surface on a place of interest. The electrons of the beam subsequently interacted with the sample and produced signals, which reproduced

information about the surface structure.[96] Samples were located in the chamber area, working at low vacuum conditions, together with the column. Scan coils was controlling the position of the electron beam. Images were acquired in a secondary electron emission mode, scan mode was DEPTH, beam density was 10 and a 10 kV accelerated voltage. Work distance was set on 15 mm.

The Sample Preparation for SEM Measurement

Sample stubs were cleaned and used as a sample support. The manipulation was provided by using clean forceps and gloves. Small representative sample size was used for measurement around 5 x 5 mm and glued to the surface of the stub. Conductive, double coated carbon tape was used as an adhesive material, which glued sample to the stub. The stubs with the samples where coated with a 20 nm thick layer of Au/Pd metals and used for measuring. Conductive metals coating was provided with Sputter coater (Leica ACE 600), high vacuum film deposition system.

3.4.2 Biomechanical Testing of Prepared Scaffolds

A measurement that yields elastic modulus of a specimen in a uniaxial strain test, in which the sample is grasped at two ends and pulled, while axial strain and stress are simultaneously measured was used to evaluate prepared scaffolds. Prepared samples were cut into strips of 40 mm length and 10 mm width. Thickness various on type of the sample (0.5 – 3 mm). Samples was mounted into the grip, in a central position. Distance between two ends of the grip was always set up on 10 mm, which represent the final length of the samples. Tensile properties of prepared scaffolds were tested with rheometer RSAG2. First biomechanical testing was carried out at room temperature 23 ℃, while the second testing involved constant hydrating conditions, where samples were immersed in ultra pure water at 36 ℃ in a built chamber, surrounding the grips. Before every measurement, 10 min of swelling was provided for every sample. The relation between stress and strain was depicted, together with appertaining elastic modulus *E.*

3.4.3 *In-vitro* testing of prepared scaffolds

3.4.3.1. Swelling test

A swelling test for each sample was performed by cutting prepared scaffolds into small pieces and putting them into aqueous solutions at ambient conditions. Every piece of scaffold was before immersion weighted at its dry state and also the weight after removing surface

water by filtrate paper was noted in following intervals: 1, 2, 5, 10, 15, 20, 30, 45, 60, 90, 120, 150 and 180 min. The swelling ratio was calculated in order to define the exact amount of swelling caused by water absorption and the swelling curve was obtained. The swelling ratio was calculated as follows:

$$Swelling\ \ Ratio = \frac{W_s}{W_i}$$

where W_s is the weight of the scaffold in swollen state and W_i is the initial weight of dry scafffold sample. The ratio of weight increase to the initial weight was characterized as water content:

$$Water Content = \frac{W_s - W_i}{W_i} \cdot 100\,[\%]$$

3.4.3.2. Degradation of collagen scaffolds by *Clostridium* collagenase

Clostridium collagenases has been already used in many illustrated studies of third-degree burns treatments and have been shown to provide effective debridement in treating various wounds.[97][98] Thus, this enzyme was used to investigate *in-vitro* degradation study of chemically cross-linked collagen scaffolds. Degradation was carried out in phosphate buffered saline (PBS) at physiological pH 7.4 at 37°C with collagenase from *Clostridium* histolyticum (≥ 125 CDU/mg). Buffer was prepared as follows: 8 g NaCL, 0.2 g KCl, 3.63 g Na_2HPO_4 $12H_2O$ and 0.24 g KH_2PO_4 was diluted in 1 L volumetric flask and used for samples swelling. After one hour of swelling, they were removed from the buffer solution, subsequently weighted and put into the solution of collagenase. After every 2, 4, 8, 24, 48, 72, 96, 120 and 144 hours, excessive surface phosphate buffer saline was blotted out with absorbent paper, following the scaffolds weightning and the percentage of weight loss was calculated using the following equation:

$$Weight\ Loss = 100 - \left(\frac{W_i \cdot 100}{W_s} \right) [\%]$$

where W_s represents the weight of the scaffold after being incubated for one hour without enzymes and W_i represents the weight of digested scaffold.

3.4.3.3. Degradation of collagen/chitosan scaffolds by lysozyme

This study was carried out to test another enzymatic degradation by exposing collagen/chitosan scaffold to human lysozyme. The same degradation process together with the same time intervals were carried out in PBS at physiological pH (7.4) with recombinant human lysozyme, expressed in rice (120530 units/mg). The extent of degradation was expressed as a percentage of weight loss of the dried scaffold after lysozyme digestion.

3.4.3.4. FGF release experiment

The experiment was performed by principe of Enzyme-Linked ImmunoSorbent Assay (ELISA). Before ELISA detection, release of FGF from the collagen scaffold and PDA-coated collagen scaffolds was provided in 20 nM phosphat buffer of 750 nM NaCl (pH 7.5) after 1, 3 and 5 hours. At the beginning, the buffer was added in 1 ml and after each interval, ¼ of the buffer was taken and replaced with a new fresh buffer. For enzyme-linked immunosorbent assay, a 96 wells plate designed for the quantitation and detection of FGF2 was used. Stored buffer solutions with FGF were diluted 3 times (10x, 50x and 100x), pipetting into the wells plate and incubated during the night at 4 °C. On the other day, plate was washed 3 times with phosphat buffer Tween20 (PBST) and then blocking buffer Bovine Serum Albumin (BSA) in PBST was added to the wells plate and incubated for one hour to remove nonspecific binding. The wells plate was then washed again 3 times with PBST.

The principle of the test rests in a target-specific antibody. In this case FGF2 – antibody is a mouse monoclonal IgG_1, which was added into the wells incubated for one hour and washed with PBST. The addition of the second antibody Anti-Mouse IgG with conjugated enzyme Horseradish peroxidase (HRP) was next added and bind to the primary antibody. After 45 min of incubation, unbound antibody was washed with PBST and substrate solution of tetramethyl benzidin (TMB) was added. Substrate reacted with the enzyme-antibody-target complex for 30 min with following blue coloration. The end of coloured reaction was caused by adding 1 M H_2SO_4 and absorbance intensity of yellow accrued solution was proportional to the concentration of FGF.

3.4.3.5. Cytotoxicity Assesment of scaffolds

In-vitro cytotoxicity test of scaffolds was performed by Eva Filová and Veronika Blahnová in Institute of Experimental Medicine, Academy of Science of the Czech Republic,Prague. The mouse fibroblast cell line 3T3 were cultured in cultivated medium involves DMEM, 10% FBS and 1% penicilin/streptomycin. 7000 cells/scaffold where seeded for a period of 14 days. Metabolic activity was determined by MTS metabolic assay, where MTS tetrazolium compound is added directly into the cell culture media. Viable cells reduce MTS reagent and generate a colored formazan dye that is soluble in cell culture media. This conversion is thought to be carried out by NAD(P)H-dependent dehydrogenase enzymes in metabolically active cells. The formazan dye is quantified by measuring the absorbance at 490-500 nm.[99]

PicoGreen assay determined cell proliferation, as it quantified the amount of double-stranded DNA. PicoGreen is a cyanine dye, binding to the dsDNA.[100] The viability of the cells was evaluated by live-dead staining and DiOC/propidium iodide was used to reveal the cell nucleus and cell membranes. Statistical, significant differences were carried out with ANOVA Test.

4 Results and Discussion

4.1. Characterization of prepared scaffolds

This chapter will consider and discuss the importance of the obtained results with potential application for the future *in-vivo* study. As it was mentioned, all types of scaffolds were prepared by two different mechanisms. Individual steps of the both processes differ in order. In the first case, electrospining is carried out in the very end of the process, what means that nanofibres are not cross-linked (**Figure 7**). The second process involves electrospinning before cross-linking, which means that nanofibres are now cross-linked with the porous collagen foam (**Figure 8**). An another difference is between PDA-coatings, whereas in first mechanism only the porous layer is coated, in the second both layers were immersed in dopamine solution.

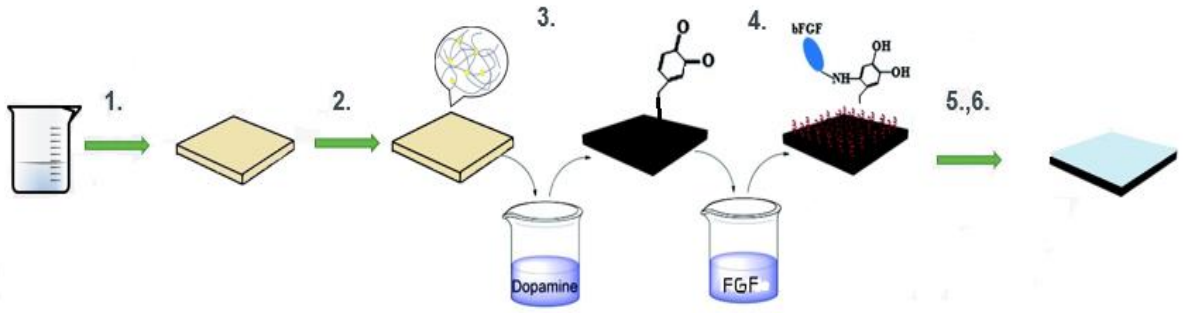

Figure 7*-First mechanism of scaffold preparation, proposing the following steps* ***1.*** *Lyofilization* ***2.*** *Cross-linking* ***3.*** *PDA coating* ***4.*** *FGF grafting* ***5.*** *Lyofilization* ***6.*** *Electrospinning process*

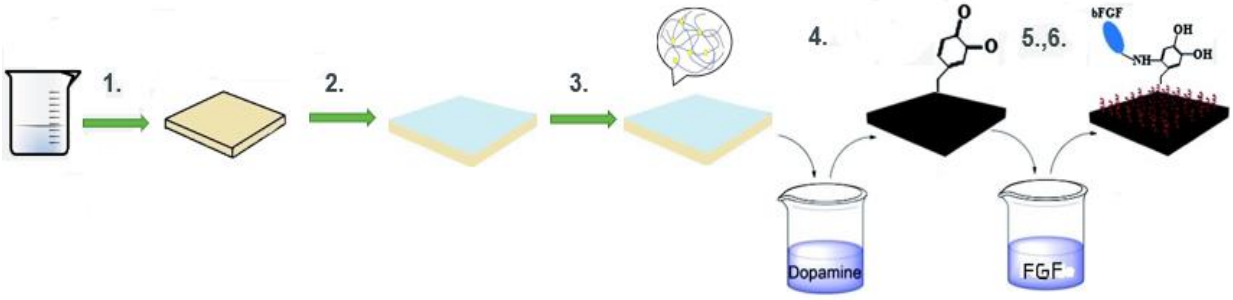

Figure 8*-Second mechanism of scaffold preparation, proposing the following steps:* ***1.*** *Lyofilization* ***2.*** *Electrospinning process* ***3.*** *Cross-linking* ***4.*** *PDA coating* ***5.*** *FGF grafting* ***6.*** *Lyofilization*

4.1.1. PDA-linker and glue material

Polydopamine (PDA) was prepared as it was described above (section 3.3.4) in a simple one-step process, but strongly depending on factors as reaction temperature, initial dopamine concentration, time of coating and pH solution. It was already studied that a dopamine concentration of 2 mg/ml in Tris buffer of pH 8.5 at ambient temperature can create adhesive PDA-linker.[63] The process of coating resulted in a black coloured scaffold apppearence, due to the oxidative polymerization of dopamine. It might be taken into the consideration – that dopamine solution might degradate chitosan, due to the alkaline environmnet of Tris-

HCl. Chitosan is soluble in aqueous solutions of organic or mineral acids under specific conditions, which have a lower pH than chitosan pK_a (around 6.3)). At low pH, the free amino groups are protonated causing electrostatic repulsion between the polymer's chains and thus enabling polymer solvation.[101] In this case, chitosan was at higher solution pH and no degradation or sample disruption occured. However, when dopamine was coated on dry collagen/chitosan surface, it led to the sample disruption. **Figure 9** non cross-linked nanofibres based on the PDA modified surface are showing poor adhesivity to the foam basics. The nanofibres were easily removed even by slight handling and were also broken in many areas of the surface. A good adhesion was attributed only to the collagen/chitosan. The good adhesion could be due to the attended PDA-linker, successfully binded to the hydrophilic collagen/chitosan surface but less attached to the hydrophobic nanofibres. Seeing that PDA can bind even very superhydrophobic surfaces[102], this case should be more dealing with electrospinning process.

Conditions need to be accurate in order to enhance addhesivity. One option could be non thermal plasma-electrospinning, where higher wettability after plasma application would improve adhesive property of nanofibres and surface, strongly supported by PDA modification. The plasma treatment can remove hydrogen atoms from PLC polymer chains and leaving free radicals. Oxygen or moisture, after nanofibres air exposure, can react with the free radicals resulting in the formation of oxygen containing groups and significantly increase the hydrophilicity of the PCL nanofibers.[103][104]

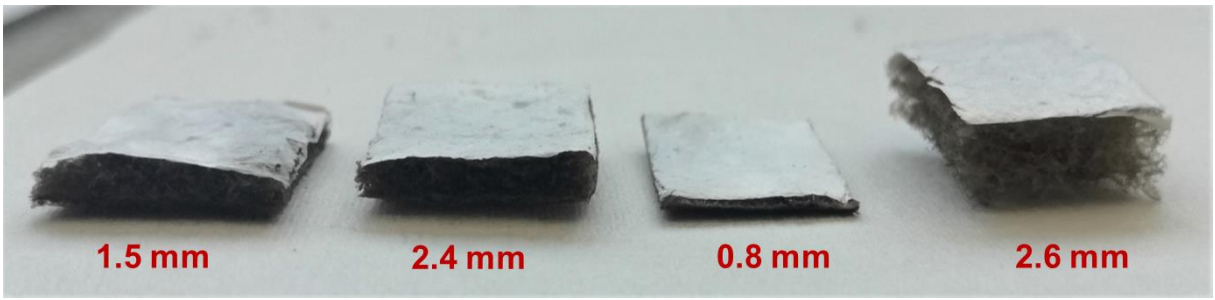

***Figure 9**-Nanofibres based on PDA coated collagen, collagen/chitosan, collagen/CaOC and collagen/CMC scaffold (from left to right)*

Small adhesivity of nanofibres was also observed with not PDA-coated samples (**Figure 10**) mainly due to the non cross-linking with porous layer. Again, weak adhesion was strongly depending on the condition of electrospinning process. The effect of humidity was also critical for fiber formation. The low humidity (40 % in this case) increased the velocity of solvent evaporation and dried the solvent, thus collected nanofibres had insufficient wettability to be strongly attached to the porous surface. The need of the humidity regulation is very important, since in contrast to this, the excess of humidity leads to a thick fiber diameter, where charges on the jet are neutralized and make stretching forces to be small. The nanofibres can not be then produced effectively.

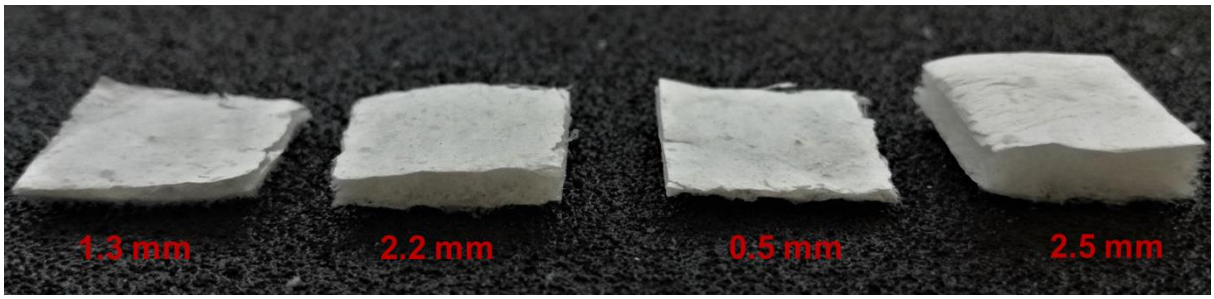

***Figure 10**-Nanofibres based on collagen, collagen/chitosan, collagen/CaOC and collagen/CMC scaffold (from left to right)*

Excess of humidity is also affecting surface morfology, which is then rich in small, dense cavities, what was slightly occuring in chitosan scaffold. It was studied that for gelatin successfull fiber formation the humidity is over 80 %.[105] The first fabrication mechanism with PDA-linker is having a good potential, but needs further development.

The obtained results pointed at the better use of the second proposed mechanism, in which nanofibres are cross-linked (**Figure 11**) and PDA-coated (**Figure 12**). The adhesion of nanofibres is enhanced in both cases, while more supported by presence of PDA. Cross-linking is favourable for many properties, from which the one is to establish biomechanical properties.

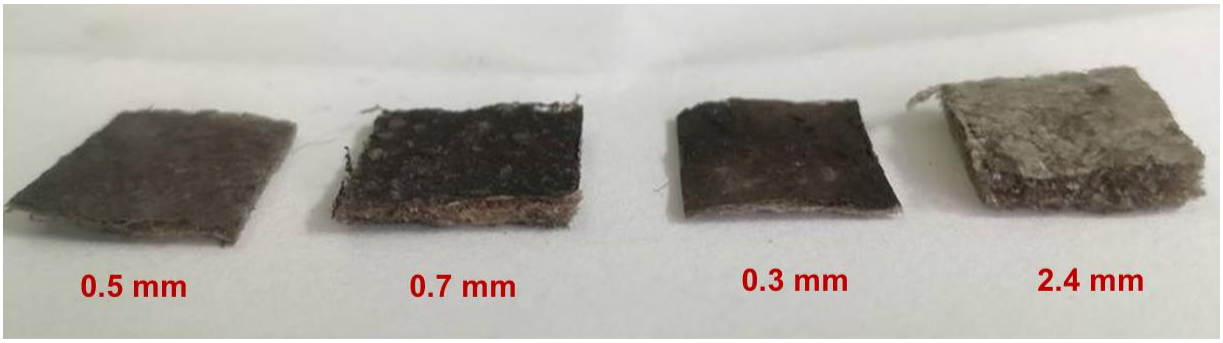

***Figure 11**-PDA-cross-linked nanofibres based on PDA coated collagen, collagen/chitosan,collagen/CaOC, collagen/CMC scaffold (from left to right)*

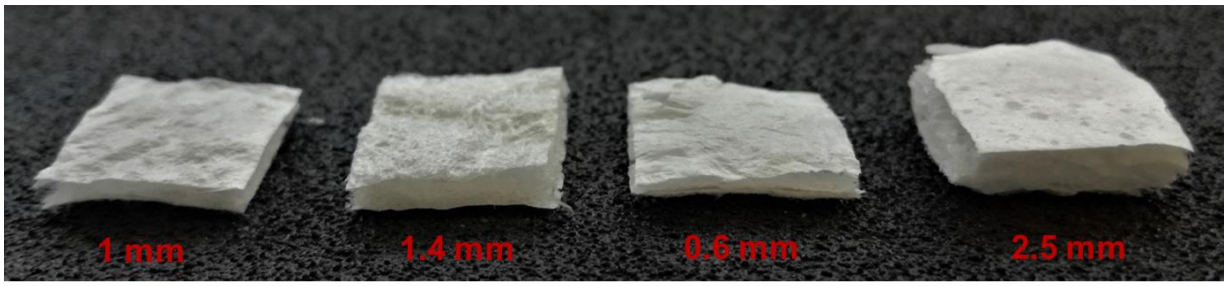

***Figure 12**-Cross-linked nanofibres based on collagen, collagen/chitosan, collagen/CaOC and collagen/CMC scaffold (from left to right)*

Differences in thickness can be observed between various scaffolds, where cross-linking caused decrease in scaffold depth, and it was more supported with PDA (**Figure 13, Figure 14**) are comparing thickness with non cross-linked nanofibres. Related with CMC, this difference has shown to be negligible (**Figure 15).** General values comparison of all axial lengths depits (**Figure 16**). From the scaffold observation it might be noted that after the PDA-coating, the more intensive black colour is attributed to the up nanofibres layer than to the only porous foam, especially for collagen/chitosan and collagen/CaOC. This suggesting that surface wettability has an influence on the PDA deposition. It seems that hydrophobic surface of nanofibres exhibited stronger PDA adhesion compared with the hydrophilic surface of porous collagen.

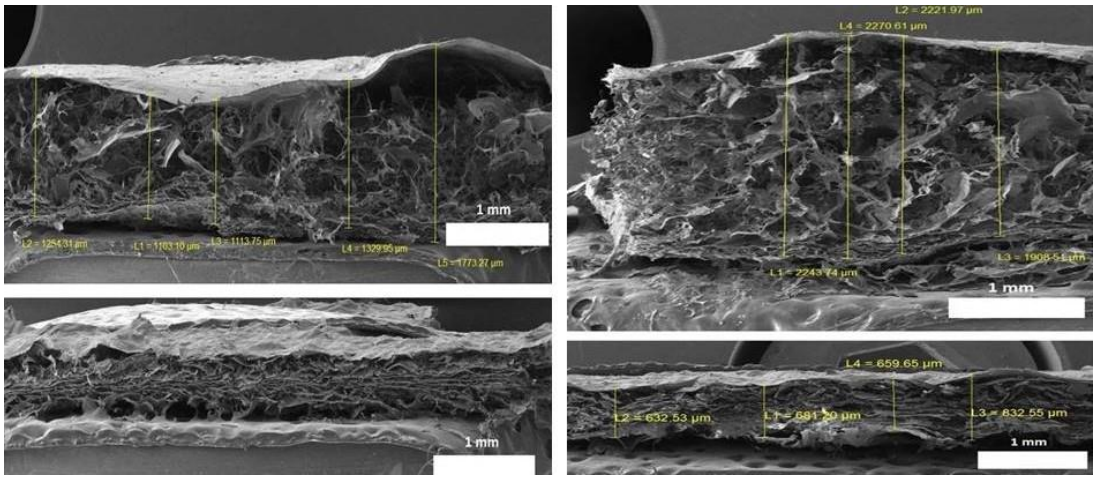

***Figure 13**-Cross-sections of non cross-linked and PDA-coated cross-linked nanofibres based on collagen (left) and collagen/chitosan (right) scaffold, differing in thickness and adhesion between two skin artificial layers*

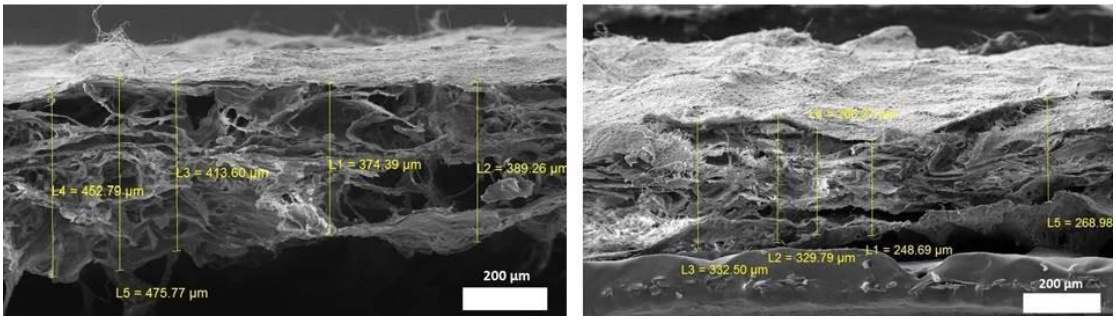

***Figure 14**-Cross-sections of non cross-linked(left) and PDA-coated cross-linked nanofibres(right) based on collagen/CaOC scaffold, differing in thickness and adhesion between two skin artificial layers.*

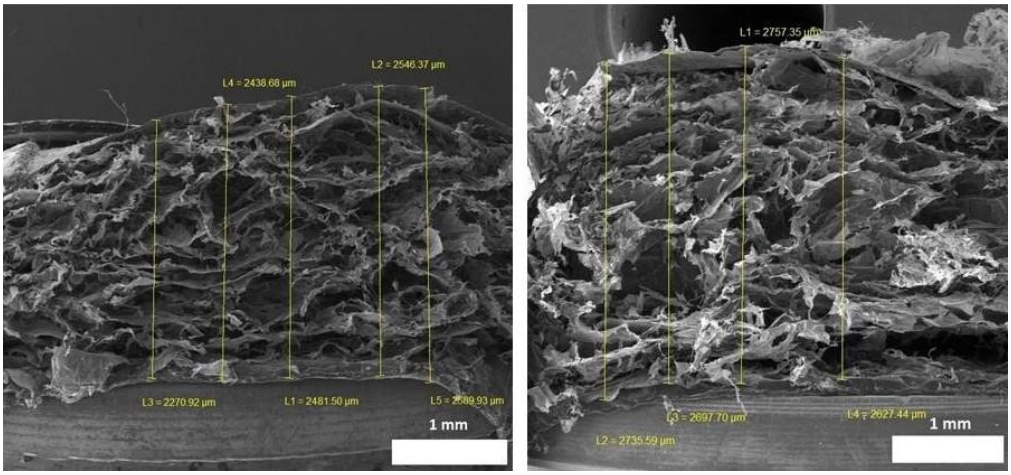

***Figure 15**-Cross-sections of non cross-linked (left) and PDA-coated cross-linked nanofibres (right) based on collagen/CMC scaffold, differing in thickness and adhesion between two skin artificial layers.*

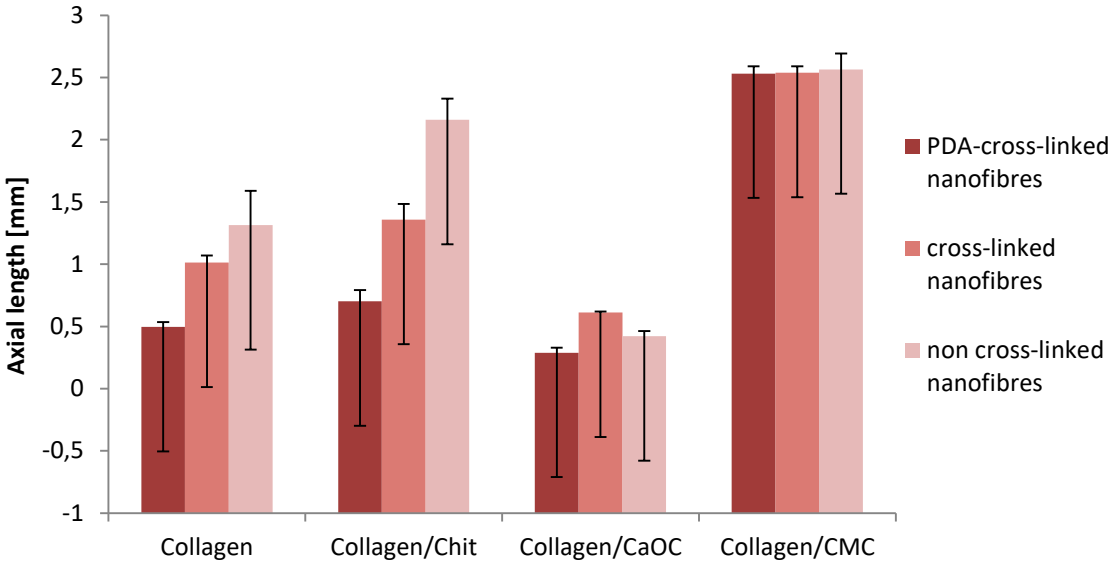

***Figure 16**-The axial length of scaffolds influenced by cross-linking and PDA*

4.1.2. Structure and Morfology of prepared scaffolds

SEM observation of prepared scaffolds was performed and following figures are representing porous and fibres structures also in presence of PDA with possible FGF grafting, as well as adhesion between the both layers.

Observing **Figure 17** (up line), the similar oval shapes were found in every scaffold type with coupled FGF. These small structures where densely accumulated all over the porous surface and from their magnification it can be seen, that some of them were found to be sticking out of the spot more, as those in collagen alone or collagen/chitosan, when compared to the not visible in collagen/CaOC structure. These shapes, probably associated with FGF, were found in more deep structure as their image appearance was in more darker parts.

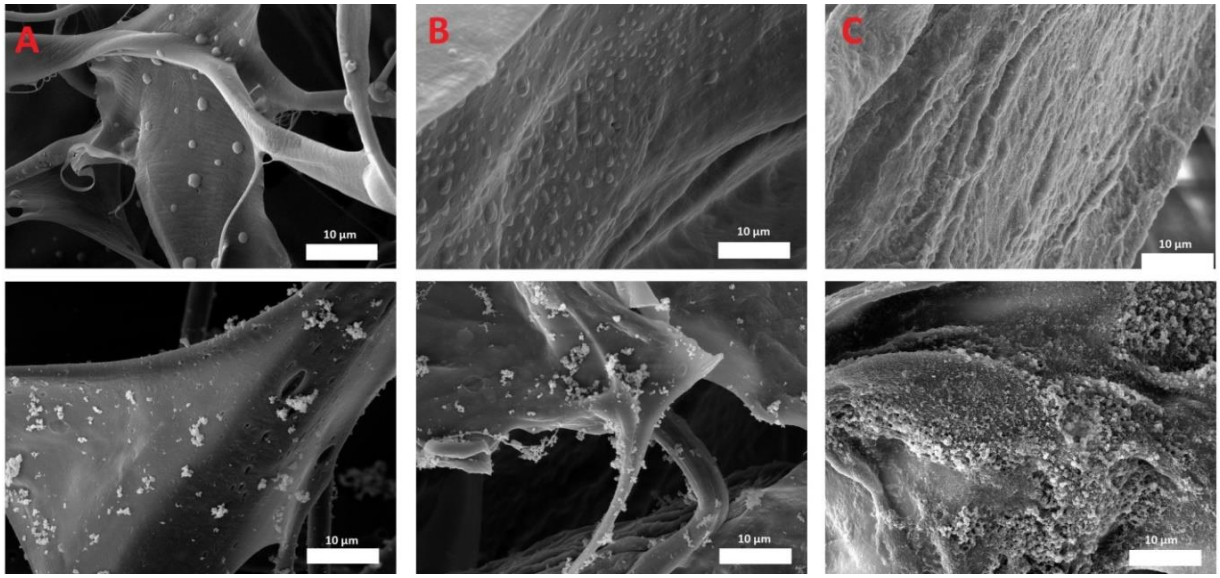

***Figure 17**-SEM observation of **A** collagen, **B** collagen/chitosan and **C** collagen/CaOC scaffold with binded FGF (up line) and in presence of PDA (bottom line).*

A self-assembly of dopamine was found in all samples, where considerable amounts of amine and catechol groups could covalently conjugate via the quinone groups and formed a stable complex containing the oxidative product, 5,6-dihydroxyindole (DHI). Subsequently, the oxidative polymerization with non-covalent self-assembly occurred and produce the PDA precipitates, which can be observed on **Figure 17** (down line). Regarding CaOC, no precipitates were found, which suggests the posibility of a continual film creation or less PDA binding, if taking into the consideration that CaOC required multiple times doing PDA removing what also resulted in less intensive black colour.

Adhesion between nanofibres and porous structure is important for mimicking the skin structure of dermis and basal membrane. The main idea of the basal membrane, as nanofibres scaffold part, is to create a barrier of keratinocytes with function of producing keratin. The porous foam acting as the skin dermis should promote fibroblast proliferation, which is responsible for formation of new connective tissue. Fibroblast proliferation is here stimulated by the presence of FGF. Since the skin dermis is tightly connected to the epidermis through the basal membrane, the good adhesive property should be part of the enginnered scaffold. The following SEM observations on **Figure 18** are refering to better adhesion in the case of cross-linked nanofibres, what was expected compared to the non cross-linking behaviour.

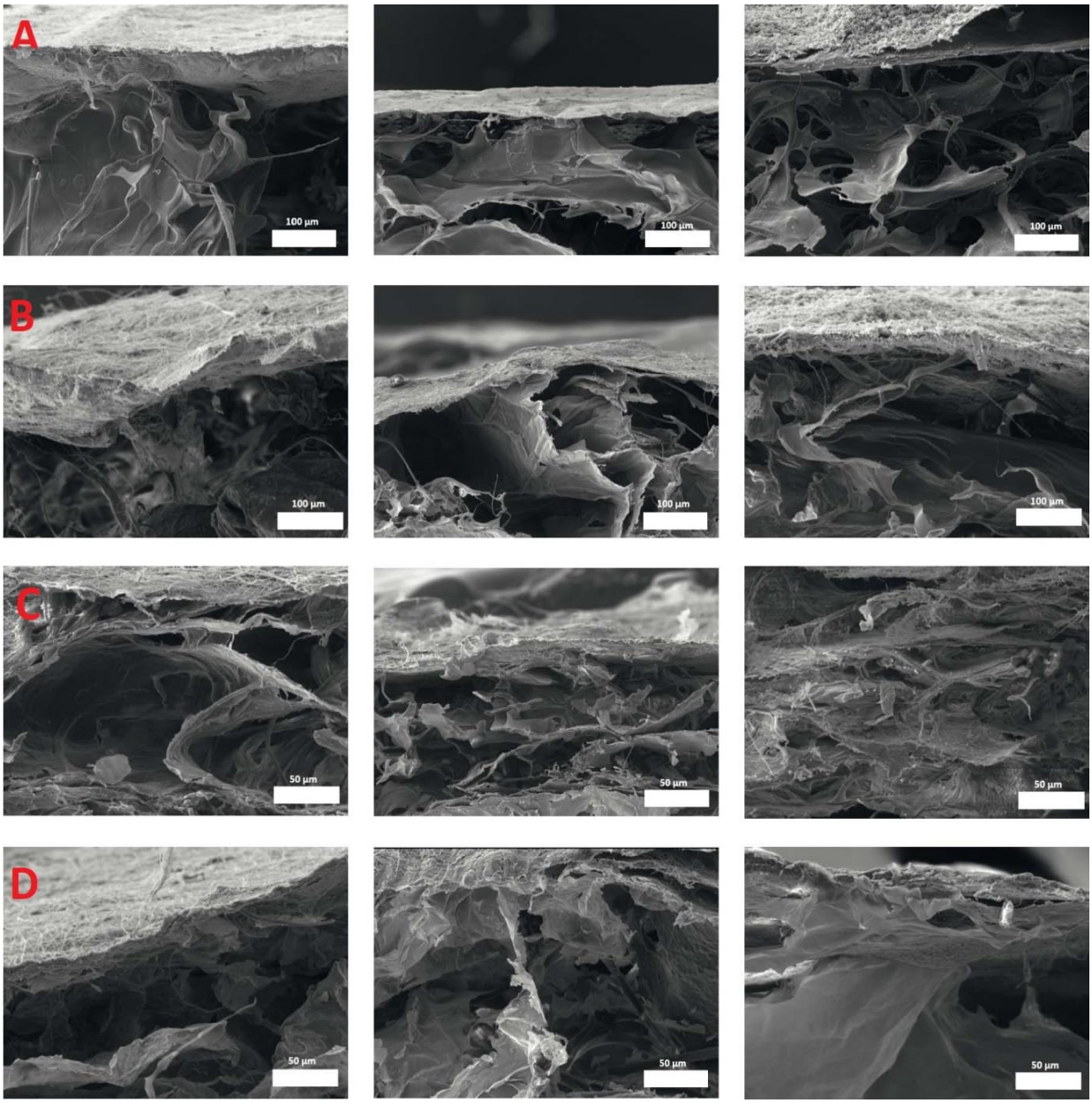

***Figure 18**-SEM images of adhesion between nanofibres and different porous collagen basements. From up to down, first column represents non cross-linked, second column are cross-linked and third column are PDA-coated cross-linked nanofibres, where **A** is collagen, **B** belongs to collagen/chitosan, **C** is collagen/CaOC and **D** characterizes collagen/CMC scaffold*

Other important function of basal membrane is to control the traffic of the cells and molecules between the dermis and the epidermis, thus the nanofibres should exhibit a mesh with interconnected pores possessing mechanical stability. Besides, the basal membrane should also serve as reservoir for cytokines and growth factors and control their release during the skin remodeling in wound healing.

Various surfaces of basal membrane mimicked by nanofibres are depicted on **Figure 19_(A-D).** Non cross-linked electrospun PLC, gelatine and CaOC, as components of engineered basal membrane were, in case of collagen scaffold, equally distributed in all observable area. They are visible more as randomly orientated bunches with larger pores, seems more as tenuous structure. Cross-linked nanofibres, in same case, were tightly attached to each other, exhibiting less porosity, while non-covalent self-assembly of dopamine created PDA precipitates, deposited on the collagen surface and forming heterogeneous layer. **Figure 19_(A)**

The same observation can be done to non cross-linked nanofibres based on chitosan. Even higher density of fibres was shown in case of cross-linking with sporadically occured nodes and a poorly porous structure. Here, less PDA agglomerates were present, which can be explained as better PDA adhesion to chitosan, thus less visible self-assembly occured. **Figure 19_(B)**

Another, similar porous structure, without cross-linking was observed in combination with CaOC, while the cross-linked as well as PDA layer created different surfaces. PDA agglomerates were becoming to be tightly connected to each other and more continually covering the surface, **Figure 19_(C)**. The most diverse was PDA coated on CMC, where a thin, adherent layer was created on nanofibres with no PDA precipitates, as they were deposited on the surface and finally forming a continuous PDA film (**Figure 19_(D)**). However, this formed layer worsened porosity, comparing to the most convenient porous surface, observed in case of CMC with only cross-linked nanofibres. No higher heterogeneities, artifacts or nanofibres nodes presence was occured, as well as in the other porosity visible, cross-linked nanofibres surface, which characterize collagen/CaOC scaffold. This time coated with PDA, **Figure 19_(C)**. This cellulase scaffolds exhibited a more compact filament interlace which may be attributed to the filling effect of PDA. Their pores have also shown to possessing more regular shapes in compare to that of non cross-linked nanofibres.

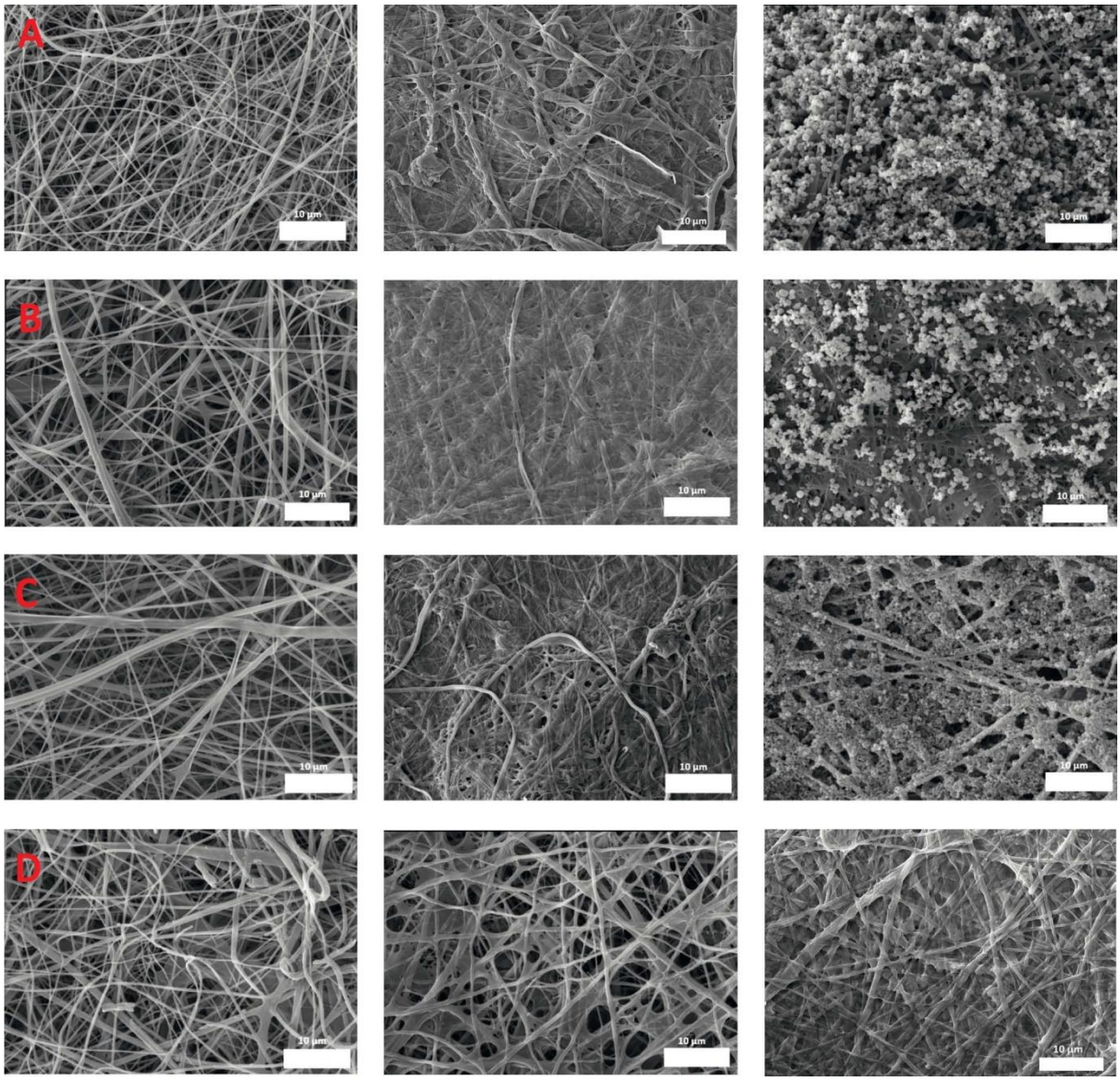

Figure 19*-SEM images of nanofibres surfaces based on different type of collagen scaffolds. From up to down, first column are non cross-linked, second column are cross-linked and third column are PDA coated cross-linked nanofibres, where* ***A*** *is representing collagen,* ***B*** *belongs to collagen/chitosan,* ***C*** *is collagen/CaOC and* ***D*** *is collagen/CMC scaffold*

4.1.3. Biomechanical testing of prepared scaffolds

The mechanical properties (Young's modulus and strength) of scaffolds are critical for handling during surgery, as well as for cell differentiation. To improve mechanical properties, series of scaffolds were prepared by different mechanisms and discussed. Elasticity of a material is typically characterized by its stress–strain relationship. The Young's modulus *E* (elastic modulus) is defined as the ratio of stress to strain. The stress represents the force acting per unit area and the strain is the fractional change in length of the specimen.

Young's modulus is a measure of linear elasticity, which material can exhibit at small applied stress. The higher applied stress or the higher Young's modulus, the higher stiffness will characterize the material. Consecutive increase of the stress makes this relation increase as well and above a certain stress level, the relation becomes non-linear and material has breaken. Final tensile curves of all scaffolds with and without nanofibres in dry and hydrated state are depicted on on following figures with their coresponding elastic modulus.

4.1.3.1. Influence of cross-linked nanofibres on biomechanical properties

All samples exhibited the linear relation, which varied on the type of the biomaterial. In the dry state, the higest relation was attributed to Collagen (118.91 kPa) and Collagen/CaOC (267.0 kPa) in the presence of cross-linked nanofibres. Very similar curves shapes were observed without nanofibres, where only a little less stress (86.7 kPa for Collagen and 184 kPa for Collagen/CaOC) was required to cause their permanent deformation (**Figure 20** and **Figure 21**). On the other hand, addition of CMC and Chitosan required much lower amount of stress (30.4 kPa and 60.49 kPa). Collagen and collagen/CaOC are characterized as more stiff and exhibiting tensile curves with low elongation. Their breakage is more fragile and the material is then less tenacious. Related with adhesivity, no significant tearing differences occurred only at the beginning, where the nanofibres had tendency to be broken at as first. This can also happen, due to a heterogeneity of the samples, but generally, their presence improved biomechanical property of the scaffolds, besides Collagen/CMC, where very negligible differences were observed.

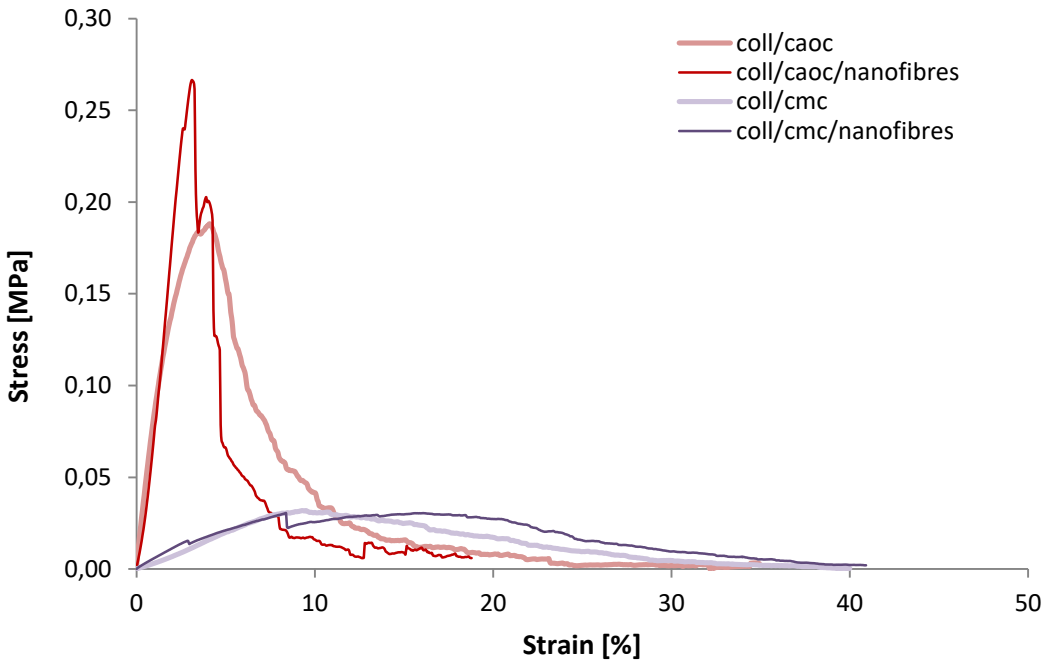

***Figure 20**-Uniaxial extension of scaffolds with and without nanofibres in dry state.*

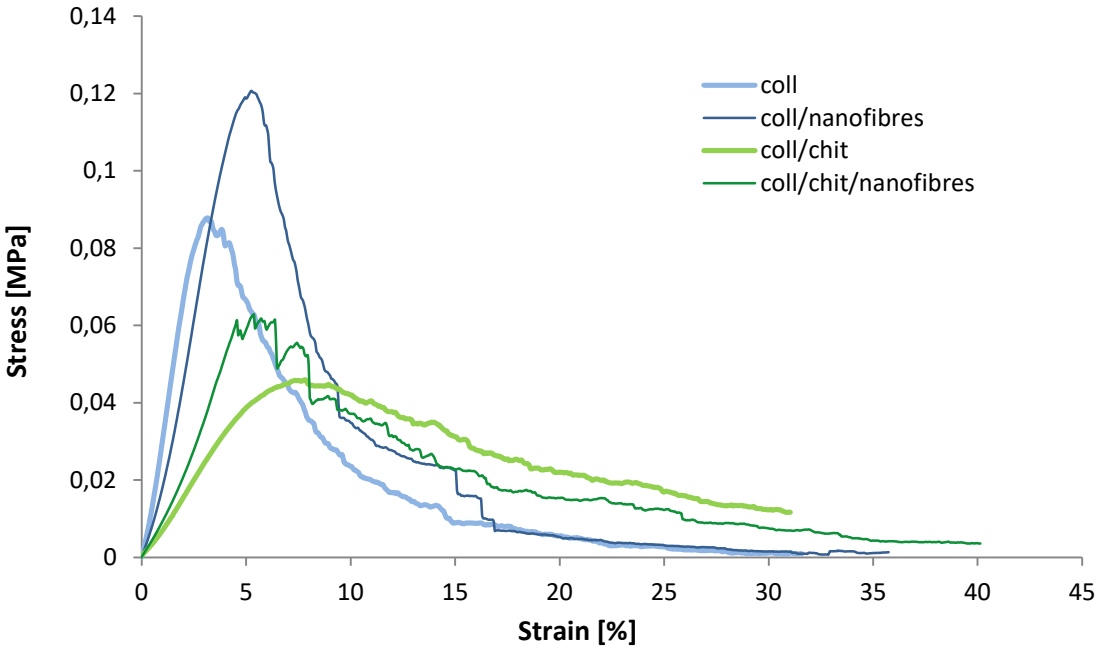

***Figure 21**-Uniaxial extension of scaffolds with and without nanofibres in dry state*

In the hydrated state, only collagen scaffold requires the highest deformation force (37.49 kPa), while Collagen/CaOC, depending on nanofibres presence (**Figure 22** and **Figure 23**) required only 6.36 kPa – 8.68 kPa to successffuly tear the material, after 10 min of swelling. Whereas the amounts of stress are negligible, the difference can be observed with tearing of material. The nanofibres were broken in different areas of surface and tearing was less continuous. Very good elongation characterizes CMC and chitosan and has become more stretched with support of nanofibres. Presence of chitosan stretched the scaffold on 34 % of its initial length, more than CMC, where the stretch was 22 %. The applied force on chitosan scaffold was compared to collagen very low 14 kPa, but time to reach deformation was longer. Tearing was also continual all over the sample compare to the others in hydrated sate, what indicates that nanofibres were better adhered on the surface of collagen/chitosan, For hydrated state, chitosan and CMC can achieve longer time and higher percentage of tensing before deformation. However, the applied stress must be sagnificantly lower to stretch them a long way. By increasing stress load, they would rupture easily. The lowest stress value was 4.09 kPa for CMC with nanofibres. An overview of biomechnical properties of all stress values are depicted on **Figure 28** for dry state and **Figure 30** for hydrated state, while all strain values are depicted on **Figure 29** for dry state and **Figure 31** for hydrated state.

The differences between cross-linked and non cross-linked nanofibres are depicted in (**Appendix 1-4**). In general cross-linking between two layers is improving the stiffness of scaffolds, as well as the adhesion. In terms of stiffness, very similar shapes of the tensile curves occured in both dry and hydrated state with slight increase in applied stresses. Scaffold with chitosan composition showed negligible differences in terms of stress loading but it stretched in case of cross-linked nanofibres from 20 % to 34 % in hydrated state. This suggest, that even if the nanofibres are non cross-linked, this scaffold exhibits the same biomechanical properties as it has with cross-linking. They are not a very usefull scaffold related with adhesivity, which was weak due to the nanofibres rupture at the very beginning, even before the porous structure disrupted and was continuing non-uniformly. Demonstrative example can be observed with CaOC, where the presence of non cross-linked nanofibres caused insufficient adhesion. For the better overview of all stress and strain values **Figure 28** and **Figure 30** for dry state, with **Figure 29** and **Figure 31** for hydrated state are shown.

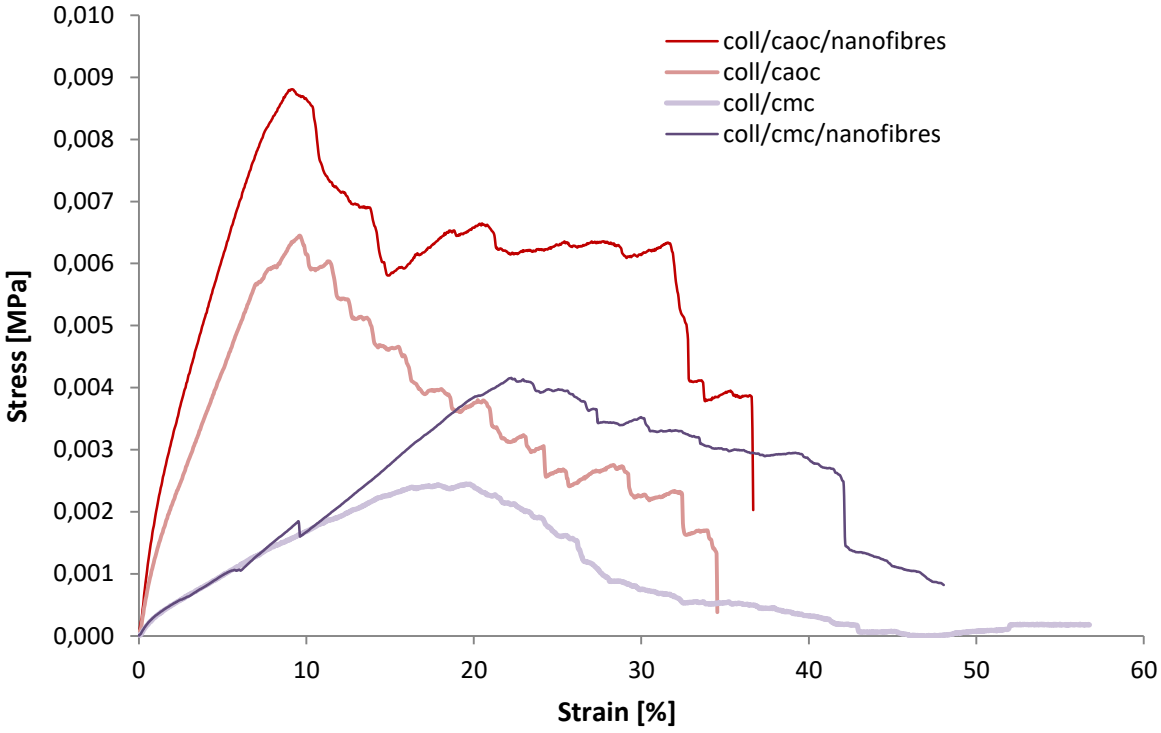

***Figure 22**-Uniaxial extension of scaffolds with and without nanofibres in hydrated state*

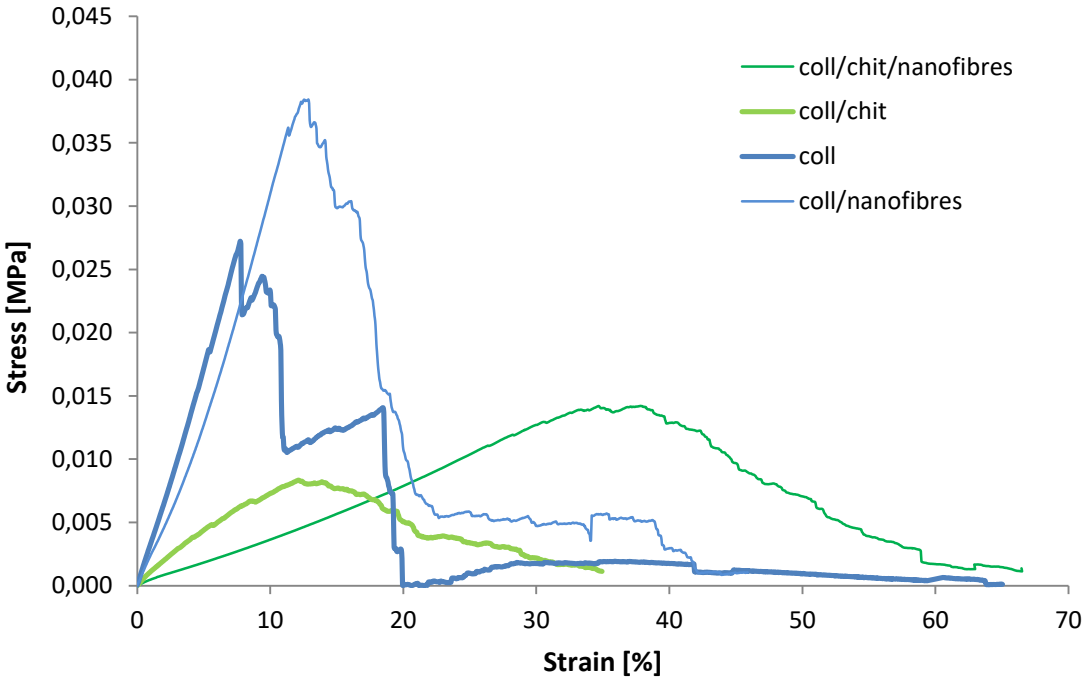

***Figure 23**-Uniaxial extension of scaffolds with and without nanofibres in hydrated state*

4.1.3.2. Influence of PDA-linker on biomechanical properties

It should be noted, that for these tests, only samples with cross-linked nanofibres were used, while the non cross-linked were excluded, mainly due to the observed worsening nanofibrous adhesion based on the porous PDA-coated foam. **Figure 24** and **Figure 25** are comparing tensile curves of cross-linked nanofibrous scaffolds in presence of PDA.

In general, PDA addition in scaffolds required higher stresses to tear the material and it was obtained for the both, dry and hydrated conditions. The most fragile sample in the dry state is connected with presence of CaOC and also for collagen alone. Collagen/CaOC with PDA was resisting plastic deformation at the most of 397.07 kPa and drop in 267 kPa with no PDA. The PDA scaffold was barely stretchable, at only 2 % of its original length. The trend of difference stress ranges within the others scaffolds of the same polymer type was obtained as follows: Collagen (277.36 – 118.91 kPa), Chitosan (154.03 – 60.49 kPa) and CMC (107.9 – 30.4 kPa). A formation of covalent bonds and hydrogen bonds between PDA layer and PCL composite nanofibres could be an attribute to that differences. Also a better gelatin immobilization on PCL nanofibres via PDA-coating could contribute to higher tensile strength, as was already studied with poly(L-lactide-co-ε-caprolactone) (PLCL).[106]

Analogous results have been done with PDA-coated porcine acellular dermal matrix (PADM) with 5 mg/ml dopamine coating concentration. This study has shown that a tensile strength increased by about 40% and elongation at break increased by about 20% compared to that of PADM.[107] Similar increased percentage of the tensile strength (57 %) occurred in case of collagen scaffold, while the elongation at break increased by about 50%. Elongation at break for PDA-coated chitosan scaffold did not express any significant tensile change and had a constant value. Stretching differences are not that significant as the stress attributes, but they support the fact that dopamine is stiffening the material. Related with the adhesivity, dopamine was added to the final nanofibrous scaffold as the last step before freeze-drying, so the adhesion was supported by its wet application, where it could have modified the both, hydrophilic and hydrophobic surface. Subsequent material tearing was after first rupture continual and similar if compares within the scaffold of the same type. Slight divert was shown within CMC scaffolds, where less continual tearing occured.

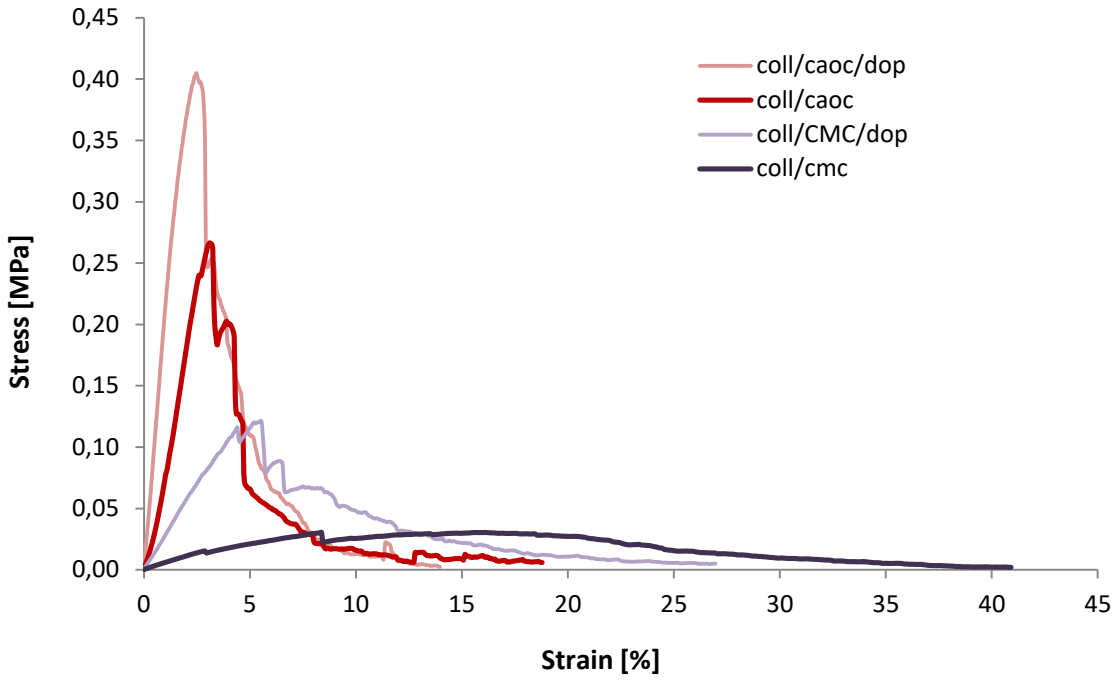

***Figure 24**-Uniaxial extension of scaffolds with not coated and PDA coated nanofibres in dry state*

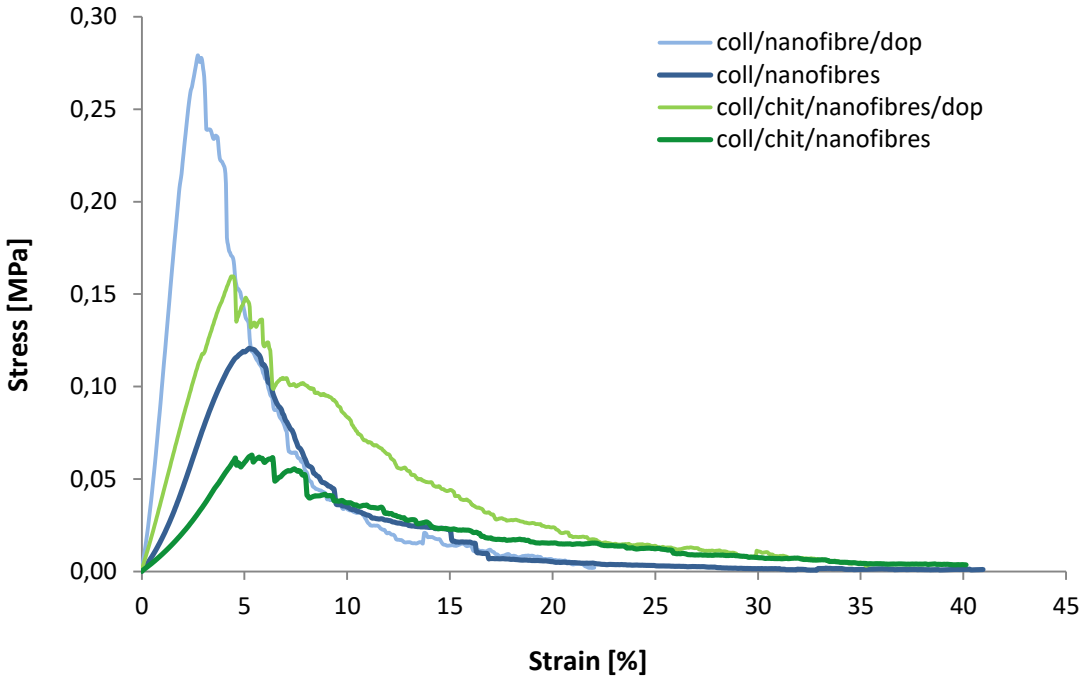

***Figure 25**-Uniaxial extension of scaffolds with not coated and PDA coated nanofibres in dry state*

In the hydrated state (**Figure 27**), the most resistant breakage was associated with collagen, where the presence of PDA had negligable influence in terms of applied stress. Similarity is occuring in terms of stretching. The collagen scaffold is „out of trend“ and with dopamine became a negligible less stiffer (29.34 kPa drop in case of PDA compare to 37.49 kPa to that of non-PDA). This time, the most significant difference is for PDA-coating Collagen/Chitosan. Interesting tensile properties were observed, when the material has been resisting for a longer time to the higher stress condition (30.9 kPa). This stress is similar to the stress applied on the most resistant collagen scaffold. On the other side, tension of chitosan scaffold with dopamine has shown decrease from 34 % to 23.4 %. Since the both scaffold layers has different hydrophilic character, the improved mechanical properties could be due to the PDA binding to gelatine in nanofibres via $–NH_2$ and –COOH groups. The gelatin PDA modification then increased the hydrophilic character of nanofibres. PDA could also cross-linked with amine groups of chitosan through the condensation polymerization of amine and carboxyl groups, since the introduction of PDA increased the amount of –C–O– and –C=O groups.[108] The formation of amide bonds between PDA and chitosan could successfully create adhesive link between the both layers.

Cellulose composites of scaffolds had difficulties to resist to the increasing load and deformed very easily at stress of 8.68 kPa for CaOC and 4.09 kPa for CMC. PDA could stiffer both scaffolds and made them resistant at 14 kPa (**Figure 26**). PDA could modified the cellulose surface with possible new π-interactions, as well as the quinone or amino groups could react with –OH and –COOH functional groups of the cellulose. Only these composites showed that the stretching with PDA was higher in hydrated state, while collagen and chitosan has shown lower stretching in presence of PDA. This can refer to the stronger PDA-linker formation in chitosan scaffold, which made material to be less tensile. An overview of biomechnical properties of all stress values are depicted on **Figure 28** for dry state and **Figure 30** for hydrated state, while all strain values are depicted on **Figure 29** for dry state and **Figure 31** for hydrated state.

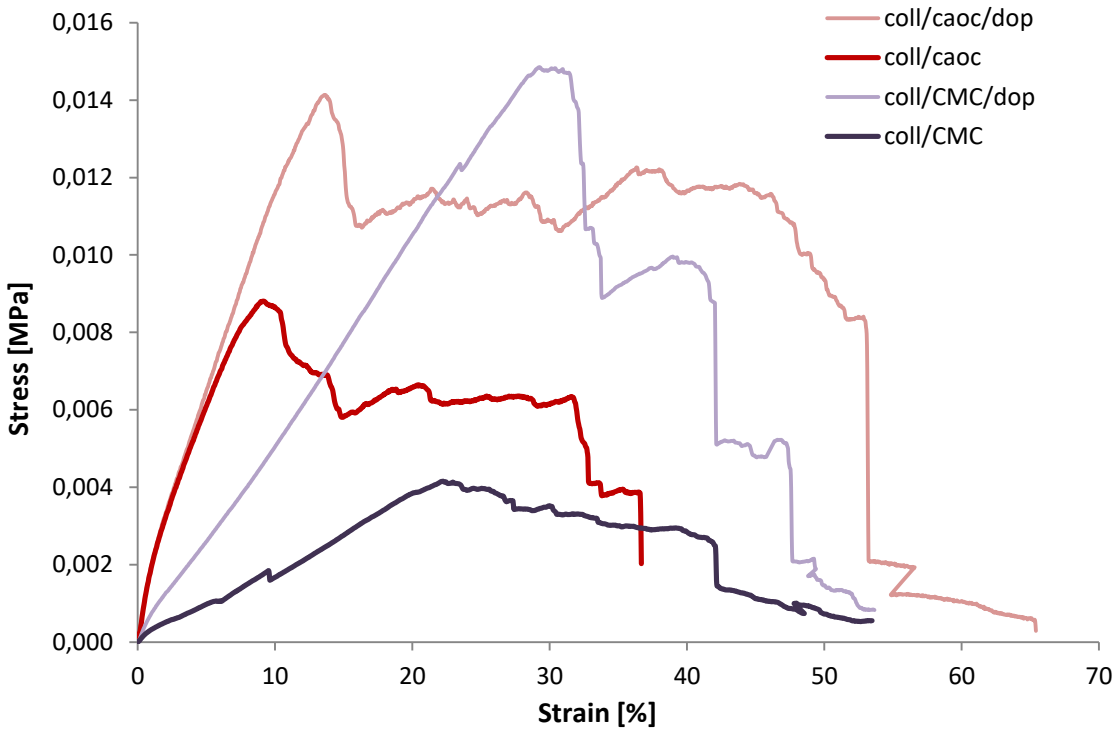

***Figure 26**-Uniaxial extension of scaffolds with nanofibres and PDA coated nanofibres in hydrated state*

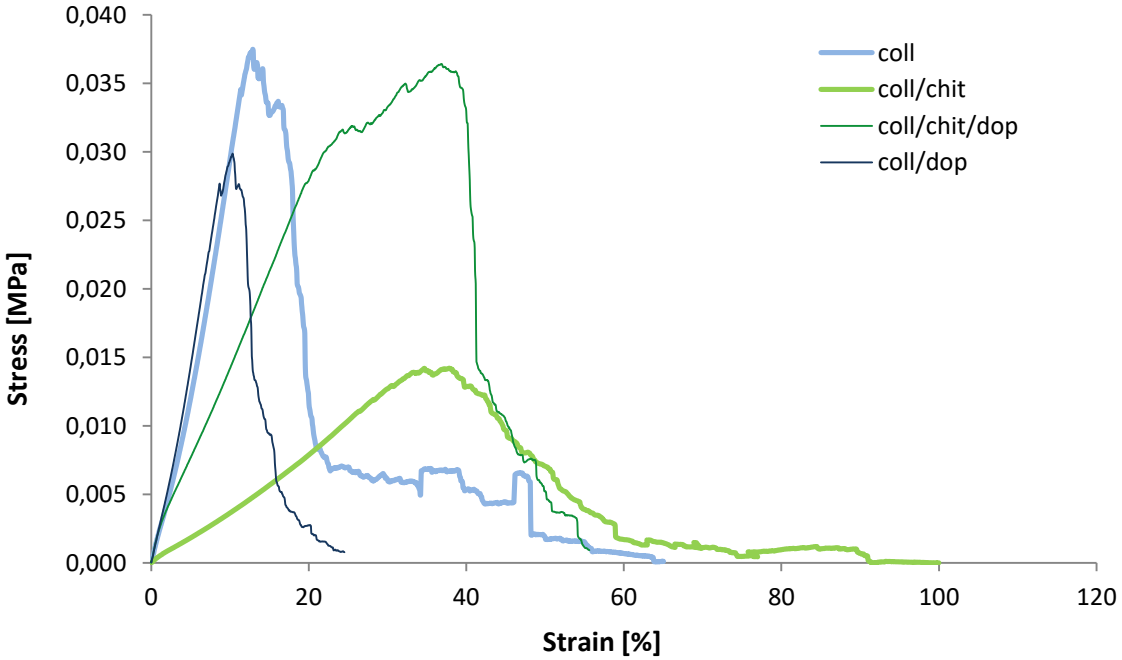

***Figure 27**-Uniaxial extension of scaffolds with nanofibres and PDA coated nanofibres in hydrated state*

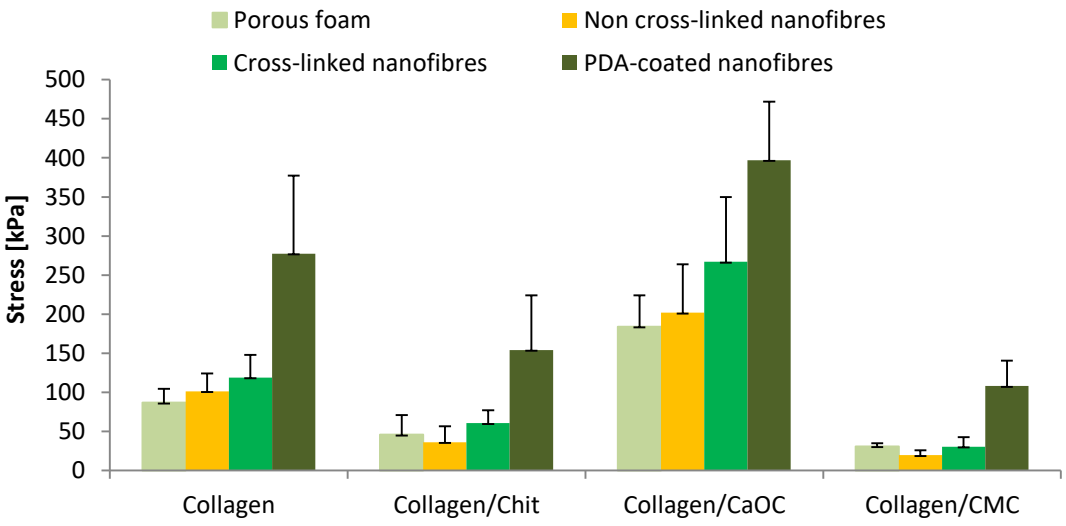

***Figure 28**-The overview of stress values for all scaffolds at dry state*

Overall from all the scaffolds in dry state, cross-linked and the PDA-coated ones can resist deformation the most and made material to be less stretched, while non-crosslinking has shown as the worst because of nanofibrous first breakage together with the decrease tense caused insufficient adhesion.

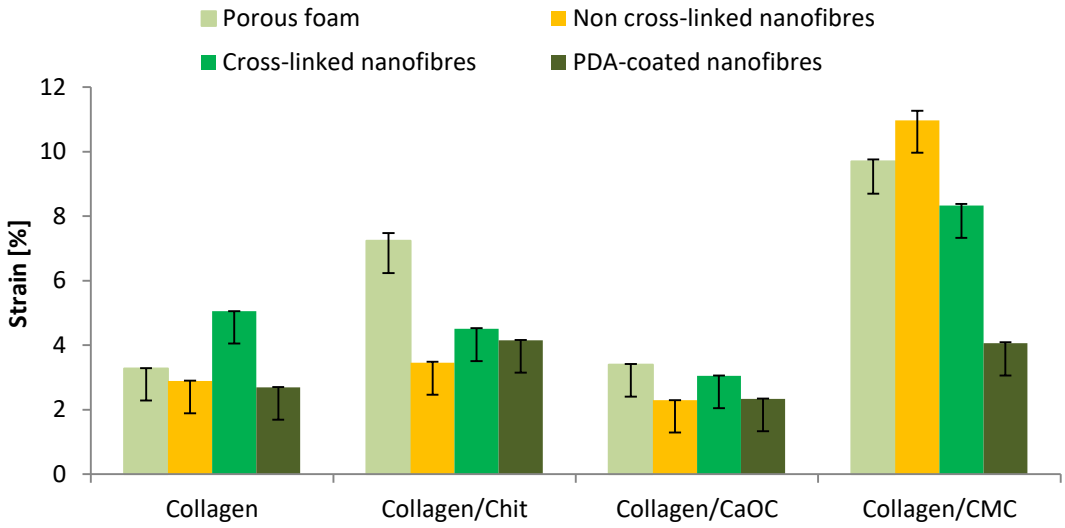

***Figure 29**-The overview of strain values for all scaffolds at dry state*

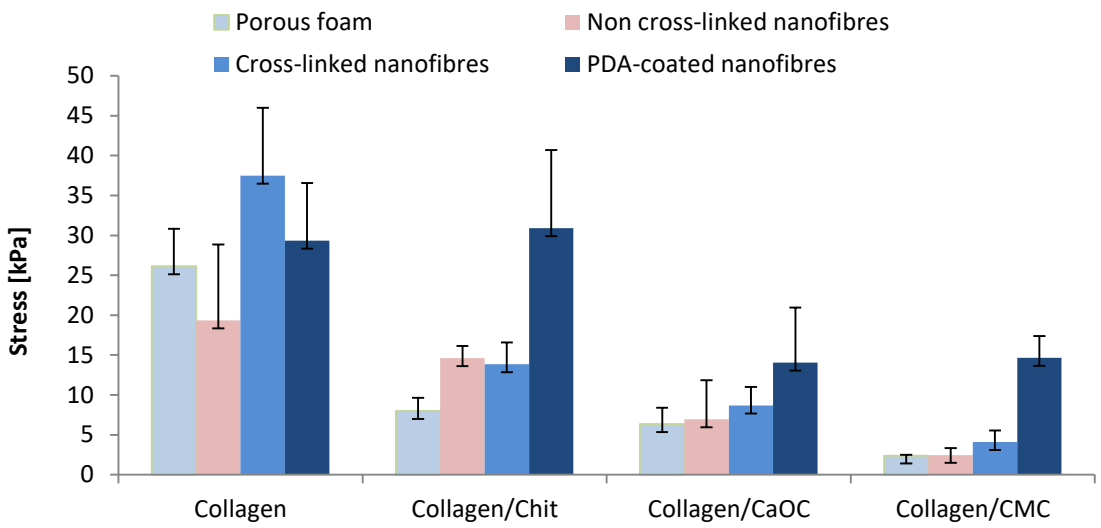

***Figure 30**-The overview of stress values for all scaffolds at hydrated state*

Overall from all the scaffolds in hydrated state, cross-linked and the PDA-coated ones can resist deformation the most and made material to be similarly or even more stretched within the same scaffold type, thus the support of nanofibres is here even more evident. Non-crosslinking has shown better mechanical support, where even collagen/chitosan has shown a bit higher amount of stress compare to cross-linked nanofibres, what suggests his good adhesive potential.

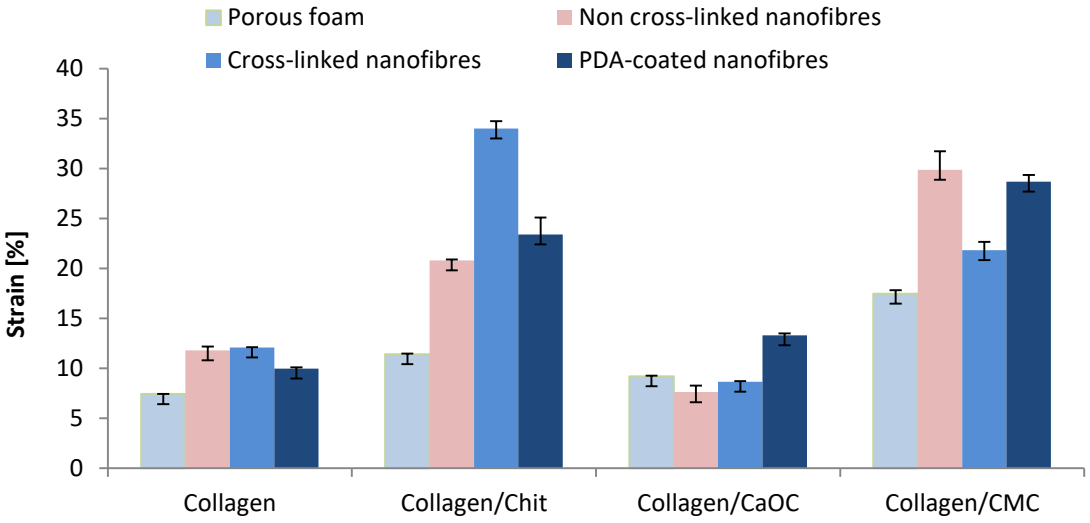

***Figure 31**-The overview of stress values for all scaffolds at hydrated state*

All measurements have shown, that hydrated collagen and collagen composite scaffolds under aqueous solution condition, which is more closely related to the situation in vivo, experienced a reduction in modulus compared to the anhydrous form. In general, highly non-linear is elastic modulus of most biologic tissue, hence the engineered scaffolds should exhibit increasing elastic modulus for higher strains. In case of this work, the most suitable in hydrated state is PDA-coated nanofibrous collagen/chitosan scaffold, which is characteristic by increasing elastic modulus, together with the high strain.

Samples differ in elastic modulus when the nanofibres are cross-linked with the porous foam or not. Non cross-linked nanofibres are characterized as less stable and less fixed on the surface of collagen hence the elastic modulus is lower. Cross-linked nanofibres are more tightly adhered on the surface of collagen foam and exhibiting higher modulus and scaffolds have higher stiffness. Those observations are seeing in both dry and hydrated state in relation to elastic modulus **Figure 32** and **Figure 33**.

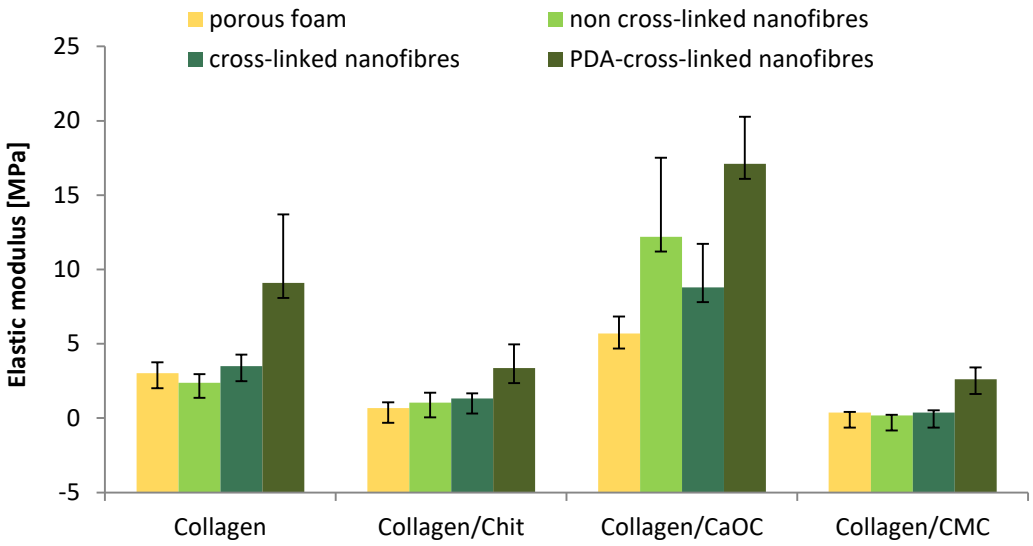

***Figure 32**-Elastic modulus of all composite collagen scaffods in dry conditions*

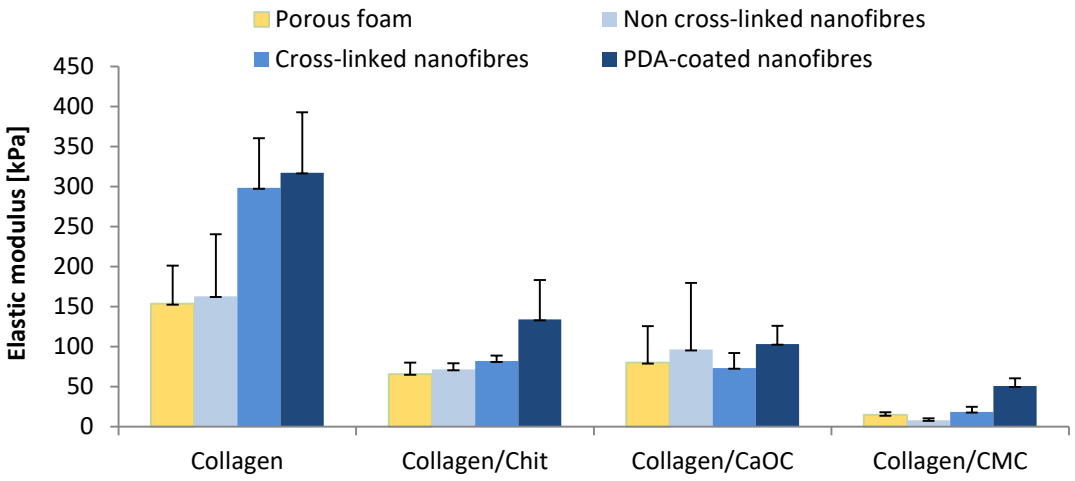

***Figure 33**-Elastic modulus of all composite collagen scaffods in hydrated conditions*

4.1.4. In-vitro testing of prepared scaffolds

4.1.4.1. Swelling test

The ability of a scaffold to preserve water is an important aspect to evaluate its property for skin tissue engineering. Swelling behaviour of collagen scaffolds was obtained upon contact with distilled water. The rate of swellings decreased with time and reached constant values, as it is illustrated on the **Figure 34**.

The highest swelling scaffold was related with CMC, then collagen and finally collagen/chitosan and collagen/CaOC. Essentially, the collagen fibres have a good affinity with water and swell when water is absorbed. As for the collagen, so as for the collagen/chitosan, the water-binding ability could be attributed to the both hydrophilicity and the maintenance of their three-dimensional structure. As the collagen cross-linked with chitosan it decreased the swelling ratio, as the cross-linking between collagen and chitosan decreased amount of free bind hydrophilic groups.

Swelling property of collagen involving CaOC was evaluated up to 60 min, due to the scaffold integrity loss with following restraint manipulation. Also, the lowest value of swelling ratio was due to the large amounts of carboxylic and hydroxyl groups of CaOC, which can form hydrogen bonds with the water, as well as with collagen. Fully protonated (COOH) groups formed several hydrogen bonds, which reduced the water uptake. As a result of such interactions the hydrophilic character of the scaffold decreased.

The collagen/CMC scaffold revealed that CMC contributed to increasing swelling as a result of strong water adsorption. However, the swelling is strongly influenced by the ionic strength, and since CMC is ionic, its Na^+ ions can hinder the repulsion of carboxylic groups, thus decreasing swelling capacity. The swelling is also strongly suppresed with increasing salt concentration.[109] In this case, the CMC scaffols exhibited the highest swelling, which could be due the strong Na^+ solvation in an aqueus medium, what revealed electrostatic repulsion between adjacent carboxylic groups with following repulsions between the polymer chains and facilitating volumetric expansion thus increased the amount of water that could enter the scaffold.

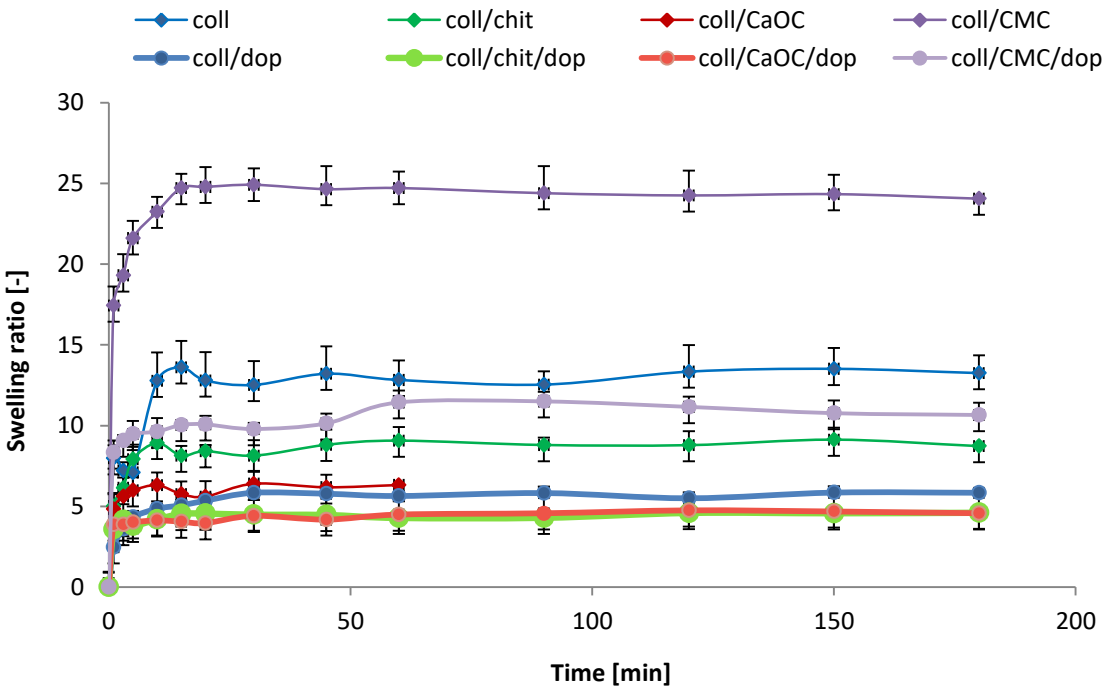

***Figure 34**-Swelling behavior of collagen composite scaffold and PDA-coated collagen composite scaffold*

Presence of PDA reduced swelling ratio in every scaffold type. It has been already demonstrated that dopamine can self-polymerize to PDA under alkaline conditions. With that chemical structure, PDA could limit the extension of collagen fibrils, thus the lower swelling ratio. PDA can bind to the collagen via hydrogen bonds, because within the dopamine structure, there are large amounts of hydroxyls groups, which tends to interact with the collagen molecules and retard the self-assembly of collagen, what then reduce porosity.

The low porosity leads to the lower swelling, since the smaller are spaces for water uptake. The same effect can be considered also for CaOC, where hydrogen bonds occured and reduced the porous structure.

The same trend was observed for CMC scaffold, the presence of PDA reduced its swelling ratio in half. However, it has the higest swelling ratio among PDA scaffolds. Polydopamine films have also a pH dependent permselectivity, where at pH higher than about four, they allow permeation of cations, where in acidic conditions they become selective for anions.[110] PDA in pH of 8.5 could permeate the Na+ cations of CMC and reveal electrostatic repulsion between carboxylic groups and by this reason the CMC was occurred with higer swelling among the others.

Negligible different swelling ratios were evaluated among the rest PDA scaffolds (**Figure 24**), but exhibiting lower values compare to their not PDA-coated models. The chitosan, which contains free amine groups can be partially charged at pH 8.5, as the pKa of chitosan is around 6.3.[101] Highly protonated $–NH_3^+$ groups can interact with the remaining free COOH of collagen, ionically crosslinking the polymeric chains and hindering the solvation, thus no repealing interactions are occurred, leading to the lower swelling.

The water retaining capacity of scaffold must be considered as very important in cell growth, where higher water retaining capacity means higher nutrients capturing ability, when the scaffold is applied as tissue engineering material. Time dependence of the water content was studied for every scaffold. The water content is illustrated as amounts of water absorbed by swelling, which is shown in **Figure 35** and **Figure 36**. The highest amount of water absorbed collagen/CMC (95.83 %), with following collagen (92.42 %), collagen/chitosan (88.48 %) and collagen/CaOC (84 %). The presence of PDA decreased water content in CMC structure (90.59 %), what was also the highest from all PDA-coated scaffolds, next collagen (79.08 %), collagen/chitosan (78.26 %) and collagen/CaOC (78 %).

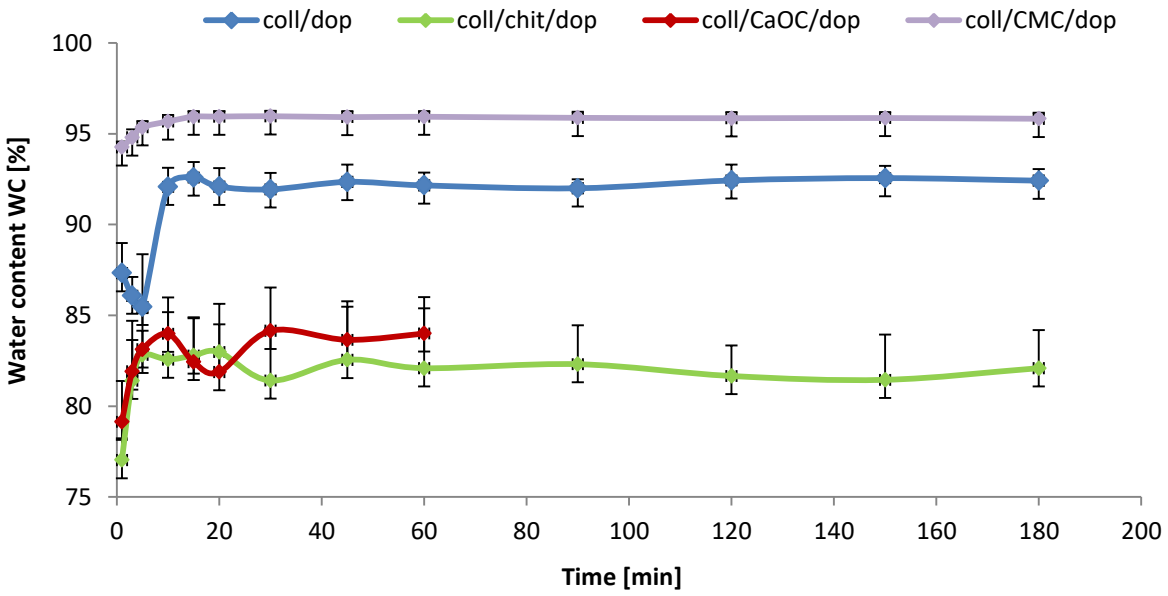

***Figure 35**-Water content of collagen composite scaffolds*

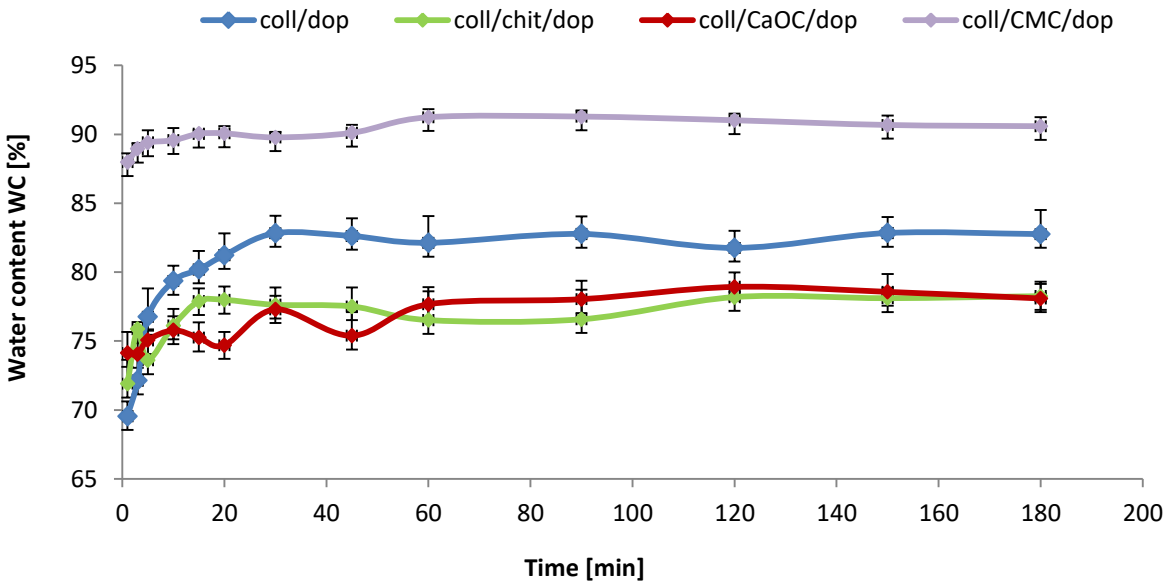

***Figure 36**-Water content of PDA-coated collagen composite scaffolds*

4.1.4.2. Degradation of collagen scaffolds by *Clostridium* collagenase

Degradation was performed in order to compare the stability effect of dopamine on collagen based scaffolds. At the begining, some of the scaffolds were swelling for 2 or 4 hours, after exposing to enzymatic activity. The swelling was observed for both collagen/chitosan and PDA-coated collagen/CMC scaffold. Significant behaviour was

observed with chitosan, where presence of dopamine caused degradation deferment on day 4. The same scaffold, but without dopamine degradated already after 8 hours. Both scaffolds reached same 60 % weight loss on day 6.

Degradation of collagen scaffold without any composite reached 77 %, where only more continual degradation occured and was continuing in the same tendency until 6. Day with PDA. (**Figure 37**). No prolonged time of degradation was occured in terms of PDA-coated collagen without composites, which might lead to the conclusion that PDA is adhesive linker, which is improving the stability between collagen and its composite biomaterials.

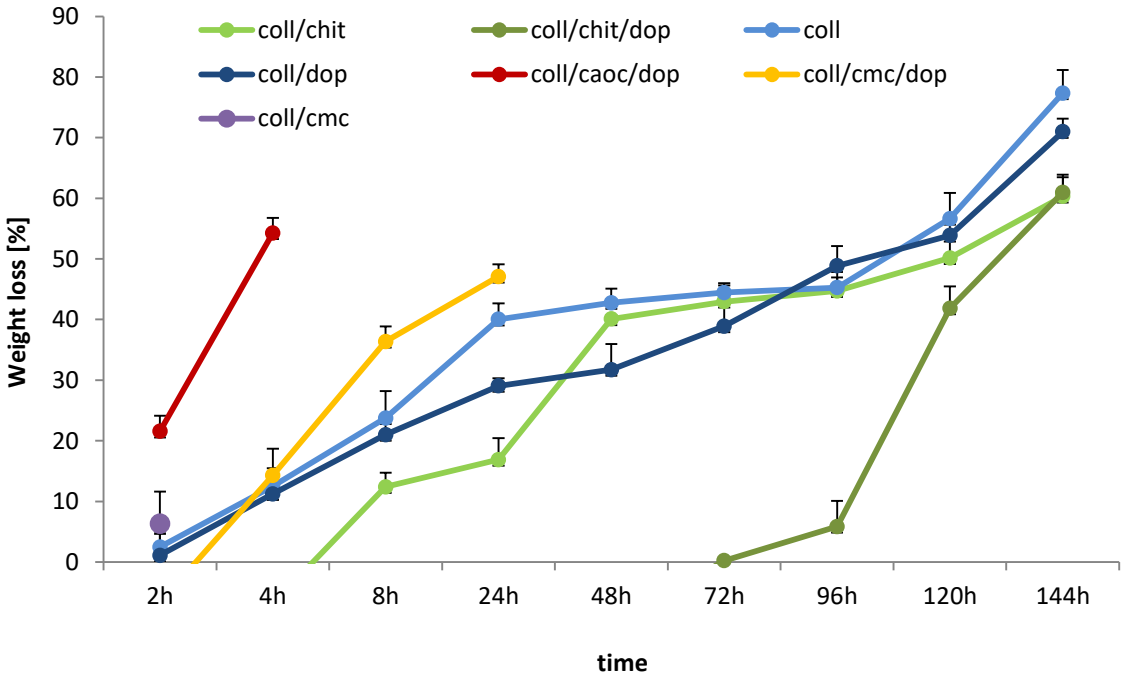

***Figure 37**-PDA influance on Clostridium collagenase degradation of collagen scaffolds*

Related with other additives, structure of collagen/CMC was disrupted very soon, 2 hours was enough to create incompact form with restraint samples manipulation. The effect of dopamine supported this structure only for more two hours, where 47 % weight loss was recorded. In case of CaOC, the same effect happened. Whereas CaOC in collagen caused unrecorded result, with dopamine presence, the degradation was postponed for more 24 hours and release 55 % weight loss.

Presence of PDA not only increased the time of collagen degradation, moreover remarkably enhanced antibacterial activity. Mainly for collagen and collagen/chitosan, where

a characteristic haze and odour of bacterial contamination were accompanied the scaffolds, observed after 24 hours of degradation. PDA was able to suspend bacterial activity until day 5 for the both scaffolds. As a consequence antibacterial tests on different bacterial stains will be evaluated.

4.1.4.3. Degradation of collagen/chitosan scaffolds by lysozyme

Collagen/chitosan scaffold was submitted to degradation in order to compare the stabilization effect of dopamine, by exposing scaffold to the human lysozyme. **Figure 38** represents what impact has dopamine during 6 days of degradation.

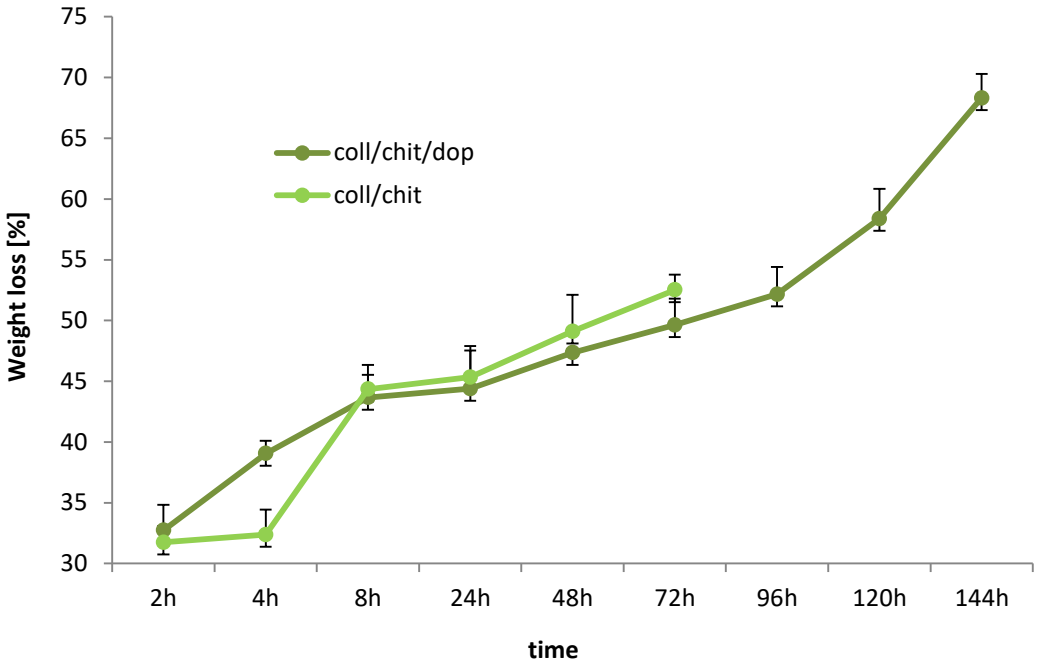

***Figure 38**-PDA influance on Lysozyme degradation of collagen/chitosan scaffolds*

The lysozyme biodegradation test demonstrated, that the presence of PDA can prolong the biodegradation of collagen/chitosan scaffolds, thus indicated scaffold higher stability. On day 3, lysozyme caused 52 % chitosan loss, following the scaffold restraint manipulation. Influence of PDA made chitosan degradation going slower and on day 6, the weight loss reached 68 % with still possible scaffold manipulation. Antibacterial effect of dopamine showed up similary as it was for degradation with collagenase. On 5. day, emergent bacterial contamination accrued in compare to the started bacterial activity after 24 hours for not PDA-linked scaffolds.

PDA degradation was already studied that it is strongly depended on the synthesis method and the nature of the substrate, on which it is coated. Degradation was provided in an oxidizing sodium hypochlorite solution in that case.[111] Also PDA degradation is largely dependent on pH of aqueous solution and organic solvents.[112] Others foundation has shown that PDA can biodegraded in soil.[113] The main factor of PDA enhanced stability could be its reaction with collagen and collagen fibrils via plenty of hydrogen bonds.

4.1.4.4. FGF release experiment

The release experiment was performed in order to find out the amount of FGF, released from the skin scaffold. Results from this experiment became negative and a new optimalization needs to be done to better facilitate and study the release of the protein. Samples releasing and dilutions are summarized in following tables:

***Table 4**-Sample releasing into 1ml of phosphat buffer*

Intervals	**Taken volumes**
1 hour	250 µl
3 hours	250 µl
5 hours	250 µl

***Table 5**-Standard and samples dilutions*

The standard dilution	**Protein solution**	**Buffer**
0,19 ng/µl	190 µl	810 µl
0,17 ng/µl	170 µl	830 µl
0,13 ng/µl	130 µl	870 µl
0,09 ng/µl	90 µl	910 µl
0,05 ng/µl	50 µl	950 µl
0,03 ng/µl	30 µl	970 µl
0,01 ng/µl	10 µl	990 µl
The samples dilution	**Protein solution**	**Buffer**
10x	100 µl	900 µl
50x	20 µl	980 µl
100x	10 µl	990 µl

The release experiment needs to be optimized again. The considering reason of no FGF detection could be the used well plates, in which samples were prepared. The main property of these plates is to increase cell attachment to the surface, where FGF as protein could also bind. Releasing time with following samples intake should be performed in longer intervals, more than 5 hours.

4.1.4.5. Cytotoxicity testing

According to the MTS metabolic assay, the metabolic activity of the cells was recorded for every type of scaffold. The significant difference caused the presence of dopamine on **Figure 39** (G-L), where the highest maintained metabolic activity (on 14. day) was shown and as the most it was observed in PDA-coated collagen scaffold (G). Very active were cells on 7th day in PDA-coated collagen/CaOC scaffold (I) and PDA-coated collagen in presence of FGF (J). Remarkable result was in presence of FGF, which didn't significantly influence the cells activity.

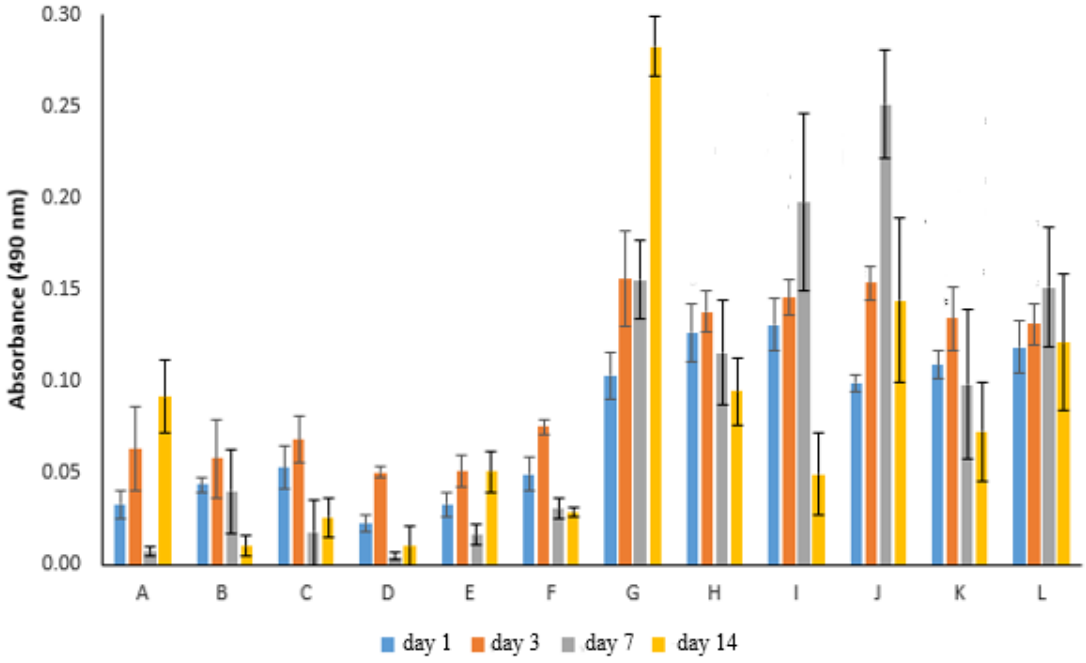

***Figure 39**-Metabolic activity of the composite scaffolds in the following order: **A**-collagen, **B**-collagen/chitosan, **C**-collagen/CaOC, **D**-collagen/FGF, **E**-collagen/chitosan/FGF, **F**-collagen/CaOC/FGF, **G**-collagen/PDA, **H**-collagen/chitosan/PDA, **I**- collagen/CaOC/PDA, **J**-collagen/PDA/FGF **K**- collagen/chitosan/PDA/FGF, **L**- collagen/CaOC/PDA/FGF*

The PicoGreen assay has shown that the cell proliferation in response to growth factor FGF didn't show significantly difference, comparing scaffolds A-C with D-F (**Figure 40**). Considering the FGF release experiment, it might be possible that FGF binded to the surface of the wells plate and loose its function. Remarkable result showed collagen/CaOC scaffold, (C,F) which promoted cell proliferation significantly more than the others composite

biopolymer scaffolds (A,B,D,E). The best result this scaffold showed in presence of PDA (I), where on day 14, the amount of double-stranded DNA reached 537 ng of dsDNA/scafffold.

In this case even FGF supported proliferation, which increased and reached 840 ng dsDNA/scafffold (L). Fibroblast proliferation was significantly greater in response to treatment with PDA-coatead collagen/CaOC scaffold, which can provide both a matrix for binding and stabilization of growth factor and hydrated scaffold, where cells can migrate and proliferate. Only here, the effect of dopamine grafting FGF was observed as enhanced cell proliferation. The other composite scaffold didn't show significant differences with FGF, besides significant proliferative activity in presence of dopamine.

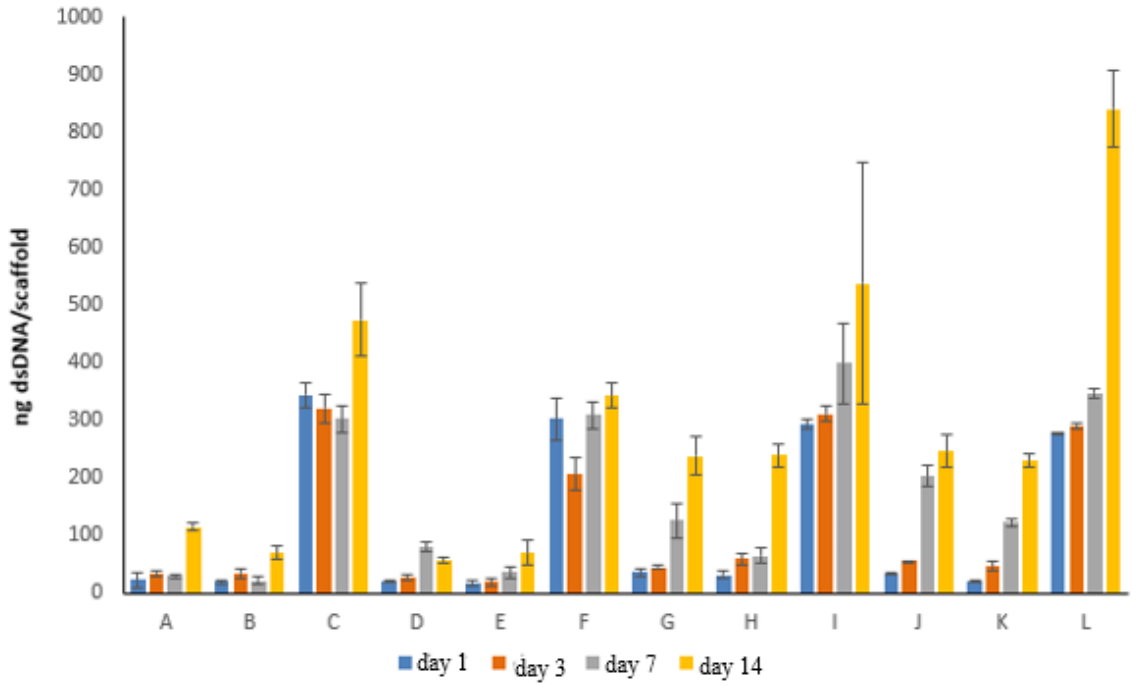

***Figure 40**-Fibroblast proliferation of the composite scaffolds in the following order: **A**-collagen, **B**-collagen/chitosan, **C**-collagen/CaOC, **D**-collagen/FGF, **E**-collagen/chitosan/FGF, **F**-collagen/CaOC/FGF, **G**-collagen/PDA, **H**-collagen/chitosan/PDA, **I**- collagen/CaOC/PDA, **J**-collagen/PDA/FGF **K**- collagen/chitosan/PDA/FGF, **L**- collagen/CaOC/PDA/FGF*

The live/dead viability of fibroblast cells where performed by staining nucleus of viable cells (expressed by green fluorescence) and nucleus of non-viable cells (expressed by red fluorescence). High proportions of viable cells were observed in collagen/chitosan/FGF and PDA-coated collagen/FGF scaffolds **Figure 42**_(E,J). No viable cells were observed in the collagen/CaOC scaffold (C), while their presence was more found within the same scaffold

but with PDA (I). On the day 7, the most visible nucleus were found to be in PDA-coated collagen/CaOC/FGF and PDA-coated collagen/FGF and cells were proliferate with good viability until day 14, where only in that of CaOC scaffold some appearing dead cells were observed (**Figure 41_**(I,L)). Since PDA improved proliferation, day 7 showed more viable cells in its presence and the viability was gradually continuing together with cell proliferation until day 14 (**Figure 42_**(G-J)). Collagen/chitosan and Collagen/CaOC with PDA and FGF (K,L) has shown higher viability on 7^{th} day, while on day 14 the more viable cells were occurred with no PDA coating (**Figure 42_**(E-F)) compare to that of PDA (K,L). PDA in role of grafting FGF significantly enhanced proliferation in collagen/CaOC but maintained the good cell viability only until day 7. Since FGF was not expressed, due to the probable binding to the plastic wells plate during scaffold fabrication, the most cells were proliferate in collagen/CaOC/FGF which suggests the possibility of CaOC higher FGF affinity.

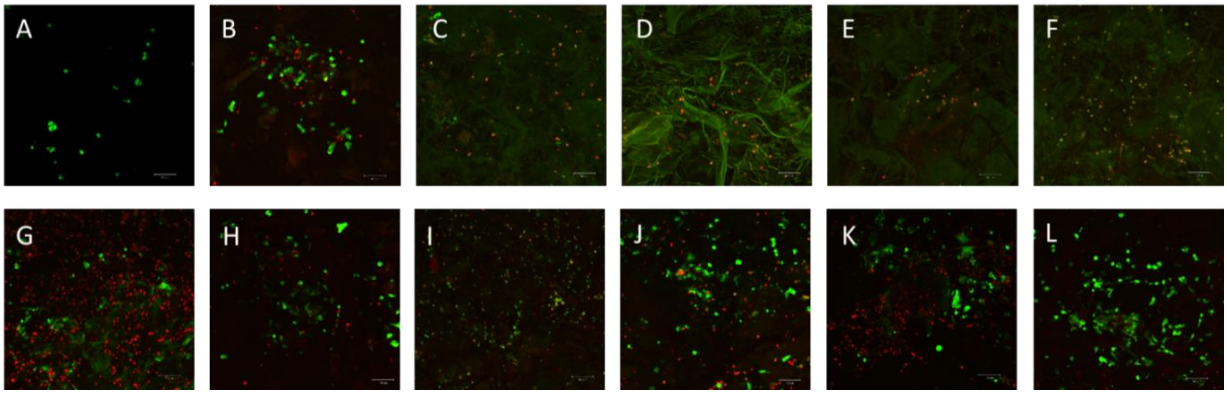

***Figure 41**-The cell viability analysis on 7^{th} day of the composite scaffolds in following order: **A**-collagen, **B**-collagen/chitosan, **C**-collagen/CaOC, **D**-collagen/FGF, **E**-collagen/chitosan/FGF, **F**-collagen/CaOC/FGF, **G**-collagen/PDA, **H**-collagen/chitosan/PDA, **I**- collagen/CaOC/PDA, **J**-collagen/PDA/FGF **K**- collagen/chitosan/PDA/FGF, **L**- collagen/CaOC/PDA/FGF*

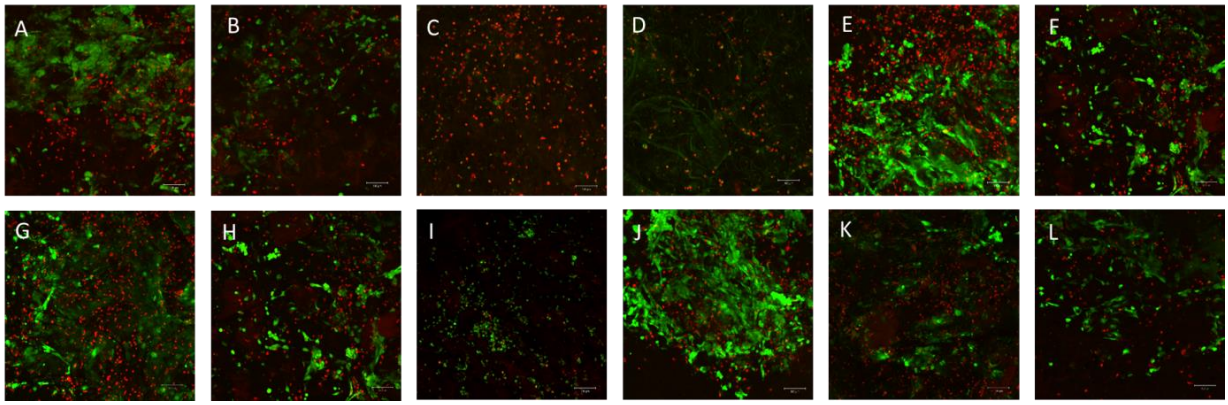

***Figure 42**-The cell viability analysis on 14th day of the composite scaffolds in following order: **A**-collagen, **B**-collagen/chitosan, **C**-collagen/CaOC, **D**-collagen/FGF, **E**-collagen/chitosan/FGF, **F**-collagen/CaOC/FGF, **G**-collagen/PDA, **H**-collagen/chitosan/PDA, **I**- collagen/CaOC/PDA, **J**-collagen/PDA/FGF **K**- collagen/chitosan/PDA/FGF, **L**- collagen/CaOC/PDA/FG*

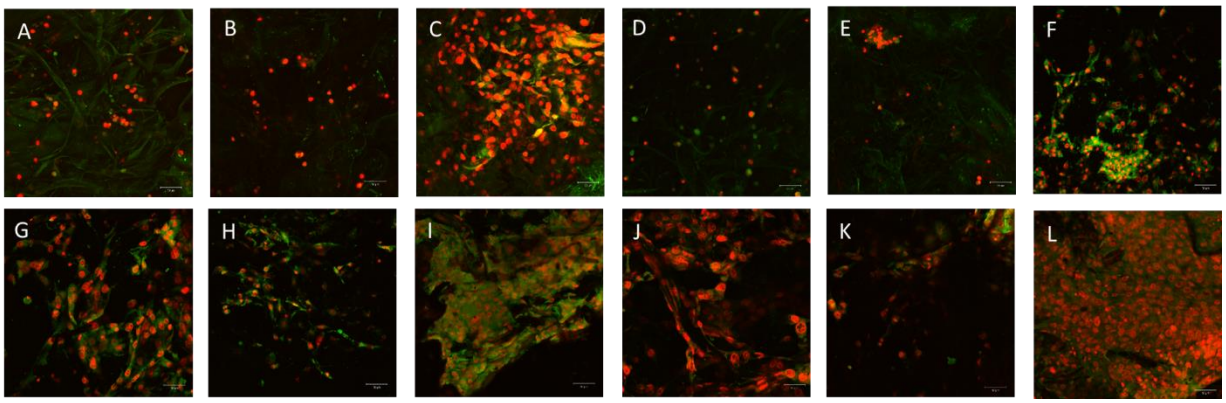

***Figure 43**-The red cell's dead nucleus visualized by propidium iodid and green cytoplasm visualized by DiOC on 14th day of the composite scaffolds in following order: **A**-collagen, **B**-collagen/chitosan, **C**-collagen/CaOC, **D**-collagen/FGF, **E**-collagen/chitosan/FGF, **F**- collagen/CaOC/FGF, **G**-collagen/PDA, **H**-collagen/chitosan/PDA, **I**- collagen/CaOC/PDA, **J**-collagen/PDA/FGF **K**-collagen/chitosan/PDA/FGF, **L**- collagen/CaOC/PDA/FGF*

To visualize the nucleus of dead cells, propidium iodide (PI) was used, since it can not permeant to live cells. However, the PI will penetrate damaged membranes, since it possesses a high affinity for nucleic acids.[114] One of the best markers for cell death is membrane integrity assessed using propidium iodide, which has shown that the most dead cells are possessed by collagen/CaOC scaffold (C), PDA-coated collagen/CaOC scaffold (L), collagen (G) and PDA-coated collagen scafffold with FGF (J) (**Figure 43**) The small amount of dead cells was observed in presence of PDA in all the rests scaffolds (H,I,K).

The extracellular matrix contributes to the fluorescence by its auto-fluorescence emission which could be caused by several different fluorophores. The figure parts of A,D and E has shown the autofluorescence of cellular components, which could include collagen itself, tryptophan as a component of most proteins or nicotinamide adenine dinucleotide (NAD), a coenzyme found in all living cells.[115] The scaffolds of collagen and collagen/chitosan exhibited the most less dead cells nucleus after 14 days.

3,3'-Dihexyloxacarbocyanine (DiOC) is a lipophilic fluorescent dye with excitation/emission spectra of 484/501 nm, used for the staining of a cell's endoplasmic reticulum (ER), vesicle membranes and also it accumulates in mitochondria. It has been already used to visualize mitochondrial dislocations, fusion, and fission in living cells, as well as cellular apoptosis.[116] In all collagen composite scaffolds, cytoplasmatic components were visualized (**Figure 43**), from which the less visible characterizes collagen/chitosan with PDA and FGF (K). Also less cytoplasmatic environment can be attributed to the rests of PDA coated scaffodls in presence of FGF (J,L). PDA-coated collagen/CaOC scaffold showed the most DiOC binding (I) compare to its model with no dopamine (C), where also intensive red fluorescence of dead cells was observed. All the rests collagen scaffolds have showed the potential environment for the cell growth. Magnification of microscopic pictures is 100 μm.

5 Conclusion

In this presented study four variants of collagen composite scaffolds were prepared by two different mechanisms in order to evaluate both, the most proper scaffold and better mechanism for *in-vivo* applications. In every mechanism, PDA-coating surface characterized the series and was the most characteristic for collagen/cellulose scaffolds. According to the surface topography, PDA precipitates deposited like a slight film on its electrospunn nanofibrous surfaces

The incorporation of PDA into collagen scaffolds has significantly improved not only adhesion between the two layers, but also scaffold stiffness property, while decreased the intensity of stretching. The PDA-coated collagen/CaOC was considered as the most stiff materials at dry testing conditions with deformation resisting at 397.07 kPa, together with the PDA-coated collagen (277.36 kPa). The PDA-coated collagen/chitosan showed much lower resistant of only 154.03 kPa, but exhibited very good properties in hydrated state, where has shown sufficient elongation (only decreased from 34 % to 23.4 % with that of

PDA) and it was good resistant to the applied stress (30.9 kPa), similar to that of the most resistant collagen (37.49 kPa). It can be suggested that this scaffold fulfilled the mechanical requirements of biological tissue in its origin environment. The difference between cross-linked and non cross-linked nanofibres has shown the similar mechanical properties in terms of stiffness and tensil properties, only adhesion of the layers is improved by cross-linking

In-vitro testing characterized the scaffolds in terms of swelling, degradation and viability/cytotoxicity assay. The highest swelling ratio was related with CMC, and collagen, while all the rest scaffolds were exhibiting lower values. The sweeling ratio was significantly redused with the presence of PDA for all the scaffolds and dropped from 24 of CMC to 10.66 of that of PDA, while collagen decreased from 13.25 to 5.84.

PDA has also large influence on collagen and chitosan degradation, where a significant time prolongation in both cases was observed. PDA caused deferment in collagenase degradation, where collagen/CaOC was postponed for more 4 hours, collagen/CMC for more 22 hours and collagen/chitosan started to degradate after more 4 days. Dopamine can also restrain the structure of collagen/chitosan in lysozyme degradation for more 3 days. The bacterial activity occured after first 24 hours during degradation was also reduced by presence of dopamine until 5^{th} day.

Scaffold with good biomechanical properties can have however, a drawback of detrimental effect of retaining a high porosity, thus the biological activity, since the less sufficient porous capacity limits cells infiltration and vascularization. When PDA redused the swelling ratio, the porosity was reduced as well. In spite of the reduced porosity, *in vitro* biocompatibility testing showed that the cell adhesion and proliferation can be significantly enhanced in presence of PDA. Analysis of cells viability has shown that a high proportion of viable cells can be maintained more in presence of PDA, throughout the whole culture period. Related with the cell viability potentially good scaffolds became PDA-coated collagen and collagen/chitosan. Many of cytotoxic cells nucleus were observed in the PDA-coated collagen/CaOC. Cells in this scaffold could proliferate as the best but did not maintain good viability until 14 day. Since FGF was not expressed, due to the probable binding to the plastic wells plate during scaffold fabrication, the most cells were proliferate in collagen/CaOC/FGF which suggests the possibility of CaOC higher FGF affinity. The balance between tension elasticity and stiffness must be created together with soft porous architecture to allow cell infiltration, adhesion and proliferation. The PDA-coated scaffolds are potential to meet this requirements and serve as good skin engineered substitutes.

6 References

[1] “Human Skin Layers Layers Of Human Skin Melanocyte And Melanin Royalty Free Stock”. 2016. Online. http://anatomybody101.org/human-skin-layers/human-skin-layers-layers-of-human-skin-melanocyte-and-melanin-royalty-free-stock/.

[2] Chaudhari, Atul, Komal Vig, Dieudonné Baganizi, Rajnish Sahu, Saurabh Dixit, Vida Dennis, Shree Singh, and Shreekumar Pillai. 2016. “Future Prospects For Scaffolding Methods And Biomaterials In Skin Tissue Engineering: A Review”. International Journal Of Molecular Sciences 17 (12): 1974-. doi:10.3390/ijms17121974.

[3] Pan, Jian-feng, Ning-hua Liu, Hui Sun, Feng Xu, and Xiaohua Liu. 2014. “Preparation And Characterization Of Electrospun Plcl/poloxamer Nanofibers And Dextran/gelatin Hydrogels For Skin Tissue Engineering”. Plos One 9 (11): e112885-. doi:10.1371/journal.pone.0112885.

[4] Basu, Poulami, U. Narendra Kumar, and I. Manjubala. 2017. “Wound Healing Materials - A Perspective For Skin Tissue Engineering”. Current Science 112 (12): 2392-. doi:10.18520/cs/v112/i12/2392-2404.

[5] Breitkreutz, Dirk, Isabell Koxholt, Kathrin Thiemann, and Roswitha Nischt. 2013. “Skin Basement Membrane: The Foundation Of Epidermal Integrity—Bm Functions And Diverse Roles Of Bridging Molecules Nidogen And Perlecan”. Biomed Research International 2013: 1-16. doi:10.1155/2013/179784.

[6] Ahmadi-Aghkand, Fateme, Shiva Gholizadeh-Ghaleh Aziz, Yunes Panahi, Hadis Daraee, Fateme Gorjikhah, Sara Gholizadeh-Ghaleh Aziz, Arash Hsanzadeh, and Abolfazl Akbarzadeh. 2015. “Recent Prospective Of Nanofiber Scaffolds Fabrication Approaches For Skin Regeneration”. Artificial Cells, Nanomedicine, And Biotechnology 44 (7): 1635-1641. doi:10.3109/21691401.2015.1111232.

[7] Piraino, Francesco, and Šeila Selimović. 2015. “A Current View Of Functional Biomaterials For Wound Care, Molecular And Cellular Therapies”. Biomed Research International. Academic Editor: Tetsuji Yamaoka.

[8] Moore, Alessandra, Clement Marshall, and Michael Longaker. 2017. “Minimizing Skin Scarring Through Biomaterial Design”. Journal Of Functional Biomaterials 8 (1): 3-. doi:10.3390/jfb8010003.

[9] Rahimnejad, Maedeh, Soroosh Derakhshanfar, and Wen Zhong. 2017. “Biomaterials And Tissue Engineering For Scar Management In Wound Care” 5 (1): -. doi:10.1186/s41038-017-0069-9.

[10] CHEN, JOHN, and GIOVANNI ABATANGELO. 1999. “Functions Of Hyaluronan In Wound Repair”. United Kingdom, and Institute of Histol- ogy, b University of Padova, Italy: ConvaTec Wound Healing Research Institute.

[11] McCarty, Sara M., and Steven L. Percival. 2013. “Proteases And Delayed Wound Healing”. Advances In Wound Care 2 (8): 438-447. doi:10.1089/wound.2012.0370.

[12] Demir, Ali, and Erdal Cevher. 2011. “Biopolymers As Wound Healing Materials: Challenges And New Strategies”. Biomaterials Applications For Nanomedicine, November. InTech. doi:10.5772/25177.

[13] Catanzano, O., V. D’Esposito, S. Acierno, M.R. Ambrosio, C. De Caro, C. Avagliano, P. Russo, et al. 2015. “Alginate–Hyaluronan Composite Hydrogels Accelerate Wound Healing Process”. Carbohydrate Polymers 131: 407-414. doi:10.1016/j.carbpol.2015.05.081.

[14] Shen, Yu-I, Hyun-Ho G. Song, Arianne E. Papa, Jacqueline A. Burke, Susan W. Volk, and Sharon Gerecht. 2015. “Acellular Hydrogels For Regenerative Burn Wound Healing:

Translation From A Porcine Model". Journal Of Investigative Dermatology 135 (10): 2519-2529. doi:10.1038/jid.2015.182.

[15] "Pharmacosmos Committed To Quality: Biogradeabillity Of Dextran". Online. https://www.dextran.com/about-dextran/dextran-chemistry/biodegradeability.

[16] Sun, G., X. Zhang, Y.-I. Shen, R. Sebastian, L. E. Dickinson, K. Fox-Talbot, M. Reinblatt, C. Steenbergen, J. W. Harmon, and S. Gerecht. 2011. "Dextran Hydrogel Scaffolds Enhance Angiogenic Responses And Promote Complete Skin Regeneration During Burn Wound Healing". Proceedings Of The National Academy Of Sciences 108 (52): 20976-20981. doi:10.1073/pnas.1115973108.

[17] Kurahashi, Toshihiro, and Junichi Fujii. 2015. "Roles Of Antioxidative Enzymes In Wound Healing". Journal Of Developmental Biology 3 (2): 57-70. doi:10.3390/jdb3020057.

[18] Lobmann, R., G. Schultz, and H. Lehnert. 2005. "Proteases And The Diabetic Foot Syndrome: Mechanisms And Therapeutic Implications". Diabetes Care 28 (2): 461-471. doi:10.2337/diacare.28.2.461.

[19] "Desio Sports Medicine: Pros And Cons Of Autograft Or Allograft Use In Acl Reconstruction". Online. Worcester. https://www.desiosportsmedicine.com/news-and-updates/pros-and-cons-of-autograft-or-allograft-use-in-acl-reconstruction/..

[20] Singh, AK, and YR Shenoy. 2012. "Skin Substitutes: An Indian Perspective". *Indian Journal Of* Plastic *Surgery* 45 (2): 388-. doi:10.4103/0970-0358.101322.

[21] Kennedy, Kelsey M., Archana Bhaw-Luximon, and Dhanjay Jhurry. 2017. "Skin Tissue Engineering: Biological Performance Of Electrospun Polymer Scaffolds And Translational Challenges". *Regenerative Engineering And Translational Medicine* 3 (4): 201-214. doi:10.1007/s40883-017-0035-x.

[22] Vig, Komal, Atul Chaudhari, Shweta Tripathi, Saurabh Dixit, Rajnish Sahu, Shreekumar Pillai, Vida Dennis, and Shree Singh. 2017. "Advances In Skin Regeneration Using Tissue Engineering". International Journal Of Molecular Sciences 18 (4): 789-. doi:10.3390/ijms18040789.

[23] Xie, Jingwei, Stephanie M. Willerth, Xiaoran Li, Matthew R. Macewan, Allison Rader, Shelly E. Sakiyama-Elbert, and Younan Xia. 2009. "The Differentiation Of Embryonic Stem Cells Seeded On Electrospun Nanofibers Into Neural Lineages". Online. Biomaterials 30 (3): 354-362. doi:10.1016/j.biomaterials.2008.09.046.

[24] Zhong, S. P., Y. Z. Zhang, and C. T. Lim. 2010. "Tissue Scaffolds For Skin Wound Healing And Dermal Reconstruction". Wiley Interdisciplinary Reviews: Nanomedicine And Nanobiotechnology 2 (5): 510-525. doi:10.1002/wnan.100.

[25] Annual Review Of Biochemistry. 2009. Vol. 78. http://www.annualreviews.org/doi/10.1146/annurev.biochem.77.032207.120833.

[26] Shoulders, Matthew D., and Ronald T. Raines. 2009. "Collagen Structure And Stability". Annual Review Of Biochemistry 78 (1): 929-958. doi:10.1146/annurev.biochem.77.032207.120833.

[27] Koide, T. 2007. "Designed Triple-Helical Peptides As Tools For Collagen Biochemistry And Matrix Engineering". Philosophical Transactions Of The Royal Society B: Biological Sciences 362 (1484): 1281-1291. doi:10.1098/rstb.2007.2115.

[28] *"Help Pharmaceuticals S.a: Collagen Menu". 2013. Online. http://www.collagenmenu.eu/our-scientific-expertise.html.*

[29] Ruszczak, Z. 2003. "Effect Of Collagen Matrices On Dermal Wound Healing". Advanced Drug Delivery Reviews 55 (12): 1595-1611. doi:10.1016/j.addr.2003.08.003.

[30] Ma, L. 2003. “Collagen/chitosan Porous Scaffolds With Improved Biostability For Skin Tissue Engineering”. Biomaterials 24 (26): 4833-4841. doi:10.1016/S0142-9612(03)00374-0.

[31] Sun, L P, S Wang, Z W Zhang, X Y Wang, and Q Q Zhang. 2009. “Biological Evaluation Of Collagen–Chitosan Scaffolds For Dermis Tissue Engineering”. Biomedical Materials 4 (5): 055008-. doi:10.1088/1748-6041/4/5/055008.

[32] Ahmed, Shakeel, and Saiqa Ikram. 2016. “Chitosan Based Scaffolds And Their Applications In Wound Healing”. Achievements In The Life Sciences 10 (1): 27-37. doi:10.1016/j.als.2016.04.001.

[33] Aravamudhan, Aja, Daisy M. Ramos, Ahmed A. Nada, and Sangamesh G. Kumbar. 2014. “Natural Polymers”. Natural And Synthetic Biomedical Polymers. Elsevier, 67-89. doi:10.1016/B978-0-12-396983-5.00004-1.

[34] Mogoşanu, George Dan, and Alexandru Mihai Grumezescu. 2014. “Natural And Synthetic Polymers For Wounds And Burns Dressing”. International Journal Of Pharmaceutics 463 (2): 127-136. doi:10.1016/j.ijpharm.2013.12.015.

[35] Meng, Xin, Feng Tian, Jian Yang, Chun-Nian He, Nan Xing, and Fan Li. 2010. “Chitosan And Alginate Polyelectrolyte Complex Membranes And Their Properties For Wound Dressing Application”. Journal Of Materials Science: Materials In Medicine 21 (5): 1751-1759. doi:10.1007/s10856-010-3996-6.

[36] Mogoşanu, George Dan, and Alexandru Mihai Grumezescu. 2014. “Natural And Synthetic Polymers For Wounds And Burns Dressing”. International Journal Of Pharmaceutics 463 (2): 127-136. doi:10.1016/j.ijpharm.2013.12.015.

[37] Chen, Shangwu, Qin Zhang, Tomoko Nakamoto, Naoki Kawazoe, and Guoping Chen. 2016. “Gelatin Scaffolds With Controlled Pore Structure And Mechanical Property For Cartilage Tissue Engineering”. Tissue Engineering Part C: Methods 22 (3): 189-198. doi:10.1089/ten.tec.2015.0281.

[38] Thein-Han, W.W., J. Saikhun, C. Pholpramoo, R.D.K. Misra, and Y. Kitiyanant. 2009. “Chitosan–Gelatin Scaffolds For Tissue Engineering: Physico-Chemical Properties And Biological Response Of Buffalo Embryonic Stem Cells And Transfectant Of Gfp–Buffalo Embryonic Stem Cells”. Acta Biomaterialia 5 (9): 3453-3466. doi:10.1016/j.actbio.2009.05.012.

[39] Rose, James, Settimio Pacelli, Alicia Haj, Harminder Dua, Andrew Hopkinson, Lisa White, and Felicity Rose. 2014. “Gelatin-Based Materials In Ocular Tissue Engineering”. Materials 7 (4): 3106-3135. doi:10.3390/ma7043106.

[40] Santoro, Marco, Alexander M. Tatara, and Antonios G. Mikos. 2014. “Gelatin Carriers For Drug And Cell Delivery In Tissue Engineering”. Journal Of Controlled Release 190: 210-218. doi:10.1016/j.jconrel.2014.04.014.

[41] Novotna, Katarina, Pavel Havelka, Tomas Sopuch, Katerina Kolarova, Vladimira Vosmanska, Vera Lisa, Vaclav Svorcik, and Lucie Bacakova. 2013. “Cellulose-Based Materials As Scaffolds For Tissue Engineering”. Cellulose 20 (5): 2263-2278. doi:10.1007/s10570-013-0006-4.

[42] Zimnitsky, Dmitry S., Tatiana L. Yurkshtovich, and Pavel M. Bychkovsky. 2004. “Synthesis And Characterization Of Oxidized Cellulose”. Journal Of Polymer Science Part A: Polymer Chemistry 42 (19): 4785-4791. doi:10.1002/pola.20302.

[43] Martina, Bajerová, Krejčová Kateřina, Rabišková Miloslava, Gajdziok Jan, and Masteiková Ruta. 2009. “Oxycellulose: Significant Characteristics In Relation To Its Pharmaceutical And Medical Applications”. Advances In Polymer Technology 28 (3): 199-208. doi:10.1002/adv.20161.

[44] Švachová, Veronika, Lucy Vojtová, David Pavliňák, Libor Vojtek, Veronika Sedláková, Pavel Hyršl, Milan Alberti, Josef Jaroš, Aleš Hampl, and Josef Jančář. 2016. "Novel Electrospun Gelatin/oxycellulose Nanofibers As A Suitable Platform For Lung Disease Modeling". Materials Science And Engineering: C 67: 493-501. doi:10.1016/j.msec.2016.05.059.

[45] Bao, Dengshan, Mingjie Chen, Haiying Wang, Jufang Wang, Chuanfu Liu, and Runcang Sun. 2014. "Preparation And Characterization Of Double Crosslinked Hydrogel Films From Carboxymethylchitosan And Carboxymethylcellulose: The Origin, Evolution, And Impact Of Doi Moi". Carbohydrate Polymers 110 (10): 113-120. doi:10.1016/j.carbpol.2014.03.095.

[46] Hollabaugh, C. B., Leland H. Burt, and Anna Peterson Walsh. 1945. "Carboxymethylcellulose. Uses And Applications: The Origin, Evolution, And Impact Of Doi Moi" 37 (10): 943-947. doi:10.1021/ie50430a015.

[47] Ke, Y., G. S. Liu, J. H. Wang, W. Xue, C. Du, and G. Wu. 2014. "Preparation Of Carboxymethyl Cellulose Based Microgels For Cell Encapsulation". Express Polymer Letters 8 (11): 841-849. doi:10.3144/expresspolymlett.2014.85.

[48] Pal, Kunal, A K Banthia, and D K Majumdar. 2006. "Development Of Carboxymethyl Cellulose Acrylate For Various Biomedical Applications". Biomedical Materials 1 (2): 85-91. doi:10.1088/1748-6041/1/2/006.

[49] Ugwoke, Michael Ikechukwu, Remigius Uchenna Agu, Hubert Vanbilloen, Jan Baetens, Patrick Augustijns, Norbert Verbeke, Luc Mortelmans, Alfons Verbruggen, Renaat Kinget, and Guy Bormans. 2000. "Scintigraphic Evaluation In Rabbits Of Nasal Drug Delivery Systems Based On Carbopol 971P® And Carboxymethylcellulose". Journal Of Controlled Release 68 (2): 207-214. doi:10.1016/S0168-3659(00)00258-3.

[50] Chen, Ray-Neng, Hsiu-O Ho, Chiao-Ya Yu, and Ming-Thau Sheu. 2010. "Development Of Swelling/floating Gastroretentive Drug Delivery System Based On A Combination Of Hydroxyethyl Cellulose And Sodium Carboxymethyl Cellulose For Losartan And Its Clinical Relevance In Healthy Volunteers With Cyp2C9 Polymorphism". European Journal Of Pharmaceutical Sciences 39 (1-3): 82-89. doi:10.1016/j.ejps.2009.10.015.

[51] Huangqin Chen, Kunal, A K Mingwen Fan, and D K Majumdar. 2008. "Novel Thermally Sensitive Ph-Dependent Chitosan/ Carboxymethyl Cellulose Hydrogels". Journal Of Bioactive And Compatible Polymers 23 (1): 38-48. doi:10.1177/0883911507085070.

[52] Matthew BA McCullo., et al. "Development of Chitosan Based Scaffolds for Bone Regeneration: A Preliminary Report". EC Orthopaedics 8.1 (2017): 15-25

[53] Reeves, Robert, Andreia Ribeiro, Leonard Lombardo, Richard Boyer, and Jennie B. Leach. 2010. "Synthesis And Characterization Of Carboxymethylcellulose-Methacrylate Hydrogel Cell Scaffolds". *Polymers* 2 (3): 252-264. doi:10.3390/polym2030252.

[54] Mondal, Debasish, May Griffith, and Subbu S. Venkatraman. 2016. "Polycaprolactone-Based Biomaterials For Tissue Engineering And Drug Delivery: Current Scenario And Challenges". International Journal Of Polymeric Materials And Polymeric Biomaterials 65 (5): 255-265. doi:10.1080/00914037.2015.1103241.

[55] Barbarisi, Manlio, Gerardo Marino, Emilia Armenia, Quagliariello Vincenzo, Francesco Rosso, Marina Porcelli, and Alfonso Barbarisi. 2015. "Use Of Polycaprolactone (Pcl) As Scaffolds For The Regeneration Of Nerve Tissue". Journal Of Biomedical Materials Research Part A 103 (5): 1755-1760. doi:10.1002/jbm.a.35318.

[56] Sun, B. K., Z. Siprashvili, P. A. Khavari, Megan E. Francis-Sedlak, Shu-wei Kao, Emmanuel C. Opara, and Eric M. Brey. 2014. "Advances In Skin Grafting And Treatment Of Cutaneous Wounds". *Science* 346 (6212): 941-945. doi:10.1126/science.1253836.

[57] Song, Xinyang, Dai Dai, Xiao He, Shu Zhu, Yikun Yao, Hanchao Gao, Jingjing Wang, et al. 2015. “Growth Factor Fgf2 Cooperates With Interleukin-17 To Repair Intestinal Epithelial Damage”. *Immunity* 43 (3): 488-501. doi:10.1016/j.immuni.2015.06.024.

[58] Dvorak, Pavel, David Bednar, Pavel Vanacek, Lukas Balek, Livia Eiselleova, Veronika Stepankova, Eva Sebestova, et al. 2018. “Computer-Assisted Engineering Of Hyperstable Fibroblast Growth Factor 2”. *Biotechnology And Bioengineering* 115 (4): 850-862. doi:10.1002/bit.26531.

[59] “Properties Of Dopamine In Chemistry”. 2017. Online. Essay, UK. https://www.ukessays.com/essays/chemistry/properties-dopamine-chemistry-5113.php.

[60] Zhao, Xingyu, Yu Han, Jiawei Li, Bo Cai, Hang Gao, Wei Feng, Shuqiang Li, Jianguo Liu, and Dongsong Li. 2017. “Bmp-2 Immobilized Plga/hydroxyapatite Fibrous Scaffold Via Polydopamine Stimulates Osteoblast Growth”. Materials Science And Engineering: C 78: 658-666. doi:10.1016/j.msec.2017.03.186.

[61] Tsai, Wei-Bor, Wen-Tung Chen, Hsiu-Wen Chien, Wei-Hsuan Kuo, and Meng-Jiy Wang. 2011. “Poly(Dopamine) Coating Of Scaffolds For Articular Cartilage Tissue Engineering”. Acta Biomaterialia 7 (12): 4187-4194. doi:10.1016/j.actbio.2011.07.024.

[62] Ho, Chia-Che, and Shinn-Jyh Ding. 2014. “Structure, Properties And Applications Of Mussel-Inspired Polydopamine”. Journal Of Biomedical Nanotechnology 10 (10): 3063-3084. doi:10.1166/jbn.2014.1888.

[63] Ding, Y.H., M. Floren, and W. Tan. 2016. “Mussel-Inspired Polydopamine For Bio-Surface Functionalization”. Biosurface And Biotribology 2 (4): 121-136. doi:10.1016/j.bsbt.2016.11.001.

[64] Rim N, Kim S, Shin Y, Jun I, Lim D, Park J, et al. Mussel-inspired surface modification of poly(L-lactide) electrospun fibers for modulation of osteogenic differentiation of human mesenchymal stem cells. Colloids and Surfaces B-Biointerfaces. 2012;91:189-97.

[65] Lee, Haeshin, Junsung Rho, and Phillip B. Messersmith. 2009. “Facile Conjugation Of Biomolecules Onto Surfaces Via Mussel Adhesive Protein Inspired Coatings”. Advanced Materials 21 (4): 431-434. doi:10.1002/adma.200801222.

[66] Sun, Xiaoming, Liying Cheng, Jingwen Zhao, Rong Jin, Baoshan Sun, Yaoming Shi, Lu Zhang, Yuguang Zhang, and Wenguo Cui. 2014. “Bfgf-Grafted Electrospun Fibrous Scaffolds Via Poly(Dopamine) For Skin Wound Healing”. J. Mater. Chem. B 2 (23): 3636-3645. doi:10.1039/C3TB21814G.

[67] Tiruvannamalai-Annamalai, Ramkumar, David Randall Armant, Howard W. T. Matthew, and Christina Chan. 2014. “A Glycosaminoglycan Based, Modular Tissue Scaffold System For Rapid Assembly Of Perfusable, High Cell Density, Engineered Tissues”. Plos One 9 (1): e84287-. doi:10.1371/journal.pone.0084287.

[68] Lu, Tingli, Yuhui Li, and Tao Chen. “Techniques For Fabrication And Construction Of Three-Dimensional Scaffolds For Tissue Engineering”. International Journal Of Nanomedicine, 337-. doi:10.2147/IJN.S38635.

[69] McGuigan, A. P., and M. V. Sefton. 2006. “Vascularized Organoid Engineered By Modular Assembly Enables Blood Perfusion”. Proceedings Of The National Academy Of Sciences 103 (31): 11461-11466. doi:10.1073/pnas.0602740103.

[70] Nichol, Jason W., and Ali Khademhosseini. 2009. “Modular Tissue Engineering: Engineering Biological Tissues From The Bottom Up”. Soft Matter 5 (7): 1312-. doi:10.1039/b814285h.

[71] Lovett, Michael, Kyongbum Lee, Aurelie Edwards, and David L. Kaplan. 2009. “Vascularization Strategies For Tissue Engineering”. Tissue Engineering Part B: Reviews 15 (3): 353-370. doi:10.1089/ten.teb.2009.0085.

[72] Nam, Yoon Sung, and Tae Gwan Park. 1999. “Biodegradable Polymeric Microcellular Foams By Modified Thermally Induced Phase Separation Method”. Biomaterials 20 (19): 1783-1790. doi:10.1016/S0142-9612(99)00073-3.

[73] Shao, Jundong, Cong Chen, Yingjun Wang, Xiaofeng Chen, and Chang Du. 2012. “Early Stage Structural Evolution Of Plla Porous Scaffolds In Thermally Induced Phase Separation Process And The Corresponding Biodegradability And Biological Property”. Polymer Degradation And Stability 97 (6): 955-963. doi:10.1016/j.polymdegradstab.2012.03.014.

[74] Lu, Tingli, Yuhui Li, and Tao Chen. “Techniques For Fabrication And Construction Of Three-Dimensional Scaffolds For Tissue Engineering”. International Journal Of Nanomedicine, 337-. doi:10.2147/IJN.S38635.

[75] Ma PX, Zhang RY. Synthetic nano-scale fibrous extracellular matrix. J Biomed Mater Res. 1999;46:60–72.

[76] Zhao, Jianhao, Wanqing Han, Haodong Chen, Mei Tu, Rong Zeng, Yunfeng Shi, Zhengang Cha, and Changren Zhou. 2011. “Preparation, Structure And Crystallinity Of Chitosan Nano-Fibers By A Solid–Liquid Phase Separation Technique”. Carbohydrate Polymers 83 (4): 1541-1546. doi:10.1016/j.carbpol.2010.10.009.

[77] Lu, Tingli, Yuhui Li, Tao Chen, Mei Tu, Rong Zeng, Yunfeng Shi, Zhengang Cha, and Changren Zhou. 2011. “Techniques For Fabrication And Construction Of Three-Dimensional Scaffolds For Tissue Engineering”. International Journal Of Nanomedicine 83 (4): 337-. doi:10.2147/IJN.S38635.

[78] Zhao, Jianhao, Wanqing Han, Haodong Chen, Mei Tu, Rong Zeng, Yunfeng Shi, Zhengang Cha, and Changren Zhou. 2011. “Preparation, Structure And Crystallinity Of Chitosan Nano-Fibers By A Solid–Liquid Phase Separation Technique”. Carbohydrate Polymers 83 (4): 1541-1546. doi:10.1016/j.carbpol.2010.10.009.

[79] L'Heureux, Nicolas, Todd N. McAllister, and Luis M. de la Fuente. 2007. “Tissue-Engineered Blood Vessel For Adult Arterial Revascularization”. New England Journal Of Medicine 357 (14): 1451-1453. doi:10.1056/NEJMc071536.

[80] Nishida, Kohji, Masayuki Yamato, Yasutaka Hayashida, Katsuhiko Watanabe, Kazuaki Yamamoto, Eijiro Adachi, Shigeru Nagai, et al. 2004. “Corneal Reconstruction With Tissue-Engineered Cell Sheets Composed Of Autologous Oral Mucosal Epithelium”. New England Journal Of Medicine 351 (12): 1187-1196. doi:10.1056/NEJMoa040455.

[81] Sawa, Yoshiki, Shigeru Miyagawa, Taichi Sakaguchi, Tomoyuki Fujita, Akifumi Matsuyama, Atsuhiro Saito, Tatsuya Shimizu, et al. 2012. “Tissue Engineered Myoblast Sheets Improved Cardiac Function Sufficiently To Discontinue Lvas In A Patient With Dcm: Report Of A Case”. Surgery Today 42 (2): 181-184. doi:10.1007/s00595-011-0106-4.

[82] Matsuura, Katsuhisa, Yuji Haraguchi, Tatsuya Shimizu, Teruo Okano, Toshiharu Kutsuna, Toshihiro Nagai, Taku Ukai, et al. 2013. “Cell Sheet Transplantation For Heart Tissue Repair: Report Of A Case”. Journal Of Controlled Release 169 (3): 336-340. doi:10.1016/j.jconrel.2013.03.003.

[83] Ohki, Takeshi, Masayuki Yamato, Masaho Ota, Ryo Takagi, Daisuke Murakami, Makoto Kondo, Ryo Sasaki, et al. 2012. “Prevention Of Esophageal Stricture After Endoscopic Submucosal Dissection Using Tissue-Engineered Cell Sheets: Report Of A Case”. Gastroenterology 143 (3): 582-588.e2. doi:10.1053/j.gastro.2012.04.050.

[84] Ito, Satoshi, Masato Sato, Masayuki Yamato, Genya Mitani, Toshiharu Kutsuna, Toshihiro Nagai, Taku Ukai, et al. 2012. “Repair Of Articular Cartilage Defect With Layered Chondrocyte Sheets And Cultured Synovial Cells: Report Of A Case”. Biomaterials 33 (21): 5278-5286. doi:10.1016/j.biomaterials.2012.03.073.

[85] Bhambere, Deepak & A. Gaidhani, Kunal & Harwalkar, Mallinath & S. Nirgude, Pallavi. (2015). LYOPHILIZATION / FREEZE DRYING – A REVIEW. World Journal of Pharmaceutical Research. 4. 516-543.

[86] "Millrock Technology Innovative By Design: What Is Ereeze-Drying". Online. Kingston, NY 12401. http://www.millrocktech.com/lyosight/lyobrary/what-is-freeze-drying/.

[87] Meyer, Michael, and Kristin Trommer. 2015. "Soft Collagen-Gelatine Sponges By Convection Drying". Brazilian Archives Of Biology And Technology 58 (1): 109-117. doi:10.1590/S1516-8913201400139.

[88] TANGSADTHAKUN, Chalonglarp, Sorada KANOKPANONT, Neeracha SANCHAVANAKIT, Tanom BANAPRASERT, and Siriporn DAMRONGSAKKUL. 2006. "Properties Of Collagen/chitosan Sc Affolds For Skin Tissue Engineering". *Journal Of Metals, Materials And Minerals*, 37-44.

[89] Lor Huai Chong, Nadira Zamal Zarith, and Naznin Sultana. 2015. "Poly(Caprolactone)/chitosan-Based Scaffold Using Freeze Drying Technique For Bone Tissue Engineering Application". *2015 10Th Asian Control Conference (Ascc)*. IEEE, 1-4. doi:10.1109/ASCC.2015.7244570.

[90] Fereshteh, Zeinab. 2018. "Freeze-Drying Technologies For 3D Scaffold Engineering". *Functional 3D Tissue Engineering Scaffolds*. Elsevier, 151-174. doi:10.1016/B978-0-08-100979-6.00007-0.

[91] Ngadiman, Nor Hasrul Akhmal, MY Noordin, Ani Idris, and Denni Kurniawan. 2017. "A Review Of Evolution Of Electrospun Tissue Engineering Scaffold: From Two Dimensions To Three Dimensions". Proceedings Of The Institution Of Mechanical Engineers, Part H: Journal Of Engineering In Medicine 231 (7): 597-616. doi:10.1177/0954411917699021.

[92] Li, Yawen, and Therese Bou-Akl. 2016. "Electrospinning In Tissue Engineering". Electrospinning - Material, Techniques, And Biomedical Applications, December. InTech. doi:10.5772/65836.

[93] Alamein, Mohammad A., Sebastien Stephens, Qin Liu, Stuart Skabo, and Patrick H. Warnke. 2013. "Mass Production Of Nanofibrous Extracellular Matrix With Controlled 3D Morphology For Large-Scale Soft Tissue Regeneration: The Origin, Evolution, And Impact Of Doi Moi". *Tissue Engineering Part C: Methods* 19 (6): 458-472. doi:10.1089/ten.tec.2012.0417.

[94] Dubský, Michal, Šárka Kubinová, Jakub Širc, Luděk Voska, Robert Zajíček, Alena Zajícová, Petr Lesný, et al. 2012. "Nanofibers Prepared By Needleless Electrospinning Technology As Scaffolds For Wound Healing". *Journal Of Materials Science: Materials In Medicine* 23 (4): 931-941. doi:10.1007/s10856-012-4577-7.

[95] SLOVIKOVÁ, A.; VOJTOVÁ, L.; JANČÁŘ, J. Preparation and modification of collagen- based scaffold for tissue engineering. *Chemical Papers,* 2008, roč. 62, č. 4, s. 417-422. ISSN: 0366- 6352.

[96] Bozzola, John J., and Lonnie Dee. Russell. c1992. *Electron Microscopy: Principles And Techniques For Biologists*. Boston: Jones and Bartlett Publishers

[97] Zhang, Yu-Zhong, Li-Yuan Ran, Chun-Yang Li, Xiu-Lan Chen, and F. E. Löffler. "Diversity, Structures, And Collagen-Degrading Mechanisms Of Bacterial Collagenolytic Proteases". doi:10.1128/AEM.00883-15.

[98] Shi, Lei, Ryan Ermis, Anastacia Garcia, Dale Telgenhoff, and Duncan Aust. "Degradation Of Human Collagen Isoforms By Clostridium Collagenase And The Effects Of Degradation Products On Cell Migration". doi:10.1111/j.1742-481X.2010.00659.x.

[99] [95]2018. Online. *Abcam*. United States. http://www.abcam.com/mts-assay-kit-cell-proliferation-colorimetric-ab197010.html

[100] Quent, Verena M.C., Daniela Loessner, Thor Friis, Johannes C. Reichert, and Dietmar W. Hutmacher. 2010. "Discrepancies Between Metabolic Activity And Dna Content As Tool To Assess Cell Proliferation In Cancer Research". *Journal Of Cellular And Molecular Medicine* 14 (4): 1003-1013. doi:10.1111/j.1582-4934.2010.01013.x.

[101] Szymańska, Emilia, and Katarzyna Winnicka. 2015. "Stability Of Chitosan—A Challenge For Pharmaceutical And Biomedical Applications". *Marine Drugs* 13 (4): 1819-1846. doi:10.3390/md13041819.

[102] You, Inseong, Young Chang Seo, and Haeshin Lee. 2014. "Material-Independent Fabrication Of Superhydrophobic Surfaces By Mussel-Inspired Polydopamine". *Rsc Advances* 4 (20): 10330-. doi:10.1039/c3ra47626j.

[103] Asadian, M, H Declercq, M Cornelissen, R Morent, and N De Geyter. 2017. "Effects Of Plasma Treatment On The Surface Chemistry, Wettability, An D Cellular Interactions Of Nanofibrous Scaffolds". MONS, BELGIUM. Online. https://biblio.ugent.be/publication/8532609/file/8532610.pdf

[104] Pappa, Anna Maria, Varvara Karagkiozaki, Silke Krol, Spyros Kassavetis, Dimitris Konstantinou, Charalampos Pitsalidis, Lazaros Tzounis, Nikos Pliatsikas, and Stergios Logothetidis. 2015. "Oxygen-Plasma-Modified Biomimetic Nanofibrous Scaffolds For Enhanced Compatibility Of Cardiovascular Implants". *Beilstein Journal Of Nanotechnology* 6: 254-262. doi:10.3762/bjnano.6.24.

[105] Huang, Zheng-Ming, Y.Z Zhang, S Ramakrishna, and C.T Lim. 2004. "Electrospinning And Mechanical Characterization Of Gelatin Nanofibers". *Polymer* 45 (15): 5361-5368. doi:10.1016/j.polymer.2004.04.005.

[106] Shin, Young Min, Hansoo Park, and Heungsoo Shin. 2011. "Enhancement Of Cardiac Myoblast Responses Onto Electrospun Plcl Fibrous Matrices Coated With Polydopamine For Gelatin Immobilization". *Macromolecular Research* 19 (8): 835-842. doi:10.1007/s13233-011-0815-y.

[107] [99] Hu, Yang, Weihua Dan, Shanbai Xiong, Yang Kang, Arvind Dhinakar, Jun Wu, and Zhipeng Gu. 2017. "Development Of Collagen/polydopamine Complexed Matrix As Mechanically Enhanced And Highly Biocompatible Semi-Natural Tissue Engineering Scaffold". *Acta Biomaterialia* 47: 135-148. doi:10.1016/j.actbio.2016.10.017

[108] Liu, Yang, Zhongxun Zhang, Huilin Lv, Yong Qin, and Linhong Deng. 2017. "Surface Modification Of Chitosan Film Via Polydopamine Coating To Promote Biomineralization In Bone Tissue Engineering". *Journal Of Bioactive And Compatible Polymers* 33 (2): 134-145. doi:10.1177/0883911517713228.

[109] Chatterji, P.R., and H. Kaur. 1992. "Interpenetrating Hydrogel Networks: 3. Properties Of The Gelatin-Sodium Carboxymethylcellulose System". *Polymer* 33 (11): 2388-2391. doi:10.1016/0032-3861(92)90532-2.

[110] Ball, Vincent, Doriane Del Frari, Valérie Toniazzo, and David Ruch. 2012. "Kinetics Of Polydopamine Film Deposition As A Function Of Ph And Dopamine Concentration: Insights In The Polydopamine Deposition Mechanism". *Journal Of Colloid And Interface Science* 386 (1): 366-372. doi:10.1016/j.jcis.2012.07.030.

[111] Del Frari, Doriane, Jérôme Bour, Vincent Ball, Valérie Toniazzo, and David Ruch. 2012. "Degradation Of Polydopamine Coatings By Sodium Hypochlorite: A Process Depending On The Substrate And The Film Synthesis Method". *Polymer Degradation And Stability* 97 (9): 1844-1849. doi:10.1016/j.polymdegradstab.2012.05.002

[112] Yang, Wei, Chanjuan Liu, Yi Chen, Jia-mei Hu, Zhi-yong Liu, He-yun Wang, and Feng Zhou. 2018. "Stability Of Polydopamine Coatings On Gold Substrates Inspected By

Surface Plasmon Resonance Imaging". *Langmuir* 34 (12): 3565-3571. doi:10.1021/acs.langmuir.7b03143.

[113] Jia, Xin, Zhi-yuan Ma, Guo-xiang Zhang, Jia-mei Hu, Zhi-yong Liu, He-yun Wang, and Feng Zhou. 2013. "Polydopamine Film Coated Controlled-Release Multielement Compound Fertilizer Based On Mussel-Inspired Chemistry". *Journal Of Agricultural And Food Chemistry* 61 (12): 2919-2924. doi:10.1021/jf3053059.

[114] Stan-Lotter, Helga, Stefan Leuko, Andrea Legat, and Sergiu Fendrihan. 2006. "24 The Assessment Of The Viability Of Halophilic Microorganisms In Natural Communities", Methods in Microbiology, . Elsevier, 569-584. doi:10.1016/S0580-9517(08)70027-8.

[115] Hegyi, J., and V. Hegyi. 2016. "New Developments In Fluorescence Diagnostics". *Imaging In Dermatology*. Elsevier, 89-94. doi:10.1016/B978-0-12-802838-4.00009-1.

[116] Sabnis, Ram W., Todor G. Deligeorgiev, Madhukar N. Jachak, and Tukaram S. Dalvi. 2009. "Dioc 6 (3): A Useful Dye For Staining The Endoplasmic Reticulum" 72 (5): 253-258. doi:10.3109/10520299709082249.

7 List of Appendix

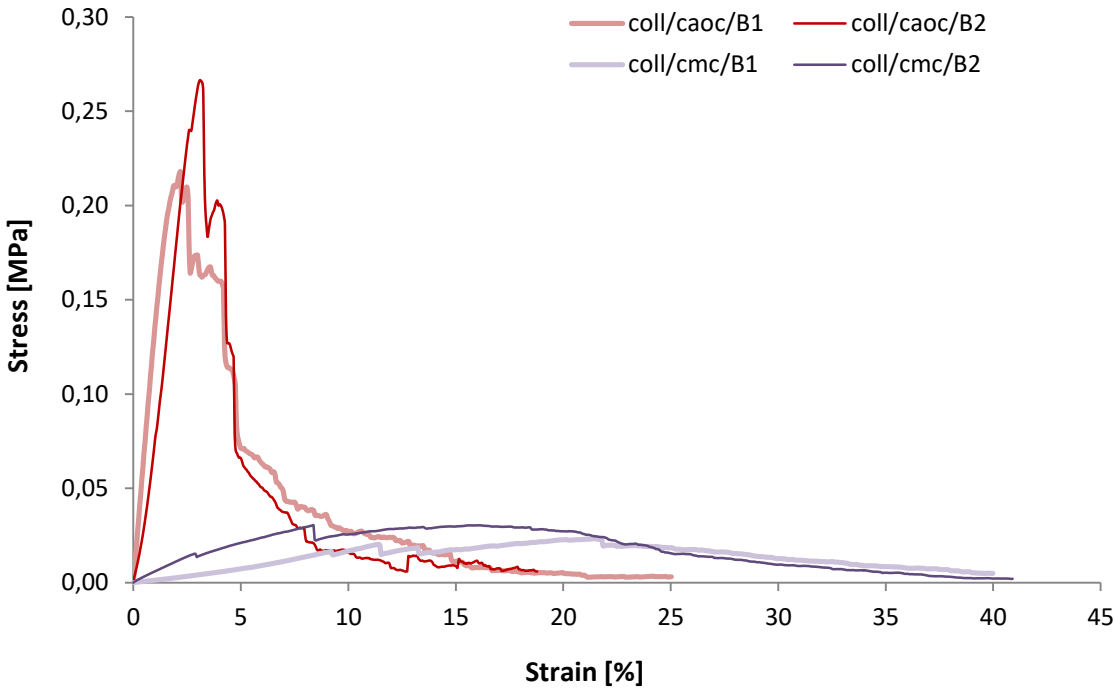

***Appendix 1**-Uniaxial extension of scaffolds with non cross-linked (B1) and with cross-linked (B2) nanofibres in dry state*

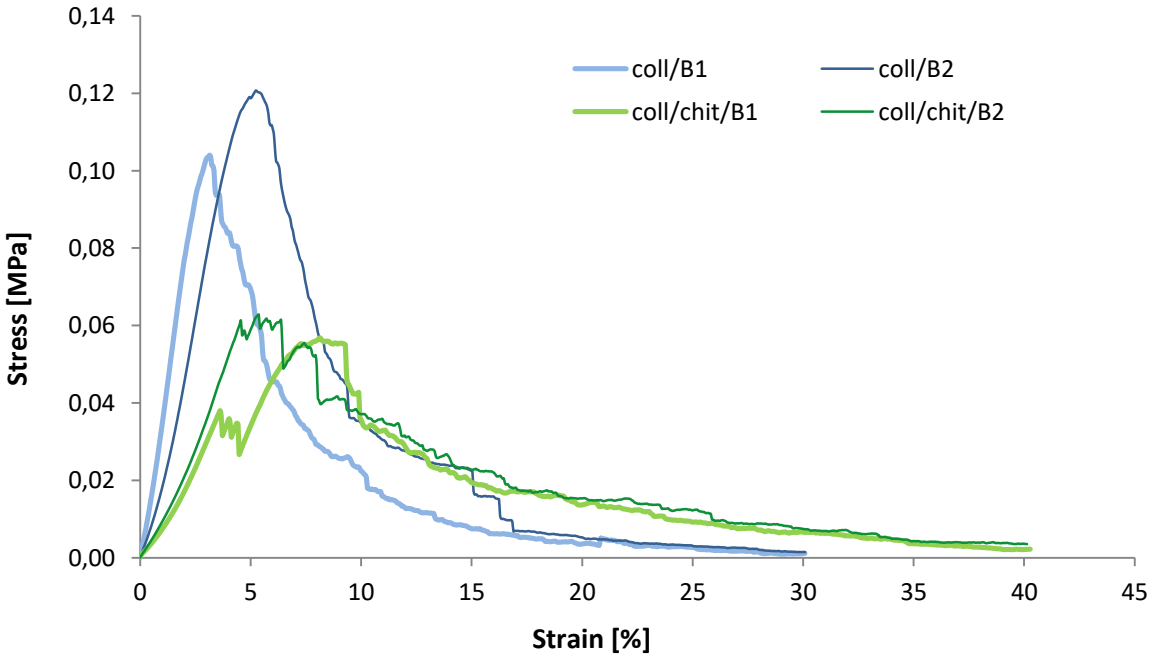

***Appendix 2**-Uniaxial extension of scaffolds with non cross-linked (B1) and with cross-linked (B2) nanofibres in dry state*

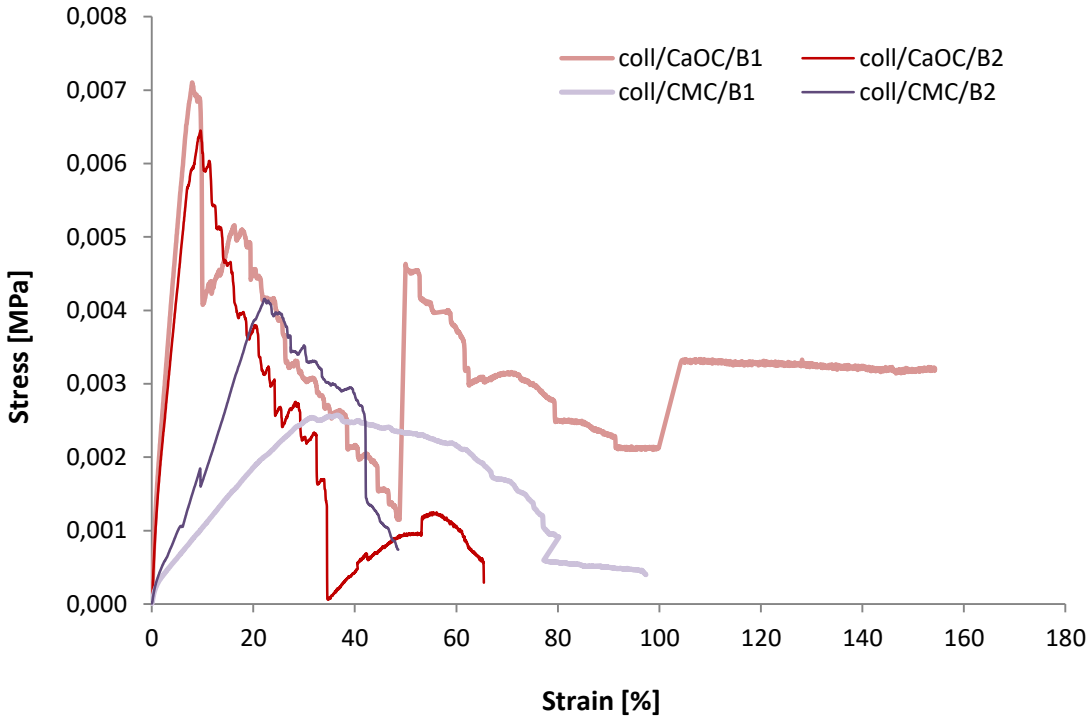

***Appendix 3**-Uniaxial extension of scaffolds with non cross-linked (B1) and with cross-linked (B2) nanofibres in hydrated state*

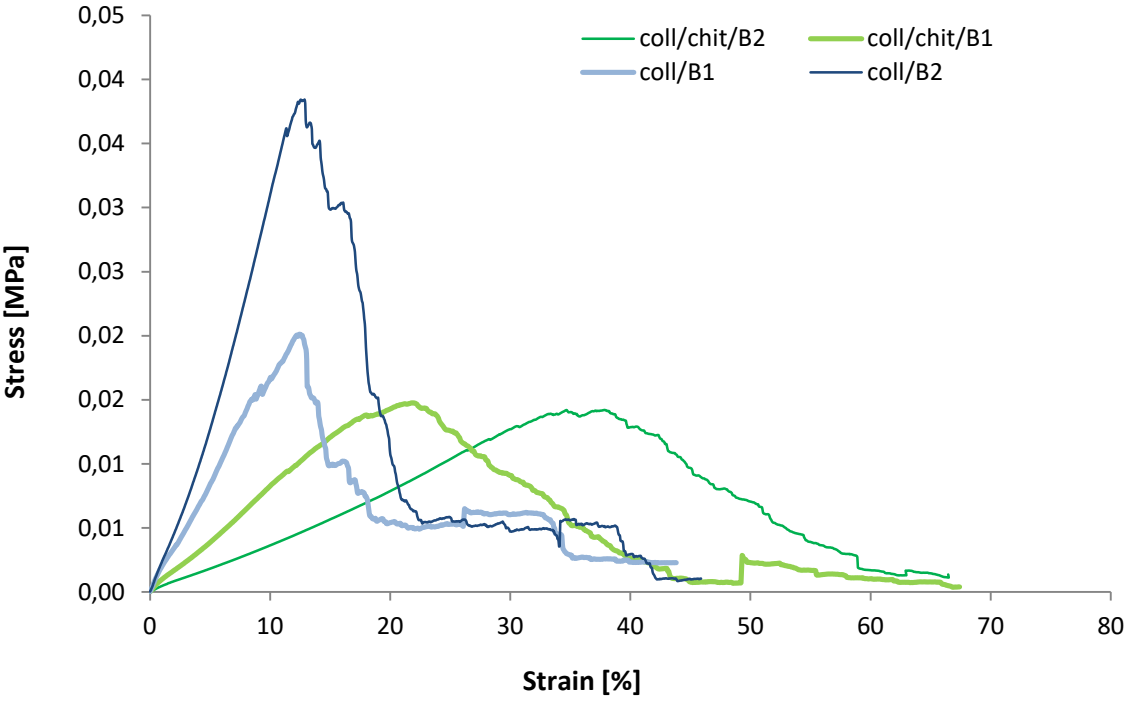

***Appendix 4**-Uniaxial extension of scaffolds with non cross-linked (B1) and with cross-linked (B2) nanofibres in hydrated state*

8 List of Abbreviations

BSA	Bovine Serum Albumin
bFGF	basic Fibroblast Growth Factor
CMC	Carboxy-Methyl Cellulose
DiOC	3,3'-Dihexyloxacarbocyanine
DHI	dihydroxyindole
ECM	Extra cellular matrix
EDC	*N*-(3-Dimethylaminopropyl)-*N′*-ethylcarbodiimide hydrochloride
EGF	Endothelial Growth Factor
ELISA	Enzyme-Linked ImmunoSorbent Assay
ER	Endoplasmic reticulum
FGF	Fibroblast Growth Factor
HA	Hyaluronic acid
hMSCs	Human Mesenchymal Stem cells
HRP	Horseradish peroxidase
IDQ	Indolequinone
IL	Interleukin
JNK	Jun amino-terminal kinases
MMPs	Matrix metalloproteinases
MTS	[3-(4,5-dimethylthiazol-2-yl)-5-(3-carboxymethoxyphenyl)-2-(4-sulfophenyl)-2H-tetrazolium
NF-ECM	Nanofibrous ECM
NHS	*N*-hydroxysuccinimide
OC	Oxidized cellulose
ORC	Oxidized regenerated cellulose
PADM	Porcine acellular dermal matrix
PBS	Phosphate Buffered Saline
PBST	Phosphat Buffer Tween20
PCL	Polycaprolactone
PDA	Polydopamine
PDGF	Platelet-derived growth factor
PEG-DM	Polyethylene glycol dimethacrylate
PI	Propidium iodide
PLGA	poly(lactic-co-glycolic acid)
PLCL	poly(L-lactide-co-ε-caprolactone)
RGD	arginine-glycine-aspartate
SEM	Scanning Electron Microscop

TGF-β1	Transforming Growth Factor beta 1
TIMPs	Tissue-derived inhibitors
TMB	Tetramethyl benzidin
VEGF	Vascular Endothelial Growth Factor

9 List of Tables

10 List of Figures